# Maximal Parallelograms in Convex Polygons and a Novel Geometric Structure \* †

## Kai Jin<sup>1</sup>

Department of Computer Science, University of Hong Kong Pokfulam Road, Hong Kong SAR cscjjk@gmail.com

#### - Abstract -

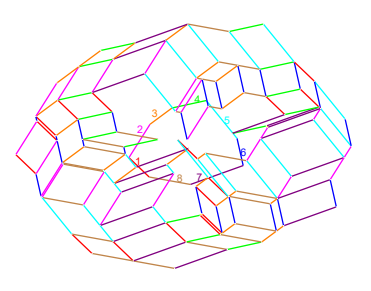
Given a convex polygon P with n edges, we propose a novel geometric structure induced by P, called Nest(P), which is an arrangement of  $\Theta(n^2)$  segments, each of which is parallel to an edge of P. This structure enjoys six simple yet nontrivial properties, which are derived from two fundamental geometric properties – convexity and parallelism.

We then apply  $\operatorname{Nest}(P)$  to solve the geometric optimization problem of computing the maximal area parallelograms in P. Specifically, we show that the essential nature of the maximal area parallelograms is captured by  $\operatorname{Nest}(P)$  and that our optimization problem reduces to answering O(n) location queries on this structure. Moreover, avoiding an explicit construction of  $\operatorname{Nest}(P)$ , which would take  $\Omega(n^2)$  time, we answer each of these queries in  $O(\log^2 n)$  time, and thus obtain an  $O(n\log^2 n)$  time algorithm for computing all the maximal area parallelograms. This is the first subquadratic time algorithm among the best-known algorithms for many related problems.

1998 ACM Subject Classification I.3.5 Computational Geometry and Object Modeling

Keywords and phrases Discrete convex geometry, Geometric optimization, Parallelograms

Digital Object Identifier 10.4230/LIPIcs.xxx.yyy.p



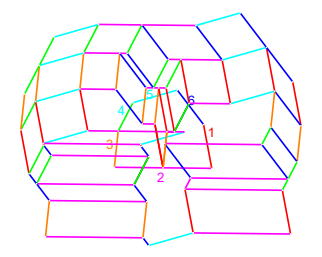


**Figure 1** Two examples of Nest(P). The edges of the given polygon P are labeled by 1 to n. The other line segments in the figure are the edges from Nest(P).

# 1 Introduction

For each convex polygon P, a geometric structure associated with P, as shown in Figure 1 and 2, which we call Nest(P), is introduced in this paper. We prove six simple yet nontrivial properties enjoyed by Nest(P), all of which manifest its good interaction with P. We then

© Kai Jin;

licensed under Creative Commons License CC-BY

Conference title on which this volume is based on.

Editors: Billy Editor and Bill Editors; pp. 1–72

Leibniz International Proceedings in Informatics

LIPICS Schloss Dagstuhl – Leibniz-Zentrum für Informatik, Dagstuhl Publishing, Germany

<sup>\*</sup> Supported by the National Basic Research Program of China Grant 2007CB807900, 2007CB807901, and the National Natural Science Foundation of China Grant 61033001, 61061130540, 61073174.

<sup>&</sup>lt;sup>†</sup> This work is mainly done during my Ph. D. in the Institute for Interdisciplinary Information Sciences at Tsinghua University.

apply Nest(P) to solve the geometric problem of computing all parallelograms in P with the maximum area. Throughout, we regard P as a compact set which contains its boundary and interior. For this and many closely related problems, the previously best algorithms run in at least  $O(n^2)$  time, where n denotes the number of edges of P. We reduce the problem to O(n) location queries on Nest(P), each of which can be answered efficiently without having an explicit construction of Nest(P), and thus obtain an  $O(n \log^2 n)$  time algorithm.

Let  $\partial P$  denote the boundary of P. If we travel along  $\partial P$  in clockwise from one point to another, we pass through a continuous portion of  $\partial P$ , which is called a **boundary-portion** (of P). We call each vertex and edge of P a **unit** (of P) and introduce an antisymmetric relation called *chasing* between the 2n units. Intuitively, unit u is chasing unit u', if the boundary-portion from u to u' (in clockwise order) is a minor arc of  $\partial P$ . This is made precise in Subsection 1.2. We regard the edges of P open, i.e. none of them contains its endpoints. Therefore, for each point X in  $\partial P$ , it lies in a unique unit (denoted by  $\mathbf{u}(X)$ ).

To introduce Nest(P), we first introduce a set  $\mathcal{T}^P$  and a function f. For each unit pair u, u' such that u is chasing u', we introduce a boundary-portion  $\zeta(u, u')$ ; see its definition in (2), which is not important here. The set  $\mathcal{T}^P$  is defined as the set of those tuples  $(X_1, X_2, X_3)$ of points in  $\partial P$  in which  $\mathbf{u}(X_3)$  is chasing  $\mathbf{u}(X_1)$  and  $X_2 \in \zeta(\mathbf{u}(X_3), \mathbf{u}(X_1))$ . Function f maps any tuple  $(X_1, X_2, X_3)$  of points to such a point that the four points constitute a parallelogram. We then define two kinds of subregions of  $f(\mathcal{T}^P) := \{ f(X_1, X_2, X_3) \mid (X_1, X_2, X_3) \in \mathcal{T}^P \}.$ A **block** is the image set under f of those tuples  $(X_1, X_2, X_3)$  in  $\mathcal{T}^P$  for which  $X_3, X_1$  are restricted to a fixed unit pair, whereas a sector is the image set under f of those tuples  $(X_1, X_2, X_3)$  in  $\mathcal{T}^P$  for which  $X_2$  is restricted to a fixed unit. Last, we define the union of the boundaries of these subregions to be Nest(P). Roughly, Nest(P) is a subdivision of  $f(\mathcal{T}^P)$ .

Although, Nest(P) seems complicated by definition, it enjoys many nontrivial properties that can be simply stated in the guise of  $f, \mathcal{T}^P$  and blocks and sectors. (See a formal description in Theorem 2.) First, the intersection of any two blocks lies in the interior of P. Second, region  $f(\mathcal{T}^P)$  has an annular shape and its inner boundary interleaves  $\partial P$ . Third, each point in  $\partial P$  has at most one preimage in  $\mathcal{T}^P$  under f. This implies a reverse function  $f^{-1}: f(\mathcal{T}^P) \cap \partial P \to \text{(the subset of } \mathcal{T}^P \text{ whose elements are mapped to } \partial P \text{ under } f).$  Forth, the second dimension of  $f^{-1}$  is monotone. Fifth, the 2n intersections between the sectors and  $\partial P$  are pairwise-disjoint and have a monotonicity. Sixth, consider the sector in which  $X_2$ is restricted to a vertex of P, we claim that its intersection with  $\partial P$  is a continuous region.

All these properties are derived from two basic properties in geometry – convexity and parallelism, and they manifest good interactions between Nest(P) and  $\partial P$ . Moreover, since Nest(P) is induced by P, they are actually properties of convex polygon P, and hence may be of interests in convex geometry. In addition, Nest(P) admits other interesting properties. For example, if we travel along Nest(P) (whose segments are connected and directional; see the leftmost picture in Figure 2) one cycle (starting and ending at the same node), the total distance would be 3 times of the perimeter of P, no matter which path we choose. This is directly implied by the definition of Nest(P). We also mention that most properties of Nest(P) still hold when P is a convex curve. These are not be proved or applied in the paper.

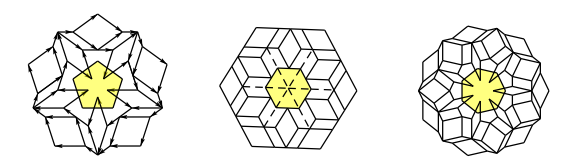


**Figure 2** Examples of Nest(P) for regular n-side polygon for n = 5, 6, 7.

Next, we apply Nest(P) to solve the aforementioned geometric optimization problem of finding the maximum area parallelograms (MAPs) in P. We say parallelogram in P is *locally maximal* if has an area larger than or equal to those of all its nearby parallelograms that lie in P. (See a rigorous definition in Definition 3 and 5.) Our algorithm first computes all the locally maximal area parallelograms (LMAPs) and then finds the MAPs among them.

Being locally maximal, the LMAPs must be inscribed in P, i.e. all their corners lie in  $\partial P$  (Fact 4). Further,  $[15]^1$  observed the following constraint on the corners of the LMAPs (Lemma 6). Briefly, a corner must lie in the aforementioned boundary-portion  $\zeta(u, u')$  when its clockwise next and previous neighboring corners are fixed on u, u' and u is chasing u'. From an overall viewpoint, this observation actually describes a relation between three consecutive corners of an LMAP, which is simply captured by  $\mathcal{T}^P$  (Lemma 8). This establishes a strong connection between  $\mathcal{T}^P$  and the LMAPs in P, which is the cornerstone of our algorithm.

We then reveal new bounds on the corners of the LMAPs hidden behind the relation  $\mathcal{T}^P$  by applying the properties of  $f(\mathcal{T}^P)$  (i.e. the properties of Nest(P) stated above). Suppose an LMAP  $A_0A_1A_2A_3$  has a corner  $A_i$  such that  $\mathbf{u}(A_{i-1})$  is chasing  $\mathbf{u}(A_{i+1})$ , where  $A_{i-1}, A_{i+1}$  denote its clockwise previous and next neighboring corners. We claim 1.  $(A_{i+1}, A_{i+2}, A_{i+3})$  equals  $f^{-1}(A_i)$ , and 2.  $A_i \in \operatorname{sector}(w) \cap \partial P$  when the opposite corner  $A_{i+2}$  lies in unit w, where  $\operatorname{sector}(w)$  denotes the sector region in which  $X_2$  is restricted to w (recall the sectors in page 2). The first claim is a corollary of the third property of Nest(P). The second is not a corollary, yet we can understand it better from the fifth property of Nest(P). By this property, Claim 2 describes a monotone relation between two opposite corners of the LMAPs.

These new bounds are powerful in that they only require (the location information of) one corner to bound the others, whereas the previous bounds in Lemma 6 require two. Thus they open the door of designing subquadratic time algorithms for computing the LMAPs.

We say a corner is anchored if it coincides a vertex of P. To compute the LMAPs, we design three routines, each takes charge of a group of LMAPs that own some special anchored corner(s). Routine 1 computes those LMAPs who have an anchored corner  $A_0$  so that  $\mathbf{u}(A_3)$  is chasing  $\mathbf{u}(A_1)$ . It first enumerates a vertex V to be  $A_0$ , and then computes the positions of  $A_1, A_2, A_3$  by computing  $f^{-1}(V)$ , noticing  $(A_1, A_2, A_3) = f^{-1}(V)$  by Claim 1. We give an O(1) time algorithm for computing  $f^{-1}(V)$  provided that the (unique) block and (unique) sector containing V have been preprocessed. Routine 2 computes those LMAPs who have an anchored corner  $A_0$  so that  $\mathbf{u}(A_1)$  is chasing  $\mathbf{u}(A_3)$ , as well as another anchored corner  $A_1$  so that  $\mathbf{u}(A_2)$  is chasing  $\mathbf{u}(A_0)$ . Under this assumption of the LMAPs, a bunch of constraints on the corners can be obtained from Claim 2, and this routine works by enumerating all parallelograms satisfying such constraints. We give an O(n) accumulated time algorithm for computing these parallelograms provided that the units intersected by each sector (more precisely, each of those sector regions in which  $X_2$  is restricted to a vertex) have been preprocessed. Routine 3 is much easier and it computes those with an anchored corner  $A_0$  so that  $\mathbf{u}(A_3), \mathbf{u}(A_1)$  are not chasing each other. To sum up, we demonstrate that computing the LMAPs reduces to computing for each vertex V, which block and sector region does V lies in and which units are intersected by the sector region in which  $X_2$  is restricted to V? Thus, our optimization problem on P is reduced to O(n) location queries on Nest(P).

Using several nontrivial algorithmic tricks, we answer each of the location query in  $O(\log^2 n)$  time. This avoids an explicit construction of Nest(P), which would take  $\Omega(n^2)$  time. Therefore we obtain an  $O(n\log^2 n)$  time algorithm for computing the LMAPs.

<sup>&</sup>lt;sup>1</sup> [15] is the full version of the conference paper [17], but contains some new results of LMAPs not stated (or not stated explicitly) in the conference paper. All notations in [15] are consistent with this paper.

## 4 Maximal Parallelograms in Convex Polygons

We have seen that two properties of Nest(P), the third and fifth, are of particular value in designing our algorithm. In fact, all the six properties are applied in the algorithm; none is redundant. We point out that the most challenging part of this paper lies in proving these properties. Our proof is built on a lot of underlying observations of the blocks and sectors, which are built above even more fundamental observations of some extremal points on  $\partial P$  called Z-points (which are used to define  $\{\zeta(u,u')\}$  and are introduced in Definition 1). The entire proof is sketched in Subsection 2.5, where the interconnections between these properties are also discussed. Moreover, we point out that the most nontrivial part in the proof is an introduction of another type of regions, called the **bounding-quadrants**, which are quadrants in the plane and are bounding areas for the block regions. See its definition in Subsection 2.4, where four interesting properties of the bounding-quadrants are stated.

## 1.1 Related Work, Motivations & Applications of computing the MAPs

The problem of computing the MAPs belongs to the polygon inclusion problems, the classic geometric optimization problems of searching for extremal figures with special properties inside a polygon, which have been studied extensively in history. For example, [7, 1, 2] computes the maximum area / perimeter k-gons in a convex polygon. For k = 3, the maximum area triangle can be computed in linear time in [9]. Recently, we presented a more elegant linear time algorithm for computing this triangle in [16], which can be regarded as a correction of the algorithm in [11] (wrong due to a recent report [19]). In addition, the currently best algorithms for computing the maximum rectangle [8], maximum similar copy of a triangle [32], maximum equilateral triangle (or inscribed square) [27] in a convex polygon take  $O(n^3)$ ,  $O(n^2 \log n)$ ,  $O(n^2)$  time respectively, much inefficient than ours. [17] gave an  $O(n^2)$  time algorithm for computing the MAPs, which is summarized in Subsection 2.2.

The extremal figures enclosing a given polygon have also attract many researchers. In particular, [31] computes the minimum area enclosing parallelogram in O(n) time using the Rotating-caliper technique [33]. We restate here that the enclosing problems are usually easier than their inclusion counterparts, as stated in [27]. For example, the minimum perimeter enclosing triangle can be found in O(n) time [9, 16, 26, 5], whereas the currently best algorithm [7] for computing the maximum perimeter enclosed triangle takes  $O(n \log n)$  time.

**Motivation.** The MAP problem is as fundamental as the above related problems yet it has special motivations. (See the details of this paragraph in [15].) First, it is a natural extension of the diameter problem [14]. By finding the diameter, we find a center O and a vector  $\beta_1$  so that  $O \pm \beta_1$  are contained in P and that a measure (i.e. length) of the vector is maximized. By finding the MAP, we find O and vectors  $\beta_1, \beta_2$  so that  $O \pm \beta_1, O \pm \beta_2$  are contained in P and that a measure (i.e. cross product) of the vectors is maximized. Second, the simplest nontrivial case m=4 of the Heilbronn triangle problem [23, 4, 30], which concerns placing m points in a region to avoid small triangles constituted by these m points, reduces to finding the MAP. Third, computing the MAPs has an application in shape approximation: The MAP serves as a  $2/\pi$ -approximation of the largest centrally symmetric body in a convex polygon. Last, by finding the MAP, we can bring the polygon into a "good position" by an affine transformation, to avoid almost degenerate, i.e., needle-like or fat polygons.

In fact, the maximum volume parallelepiped in convex bodies has been extensively studied in convex geometry. Assume C is a convex body in  $\mathbb{R}^d$  and Q is the maximum volume parallelepiped in C. [21] proved that the concentric scaling of Q by factor 2d-1 covers C; and [13] proved that there exists one scaling of Q by factor d which covers C. (Notice some similar results proved by Fritz John [18] for the maximum volume ellipsoid in convex bodies.)

[6] proved that any convex body in  $\mathbb{R}^3$  admits an inscribed parallelepiped. [12] proved that if C is a convex curve, there must be a parallelogram inscribed in C of area  $\frac{1}{2} \cdot Area(C)$ . A similar result in  $\mathbb{R}^3$  is proved in [28], and the ratio is  $3!/3^3$ . See also [24] and [22]. Other researches of parallelograms inscribed in curves can be found in [10, 29, 25, 3].

#### 1.2 Preliminaries

Let  $e_1, \ldots, e_n$  be a clockwise enumeration of the edges of P. Denote the vertices of P by  $v_1, \ldots, v_n$  such that  $e_i = (v_i, v_{i+1})$  ( $v_{n+1} = v_1$ ). Denote by  $\ell_i$  the extended line of  $e_i$ . Unless otherwise stated, an edge or a vertex refers to an edge or a vertex of P, respectively. A unit is a vertex or an edge, and each unit has two *incident units*:  $e_i$  has  $v_i, v_{i+1}$ ; whereas  $v_i$  has  $e_{i-1}, e_i$ . (So  $e_i, e_{i+1}$  are **not** incident.) For simplicity, assume all edges are **pairwise-nonparallel**.

Chasing relation between edges. Given two distinct edges  $e_i, e_j$ , we say that  $e_i$  is **chasing**  $e_j$ , denoted by  $e_i \prec e_j$ , if  $v_j$  is closer to  $\ell_i$  than  $v_{j+1}$ ; equivalently, if  $v_{i+1}$  is closer to  $\ell_j$  than  $v_i$ . By the pairwise-nonparallel assumption of edges, for any pair of edges, exactly one of them is chasing the other. For example, in Figure 3,  $e_1$  is chasing  $e_2$  and  $e_3$ , whereas  $e_4, e_5, e_6, e_7$  are chasing  $e_1$ . Denote by  $e_i \preceq e_j$  if  $e_i = e_j$  or  $e_i \prec e_j$ .

Backward and forward edges of units. The backward and forward edges of  $v_i$  are defined as  $e_{i-1}$  and  $e_i$ , respectively. The backward and forward edges of  $e_i$  are  $e_i$  itself. Intuitively, when you start at any point in a unit u and move backward (forward) in clockwise along  $\partial P$  by an infinite small step, you will be located at the backward (forward) edge of u. Denote the backward and forward edge of u by back(u) and forw(u) respectively.

Chasing relation between units. We say unit u is **chasing** unit u' if

$$back(u) \prec back(u') \text{ and } forw(u) \prec forw(u').$$
 (1)

The relation "chasing between units" is a compatible extension of "chasing between edges". **Note**: Considering chasing, there are three cases between two units u, u': 1. u is chasing u' while u' is not chasing u. 2. u' is chasing u while u is not chasing u'. 3. Neither of them is chasing the other. See Figure 3:  $v_1$  is chasing  $v_2, e_2, v_3, e_3$ ; whereas  $e_4, v_5, e_5, v_6, e_6, v_7$  are chasing  $v_1$ . Other units are not chasing  $v_1$  and  $v_1$  is not chasing them.

**Boundary-portions of** P. We consider every boundary-portion directed and the direction conforms with the clockwise order. When X, X' are respectively the *starting* and *terminal* points, the endpoints-inclusive and endpoints-exclusive versions of the portion are denoted by  $[X \circlearrowright X']$  and  $(X \circlearrowright X')$ . **Note**:  $[X \circlearrowright X']$  only contains the single point X if X = X'. For two points A, B on a boundary-portion  $\rho$ , we state that  $A <_{\rho} B$  if A would be encountered earlier than B traveling along  $\rho$ ; and that  $A \leq_{\rho} B$  if A = B or  $A <_{\rho} B$ .

**Inferior portion.** When  $e_i \leq e_j$ , we call  $[v_i \circlearrowright v_{j+1}]$  an *inferior portion*; see Figure 4.

**Reflection &** k-scaling. Given a figure F and a point O (in the same plane) and a ratio k, we define the reflection and k-scaling of F with respect to O in the standard way; as shown in Figure 5. See formal definitions in [15].

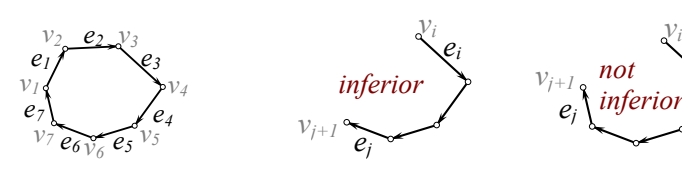


**Figure 3** Illustration **Figure 4** Illustration of inferior portion. of the relation chasing.

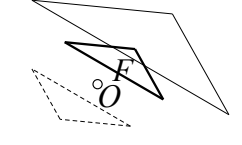


Figure 5 Illustration of reflection & 2-scaling.

# 2 Extended Technique Overview

# 2.1 Introduction of Nest(P) and some underlying geometric objects

In this subsection, we introduce Nest(P) and state its main properties. Shortly speaking, Nest(P) is a subdivision of a planar region  $f(\mathcal{T}^P)$ , where  $\mathcal{T}^P$  is a subset of  $\partial P^3 = (\partial P, \partial P, \partial P)$  defined on P and f is the geometric function that maps any tuple of points  $(X_1, X_2, X_3)$  to X so that the four points  $X_1X_2X_3X$  constitute a parallelogram; i.e.  $f(X_1, X_2, X_3)$  equals the reflection of  $X_2$  around the mid point of  $X_1$  and  $X_3$ . (f(S) is short for  $\{f(X_1, X_2, X_3) \mid (X_1, X_2, X_3) \in S\}$  for any subset S of  $\partial P^3$ .) More specifically, Nest(P) is the union of the boundaries of some subregions of  $f(\mathcal{T}^P)$  called blocks and sectors that are defined below.

Given two lines l, l' and a point X, the **distance-product** from X to l, l', denoted by  $\operatorname{disprod}_{l,l'}(X)$ , is defined to be  $d_l(X) \times d_{l'}(X)$ , where  $d_l(X)$  denotes the distance from X to l.

▶ **Definition 1** ([15] Z-points). Given two edges  $e_i, e_j$  such that  $e_i \prec e_j$ , in domain P, disprod $_{\ell_i,\ell_j}$ () achieves maximum value at a unique point; this point is denoted by  $Z_i^j$  (short for  $Z_{e_i}^{e_j}$ ). We call the  $\Theta(n^2)$  points in  $\{Z_i^j \mid e_i \prec e_j\}$  the Z-points.

Note that all the Z-points lie in  $\partial P$ . (See Fact 21 below and a proof in [15].)

Recall the chasing relation between units in (1). For every unit pair (u, u') such that u is chasing u', we have back(u) chasing back(u') and forw(u) chasing forw(u') and define

$$\zeta(u, u') = \left[ Z_{back(u)}^{back(u')} \circlearrowright Z_{forw(u)}^{forw(u')} \right]. \tag{2}$$

The above equation is complicated at the first glimpse, so we illustrate it by Figure 6.

**Figure 6** Illustration of  $\zeta(u, u')$  when u is chasing u'

The aforementioned set  $\mathcal{T}^P$  (abbreviated as  $\mathcal{T}$  when P is clear) is defined as follow.

$$\mathcal{T}^{P} := \{ (X_1, X_2, X_3) \in \partial P^3 \mid \mathbf{u}(X_3) \text{ is chasing } \mathbf{u}(X_1), X_2 \in \zeta(\mathbf{u}(X_3), \mathbf{u}(X_1)) \}.$$
(3)

Next, we define the aforementioned subregions of  $f(\mathcal{T})$ , called blocks and sectors. For unit pair (u, u') such that u is chasing u', let

$$\mathsf{block}(u, u') := f(\{(X_1, X_2, X_3) \in \mathcal{T} \mid X_3 \in u, X_1 \in u'\}). \tag{4}$$

For any unit w, let

$$\mathsf{sector}(w) := f(\{(X_1, X_2, X_3) \in \mathcal{T} \mid X_2 \in w\}). \tag{5}$$

▶ Remark. 1. We call each element in  $\{\mathsf{block}(u,u') \mid u \text{ is chasing } u'\}$  a **block**. The blocks are important objects throughout this paper, yet their definitions in (4) are lack of intuition, so we give their equivalent geometric definitions as follows. For distinct units u, u', denote  $u \oplus u' = \{\text{the mid point of } X \text{ and } X' \mid X \in u, X' \in u'\}$ , which is a parallelogram, a segment, or a point as shown in Figure 7. Consider the case where u, u' are both edges; e.g.

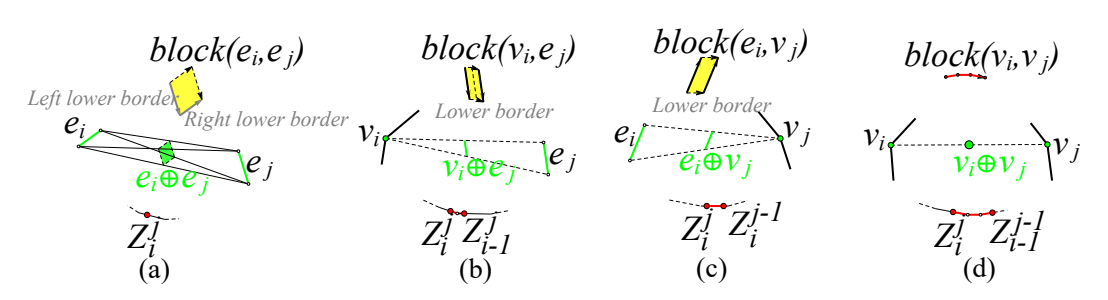


**Figure 7** Geometric definition of blocks.

 $(u, u') = (e_i, e_j)$  and  $e_i \prec e_j$ ; see Figure 7 (a). The 2-scaling of  $e_i \oplus e_j$  is a parallelogram with two edges congruent to  $e_i$  and two edges congruent to  $e_j$ , and is defined as  $\mathsf{block}(e_i, e_j)$ . The other cases are illustrated in Figure 7 (b),(c),(d) and discussed in Subsection 3.1, where we further define the **borders** of each block, and the **direction of each border**.

2. We call each element in  $\{\mathsf{sector}(w) \mid w \text{ is a unit of } P\}$  a  $\mathsf{sector}$ . The sectors are also important objects and are not easy to understand according to the above definition (5). We investigate the shape of  $\mathsf{sector}(V)$  for every vertex V in Subsection 2.5, where we show that it is a connected region and we define explicitly two of its  $\mathsf{boundaries}$ . These two boundaries are drawn by blue and red polygonal curves in the middle picture of Figure 8.

According to (4) and (5), the planar region  $f(\mathcal{T})$  is the union of all  $\Theta(n^2)$  blocks and the union of all 2n sectors. The union of the boundaries of the blocks and sectors is defined as Nest(P). Equivalently, we define Nest(P) to be the union of the borders of each block and the two boundaries of each sector in  $\{\text{sector}(V) \mid V \text{ is a vertex of } P\}$  (these borders or boundaries are defined explicitly in the paper as remarked above) – we adopt the second definition to avoid a complicated definition of the boundaries of sector(E) for every edge E of P. Clearly, Nest(P) is induced by the given polygon P. Moreover, it is an "arrangement" of  $\Theta(n^2)$  line segments, each of which is parallel to an edge of P. (The observation is of no use for understanding the main results of this paper; proof omitted.) We name it Nest(P) because its shape resembles that of a bird nest. See Figure 8 for an example.

We state the main properties of Nest(P) in the guise of blocks and sectors in the next theorem. First, we introduce a few symbols to describe these properties.

Note that region  $f(\mathcal{T})$  is annular (as shown in Figure 8) and thus has an *inner boundary* (denoted by  $\sigma P$ ) and an *outer boundary*, which are both oriented and polygonal closed curve (easy proofs are given later). See the explicit definition of  $\sigma P$  in Subsection 3.4.

Given two oriented closed curves, we say that they interleave if starting from any

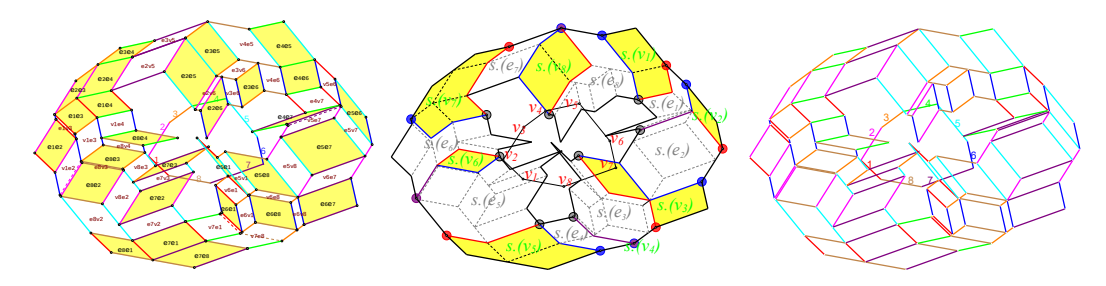


**Figure 8** Blocks, sectors, and Nest(P). The first two pictures draw the blocks and sectors of  $f(\mathcal{T}^P)$  respectively. The third picture draws Nest(P), where the edges of the given polygon P are labeled by 1 to n and the other line segments in this picture are the edges from Nest(P).

intersection between them, regardless of whether we travel around the first curve of a cycle or around the second curve of a cycle, we meet their intersections in identical order.

Let  $\mathcal{T}^*$  denote the subset of  $\mathcal{T}$  that is mapped to the boundary of P under f.

▶ **Theorem 2** (Six main properties of  $\mathcal{T}$  under function f).

**Block-disjointness** The intersection of any pair of blocks lies in the interior of P.

**Interleavity-of-**f The inner boundary of  $f(\mathcal{T})$  (i.e. the curve  $\sigma P$ ) interleaves  $\partial P$ .

**Reversibility-of-**f Function f is a bijection from  $\mathcal{T}^*$  to its image set  $f(\mathcal{T}^*) = f(\mathcal{T}) \cap \partial P$ . Henceforth, we denote the reverse function of f on  $f(\mathcal{T}) \cap \partial P$  by  $f^{-1}$ . Moreover, denote the 1st, 2nd, and 3rd dimension of  $f^{-1}(X)$  by  $f_1^{-1}(X)$ ,  $f_2^{-1}(X)$  and  $f_3^{-1}(X)$  respectively.

**Monotonicity-of-**f Noticing that  $f_2^{-1}$  is a mapping from  $f(\mathcal{T}) \cap \partial P$  to  $\partial P$ , we claim that it is "circularly monotone". Specifically, if a point X travels around  $f(\mathcal{T}) \cap \partial P$  in clockwise, point  $f_2^{-1}(X)$  would shift in clockwise around  $\partial P$  non-strictly, and moreover, when X has traveled exactly a cycle,  $f_2^{-1}(X)$  would also have traveled exactly a cycle.

**Sector-monotonicity** The 2n regions  $sector(v_1) \cap \partial P$ ,  $sector(e_1) \cap \partial P$ , ...,  $sector(v_n) \cap \partial P$ ,  $sector(e_n) \cap \partial P$  are pairwise-disjoint and arranged in clockwise order on  $\partial P$ .

**Sector-continuity** For any vertex V, the intersection between sector(V) and  $\partial P$  is continuous; to be more clear, it is either empty or a boundary-portion of P.

Note: The Block-disjointness does not state that all blocks are pairwise-disjoint.

Although simply stated, the above properties are nontrivial and their proofs are lengthy (given in Section 4 and 5). We sketch the main ideas of the proofs in Subsection 2.5.

- ▶ Remark. 1. With several cascading notation, the definition (3) of  $\mathcal{T}$  looks complicated, yet it enjoys rich properties as stated in Theorem 2, which implies that  $\mathcal{T}$  is well-structured.
- 2. The elements in  $\mathcal{T}$  that deserve special attention are those in  $\mathcal{T}^*$ , i.e. those mapped to  $\partial P$  under f. All of the properties above concern  $f(\mathcal{T}^*)$ , rather than  $f(\mathcal{T})$ .
  - 3. All of these properties manifest good relations between Nest(P) and  $\partial P$ .

## 2.2 Previous quadratic time algorithm for computing the LMAPs

In this subsection, we define the LMAPs rigorously and present its basic properties, and then outline the previous  $O(n^2)$  time algorithm for computing the LMAPs.

We say a parallelogram lies in P if all its corners lie in P. A parallelogram is *inscribed* (in P), if all its corners lie in  $\partial P$ . Given points A and B, denote by |AB| their distance.

▶ Definition 3 ([15] maximum & locally maximal). Consider any parallelogram  $Q = A_0A_1A_2A_3$  that lies in P. We say Q is maximum, if it has the largest area among all parallelograms that lie in P. We say Q is locally maximal, if it has an area larger than or equal to those of its "nearby" parallelograms that lie in P; formally, if  $\exists \delta > 0$  such that  $\forall Q' \in N_{\delta}(Q)$ ,  $Area(Q) \geq Area(Q')$ , where  $N_{\delta}(A_0A_1A_2A_3) = \{B_0B_1B_2B_3 \text{ is a parallelogram in } P \mid \forall i, |A_i - B_i| < \delta\}$ .

A parallelogram is *slidable*, if it has two corners lying in the same edge of P. (If corner A lies in  $e_i$  while corner B lies at an endpoint of  $e_i$ , these two corners are not counted as lying in the same edge – because  $e_i$  is an open segment.) Otherwise, it is said *non-slidable*.

- ▶ Fact 4 ([15]). 1. Maximum implies locally maximal and locally maximal implies inscribed.
- 2. For each slidable inscribed parallelogram, we can find a non-slidable inscribed parallelogram with the same area (by sliding the corners on the same edge to the end of the edge).

▶ **Definition 5** ([15] MAP and LMAP). A parallelogram is an *MAP* (Maximum Area Parallelogram) if it is <u>maximum and non-slidable</u>. A parallelogram is an *LMAP* (Locally Maximal Area Parallelogram) if it is <u>locally maximal and non-slidable</u>. (Note that we safely exclude the slidable parallelograms according to Fact 4.)

The following observation of the LMAPs is crucial for the quadratic time algorithm of [15]. It roughly states that each corner  $A_i$  of the LMAP can be bounded by a well-defined boundary-portion, once two neighboring corners of  $A_i$  are known to lie in two given units. The next observation is a corollary. All subscripts of A are taken modulo 4 in these lemmas.

- ▶ Lemma 6 ([15]). Assume  $A_0A_1A_2A_3$  is an LMAP, whose corners  $A_0, A_1, A_2, A_3$  lie in clockwise order. Assume  $0 \le i \le 3$  and corners  $A_{i+1}, A_{i-1}$  respectively lie in units u, u'. Recall  $\zeta(u, u')$  in (2); see Figure 6. We claim that  $A_i \in \zeta(u, u')$  if u is chasing u'.
- ▶ Lemma 7 ([15]). Assume  $A_0A_1A_2A_3$  is an LMAP, whose corners  $A_0, A_1, A_2, A_3$  lie in clockwise order. Assume  $0 \le i \le 3$  and corners  $A_{i-1}, A_{i+1}$  respectively lie in units u, u'. Recall block(u, u') in (4); see Figure 7. We claim that  $A_i \in \mathsf{block}(u, u')$  if u is chasing u'.

Outline of the previous algorithm in [15]. Suppose  $A_0A_1A_2A_3$  is an LMAP, whose corners  $A_0, A_1, A_2, A_3$  lie in clockwise order. According to Fact 4.1, all the corners lie in  $\partial P$ . In particular, let u, u' respectively denote the units containing  $A_3, A_1$ . Assume the following case occurs: u is chasing u' and  $A_0$  coincides a vertex of P. (According to a simple analysis in [17], two other cases may occur, but they are either similar or trivial.) Since u is chasing u', applying the above lemmas,  $A_0$  lies in  $\mathsf{block}(u,u')$  whereas  $A_2$  lies in  $\zeta(u,u')$ . The algorithm enumerates three units – the unit pair (u,u') and a vertex V in  $\mathsf{block}(u,u')$  to be the position of  $A_0$ . Since two diagonals of parallelogram  $A_0A_1A_2A_3$  bisect each other, the mid point of  $A_0, A_2$  lie in  $u \oplus u'$ . This means the position of  $A_2$  can be easily computed from u, u' and  $A_0$ . Further, the positions of  $A_3, A_1$  can be computed, given that their mid point coincides the mid point of  $A_0, A_2$  and that they lie in u, u' respectively. The running time is trivially  $O(n^3)$  since we enumerate three units. However, utilizing the fact  $V \in \mathsf{block}(u, u')$  with a monotonicity about the positions of the blocks (Lemma 15 in [17]), the time for enumerating (u', V) can be reduced to O(n) for any fixed u. Thus the total running time is  $O(n^2)$ .

There are  $\Theta(n^2)$  different choices of the units containing a pair of opposite corners of the LMAPs and  $\Theta(n^2)$  corresponding bounds, so it seems that the previous algorithm apply these bounds quite efficiently. In the next subsection, however, we show that a subquadratic time algorithm can be obtained via a much better utilization of these  $\Theta(n^2)$  bounds.

## 2.3 Sketch of our subquadratic algorithm for finding the LMAPs

The improvement over the previous algorithm first comes from an overall understanding of the previous bounds. Lemma 6 uses  $\zeta(u, u')$  to bound a corner when its neighboring corners are fixed on u, u'. By changing a viewpoint, these  $\Theta(n^2)$  bounds together describe a relation between three consecutive corners of an LMAP, which is exactly captured by  $\mathcal{T}$ . This is made precise in the following lemma, which follows from (3) and Lemma 6; proof omitted.

▶ **Lemma 8.** Assume that  $A_0A_1A_2A_3$  is an LMAP and  $A_0, A_1, A_2, A_3$  lie in clockwise order. For any i  $(0 \le i \le 3)$ , if  $\mathbf{u}(A_{i+1})$  is chasing  $\mathbf{u}(A_{i-1})$ , then  $(A_{i-1}, A_i, A_{i+1})$  belongs to  $\mathcal{T}$ .

The improvement also comes from revealing new bounds (for corners of the LMAPs) hidden behind the previous bounds. Lemma 9 reveals a type of bounds which describe a *relation* between two opposite corners of the LMAPs. Lemma 10 reveals even more interesting bounds by which we can determine the entire LMAP if one special corner is determined.

▶ **Lemma 9.** Assume  $A_0A_1A_2A_3$  is an LMAP and  $A_0, A_1, A_2, A_3$  lie in clockwise order. Assume  $0 \le i \le 3$  and  $\mathbf{u}(A_{i-1})$  is chasing  $\mathbf{u}(A_{i+1})$ . Then,  $A_i \in \mathsf{sector}(\mathbf{u}(A_{i+2})) \cap \partial P$ .

**Proof.** By Lemma 8,  $(A_{i+1}, A_{i+2}, A_{i+3})$  belongs to  $\mathcal{T}$ , and hence belongs to  $\{(X_1, X_2, X_3) \in \mathcal{T} \mid X_2 \in \mathbf{u}(A_{i+2})\}$ . Therefore, its image under f, which equals  $A_i$ , lies in  $\mathsf{sector}(\mathbf{u}(A_{i+2}))$ . Further because the LMAPs are inscribed (Fact 4.1),  $A_i \in \mathsf{sector}(\mathbf{u}(A_{i+2})) \cap \partial P$ .

- ▶ Lemma 10. Recall function  $f_1^{-1}$ ,  $f_2^{-1}$ ,  $f_3^{-1}$  in Theorem 2. Assume that  $A_0A_1A_2A_3$  is an LMAP whose corners  $A_0$ ,  $A_1$ ,  $A_2$ ,  $A_3$  lie in clockwise order, where  $\mathbf{u}(A_3)$  is chasing  $\mathbf{u}(A_1)$ . We claim that 1. corner  $A_0$  lies in region  $f(\mathcal{T})$  and thus  $f^{-1}(A_0)$  is defined, and more importantly, 2. corners  $A_1$ ,  $A_2$ ,  $A_3$  lie at  $f_1^{-1}(A_0)$ ,  $f_2^{-1}(A_0)$ ,  $f_3^{-1}(A_0)$  respectively.
- **Proof.** Because  $\mathbf{u}(A_3)$  is chasing  $\mathbf{u}(A_1)$ , corner  $A_0$  lies in  $f(\mathcal{T})$  (using Lemma 7 or Lemma 9). Further since all LMAPs are inscribed (Fact 4.1),  $A_0 \in f(\mathcal{T}) \cap \partial P$ . Further according to REVERSIBILITY-OF-f, (i)  $A_0$  has a unique preimage in  $\mathcal{T}$  under f, which is  $f^{-1}(A_0)$ .

Because  $\mathbf{u}(A_3)$  is chasing  $\mathbf{u}(A_1)$ , we get  $(A_1, A_2, A_3) \in \mathcal{T}$  by Lemma 8. Because  $A_0A_1A_2A_3$  is a parallelogram,  $f(A_1, A_2, A_3) = A_0$ . Together, (ii)  $(A_1, A_2, A_3)$  is a preimage of  $A_0$  in  $\mathcal{T}$  under f. Combine (i) and (ii),  $(A_1, A_2, A_3) = f^{-1}(A_0)$ .

▶ Remark. 1. Lemma 8 establishes a strong connection between  $\mathcal{T}$  and the LMAPs. It implies that all LMAPs are almost contained in set  $\{X_1X_2X_3f(X_1,X_2,X_3) \mid (X_1,X_2,X_3) \in \mathcal{T}\}$ . But be aware of the existence of other LMAPs; for example, there could be an LMAP  $A_0A_1A_2A_3$  in which units  $\mathbf{u}(A_0), \mathbf{u}(A_2)$  are not chasing each other and so as  $\mathbf{u}(A_1), \mathbf{u}(A_3)$ . Nevertheless, it is safe to claim that set  $\mathcal{T}$  captures the crucial information of the LMAPs.

Due to this connection, the properties of  $\mathcal{T}$  under f (in Theorem 2) are of great value in understanding the LMAPs. For example, the Reversiblity-of-f are applied in deducing the new bounds of LMAPs in Lemma 10. From the Sector-Monotonicity, we see Lemma 9 reveals a monotone relation between two opposite corners of the LMAPs. It is surprisingly that such a relation is hidden in the relation  $\mathcal{T}$  which concerns the relation between three consecutive corners. This monotone relation is a key for analyzing our main algorithm below. We will also see the importance of the Sector-continuity in applying Lemma 9.

2. The new bounds in Lemma 9 and 10 are powerful in that they only require (the location information of) one corner to bound the others, whereas the previous bounds require two. Thus they open the door of designing the subquadratic time algorithm below. However, the drawback is that the new bounding regions  $\operatorname{sector}(\mathbf{u}(A_{i+2})) \cap \partial P$  and  $f^{-1}(A_0)$  are less accessible. In fact, our algorithm only needs a part of Lemma 9 and Lemma 10 – only when the fixed corner  $(A_{i+2})$  in Lemma 9 and  $A_0$  in Lemma 10) coincides a vertex, so we only need to compute  $\operatorname{sector}(V) \cap \partial P$  and  $f^{-1}(V)$  for each vertex V, yet this is still not so easy. The issue on calculating these bounding regions will be addressed later in this section.

Before sketching our main algorithm, we note some facts.

- (a) If some vertex V lies in f(T), it lies in a unique block and a unique sector. So, we can say "the block containing V" and "the sector containing V" and store their indices in O(1) space. (The index of block(u, u') is (u, u'), and the index of sector(w) is w.)
- (b) For each vertex V, the units intersected by sector(V) are consecutive and thus can be stored implicitly in O(1) space.
- (a) and (b) follow from the REVERSIBLITY-OF-f and SECTOR-CONTINUITY respectively.

We also note that there is a *preprocessing procedure* independent with our main algorithm, which is in charge of computing the following information:

For each vertex 
$$V$$
 of  $P$ , which block and sector does  $V$  lie in and which units are intersected by  $sector(V)$ ? (6)

This procedure is sketched later in Subsection 2.6 and here we assume that the information is given. Note that this information can be stored in O(n) space due to (a) and (b).

In the following, we always assume that  $A_0, A_1, A_2, A_3$  lie in clockwise order. We say a corner is anchored if it coincides a vertex of P. Our main algorithm consists of three routines, each of which computes a group of LMAPs that admit some special anchored corners.

**Routine 1.** This routine aims to compute those LMAPs  $A_0A_1A_2A_3$  in which  $A_0$  is anchored and  $\mathbf{u}(A_3)$  is chasing  $\mathbf{u}(A_1)$ ; see Figure 9 (a). It simply applies Lemma 10 as follows. First, enumerate a vertex V of P to be the position of  $A_0$ . Then, compute  $f^{-1}(V)$  and assign  $(A_1, A_2, A_3) = (f_1^{-1}(V), f_2^{-1}(V), f_3^{-1}(V))$ , and report  $A_0 A_1 A_2 A_3$ . Sometimes  $f^{-1}(V)$  is undefined (because  $V \notin f(\mathcal{T})$ ), and we ignore such V according to Lemma 10.1. The difficulty in this routine lies in computing  $f^{-1}(V)$ , for which we need the following lemma. Routine 1 runs in linear time (after the preprocessing) according to this lemma.

- ▶ Lemma 11. 1. Assume a point Y lies in  $f(\mathcal{T}) \cap \partial P$ . Then, (a)  $Y \in \mathsf{block}(u, u')$  is
- equivalent to  $[f_3^{-1}(Y) \in u, f_1^{-1}(Y) \in u']$ ; (b)  $Y \in \text{sector}(w)$  is equivalent to  $f_2^{-1}(Y) \in w$ . 2. Given a vertex V of P, we can determine whether  $V \in f(\mathcal{T})$  and compute  $f^{-1}(V)$  in O(1) time if we know "which block and sector V lies in."

(Hint of Claim 2: If  $V \in \mathsf{block}(u, u')$  and  $V \in \mathsf{sector}(w)$ , points  $f_1^{-1}(V), f_2^{-1}(V), f_3^{-1}(V)$ are respectively restricted to u', w, u due to Claim 1. Further since these points form a parallelogram with V, in O(1) extra time we can compute their positions. See Subsection 7.1.)

**Routine 2.** This routine aims to compute those LMAPs  $A_0A_1A_2A_3$  in which

- 1.  $A_0$  is anchored and  $\mathbf{u}(A_1)$  is chasing  $\mathbf{u}(A_3)$ ; meanwhile,
- **2.**  $A_1$  is anchored and  $\mathbf{u}(A_2)$  is chasing  $\mathbf{u}(A_0)$ . (See Figure 9 (b).)

Apparently, it will be more involved than Routine 1 since it computes some more complicated LMAPs. This routine consists of two steps. First, enumerate the positions of  $A_0$ ,  $A_1$ . To this end, we prove a relation between  $A_0$ ,  $A_1$  (as stated in Lemma 12.2 below) and enumerate all vertex pairs satisfying this relation. Second, compute the positions of  $A_2, A_3$ . Notice that the positions  $A_2$ ,  $A_3$  are uniquely determined given  $A_0$ ,  $A_1$ . Because  $A_0A_1A_2A_3$  is an inscribed parallelogram,  $\overline{A_2A_3}$  must be the unique chord of P that is a translation of  $\overline{A_0A_1}$  (other than  $\overline{A_0A_1}$  itself), which can be computed easily in  $O(\log^2 n)$  time by a binary search or in  $O(\log n)$  time by the tentative prune-and-search technique [20]. Yet we devise a more elegant and efficient subroutine for computing  $A_2, A_3$ . For any pair of  $(A_0, A_1)$ , we prove a unit interval which contains  $A_2$  and a unit interval which contains  $A_3$  (as stated in Lemma 12.1 below), and compute  $A_2, A_3$  in time proportional to the size of the two intervals. In this way, however, the accumulated time complexity over all pairs of  $(A_0, A_1)$  is  $\Omega(n^2)$  in the worst case. Nevertheless, it can be optimized by a common batch technique. Roughly, for any fixed vertex V, we can compute  $(A_2, A_3)$  for those pairs  $(A_0, A_1)$  in which  $A_0 = V$  in a batch, so that a monotonicity property of  $A_2, A_3$  with respect to  $A_1$  is utilized. The final running time is again linear (after the preprocessing). See the details in Subsection 7.2.

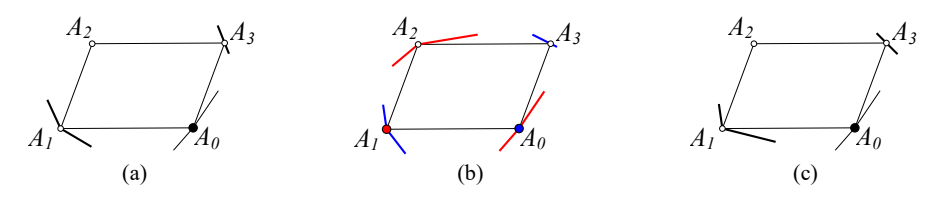


**Figure 9** Illustration of the targets of the three routines of our main algorithm.

Next, we describe the aforementioned relation between  $A_0, A_1$  and bounds on  $A_2, A_3$ . Some notation are required. For each vertex V of P, denote  $\mathbb{G}_V = \{u \mid u \text{ intersects sector}(V)\}$ ,

$$\mathbb{G}_V^- := \{u \in \mathbb{G}_V \mid V \text{ is chasing } u\}. \quad \psi_V^- := \bigcup_{u \in \mathbb{G}_V^-} \zeta(V, u).$$

$$\mathbb{G}_V^+ := \{u \in \mathbb{G}_V \mid u \text{ is chasing } V\}. \quad \psi_V^+ := \bigcup_{u \in \mathbb{G}_V^+} \zeta(u, V).$$

▶ Lemma 12. Assume  $A_0A_1A_2A_3$  is as above. We claim that

$$1.\mathbf{u}(A_2) \in \mathbb{G}_{A_0}^+, \mathbf{u}(A_3) \in \mathbb{G}_{A_1}^-; \quad and \quad 2.A_1 \in \psi_{A_0}^+, A_0 \in \psi_{A_1}^-.$$

Hint: These formulas simply follow from Lemma 9 and 6 (proved in Subsection 7.2).

For a better understanding of the above formulas, we state some basic observations on the new notation in the following. These observations follow from Sector-Monotonicity and Sector-Continuity in Theorem 2 and are stated more formally in Lemma 67.

- (i) For each vertex V, sets  $\mathbb{G}_V^-$  and  $\mathbb{G}_V^+$  consist of consecutive units,  $\psi_V^-$  and  $\psi_V^+$  are boundary-portions of P. So, each of them can be stored implicitly in O(1) space.
- (ii) The unit intervals  $\mathbb{G}_{v_1}, \dots, \mathbb{G}_{v_n}$  lie in clockwise order and are *almost-disjoint* (see details in Lemma 67.) Array  $\mathbb{G}^+$  and  $\mathbb{G}^-$  have the same monotonicity property as  $\mathbb{G}$ .
- (iii)  $\psi_{v_1}^-, \ldots, \psi_{v_n}^-$  are pairwise-disjoint (neighboring elements may share a common endpoint) and lie in clockwise order on  $\partial P$ . Array  $\psi^+$  has the same monotonicity property as  $\psi^-$ .

These observations are crucial for analyzing the running time of our algorithm. By (iii), only O(n) vertex pairs satisfies the relation in Lemma 12.2. By (ii), the sizes of the bounding intervals on  $\mathbf{u}(A_2)$ ,  $\mathbf{u}(A_3)$  given in Lemma 12.1 have a small accumulated complexity.

▶ Remark. Thus far we have sketched two most important routines of our main algorithm, from which we can see our improvement essentially comes from applications of the non-trivial properties of  $\mathcal{T}$ . Routine 1 is simply based on Lemma 10, which is a corollary of the REVERSIBLITY-OF-f. The efficiency of Routine 2 relies on the monotonicities of  $\mathbb{G}^-$ ,  $\mathbb{G}^+$ ,  $\psi^-$ ,  $\psi^+$  stated in (ii) and (iii), which are derived from the Sector-Monotonicity.

As a comparison, Routine 1 first enumerates a vertex and then locates it among the blocks and sectors, whereas the previous algorithm first enumerates a block and then queries all vertices inside the block. This striking diversity leads to the different efficiency.

Routine 3. This routine aims to compute those LMAPs  $A_0A_1A_2A_3$  in which  $A_0$  is anchored and  $\mathbf{u}(A_3)$ ,  $\mathbf{u}(A_1)$  are not chasing each other; see Figure 9 (c). Our algorithm for this routine is similar to that for Routine 2 in that it first determines two adjacent anchored corners and then computes the other two. One major difference is that it does not preprocess anything and does not apply any properties of  $f(\mathcal{T})$ . Another is that it applies different bounds of the LMAPs – yet these bounds have the same spirit as the previous bounds in Lemma 6. Specifically, Lemma 6 bounds  $A_i$  by  $\zeta(\mathbf{u}(A_{i+1}),\mathbf{u}(A_{i-1}))$  when  $\mathbf{u}(A_{i+1})$  is chasing  $\mathbf{u}(A_{i-1})$ , whereas the new bounds (Lemma 71) constrain  $A_i$  when  $\mathbf{u}(A_{i+1})$ ,  $\mathbf{u}(A_{i-1})$  are not chasing each other. Correspondingly, we have to extend the scope of definition of  $\zeta(u, u')$  (see (2)) to every pair of distinct units u, u'; this will be shown in Subsection 7.3. The running time of Routine 3 is  $O(n \log n)$ . However, by an intricate optimization, in which we apply the bounds on the LMAPs much more subtly, the running time can be reduced to O(n). We omit this optimization in this version since it does not effect the final running time.

The above three routines are sufficient for computing all LMAPs (see Lemma 66). So,

▶ **Theorem 13.** Given an n-sided convex polygon P and the information in (6), we can compute the LMAPs in P in  $O(n \log n)$  time (or even in O(n) time).

## 2.4 Introduction of bounding-quadrants for the blocks

In order to prove the properties of  $\mathcal{T}$  (Theorem 2) and compute the information (6), we have to first introduce another type of regions, which are quadrants in the plane and which are mainly used for bounding the blocks and are thus called **bounding-quadrants**. Moreover, associated with each such quadrant  $\mathsf{quad}_i^j$ , we introduce a boundary-portion  $\langle \mathsf{quad} \rangle_i^j$ .

▶ **Definition 14.** Notice that each edge is a boundary-portion and is directed; the direction of  $e_i$  is from  $v_i$  to  $v_{i+1}$ . Assume  $e_i \leq e_j$ . Let M denote the mid point of  $v_i$  and  $v_{j+1}$ .

Case1:  $e_i \prec e_j$ ; see Figure 10 (a). Make two rays at M, one with the opposite direction to  $e_j$  while the other with the same direction as  $e_i$ . Denote by  $quad_i^j$  the **open** region bounded by these two rays, and denote by  $\langle quad \rangle_i^j$  the intersection between  $quad_i^j$  and  $\partial P$ .

Case2:  $e_i = e_j$ ; see Figure 10 (b). Denote by  $\mathsf{quad}_i^j$  the  $\mathsf{open}$  half-plane that is bounded by the extended line of  $e_i$  and lies to the left of  $e_i$ , and denote by  $\langle \mathsf{quad} \rangle_i^j$  the midpoint of  $e_i$ . We regard the half-plane  $\mathsf{quad}_i^i$  as a special quadrant whose apex lies at the midpoint of  $e_i$ ; therefore, all the regions in  $\{\mathsf{quad}_i^j \mid e_i \leq e_j\}$  are quadrants in the plane.

The regions in  $\{\langle \mathsf{quad} \rangle_i^j \mid e_i \leq e_j \}$  are boundary-portions of P. In particular,  $\langle \mathsf{quad} \rangle_i^j$  is a single point when  $e_i = e_j$ . Notice that  $\langle \mathsf{quad} \rangle_i^j$  always contains  $\mathsf{quad}_i^j \cap \partial P$  for  $e_i \leq e_j$ .

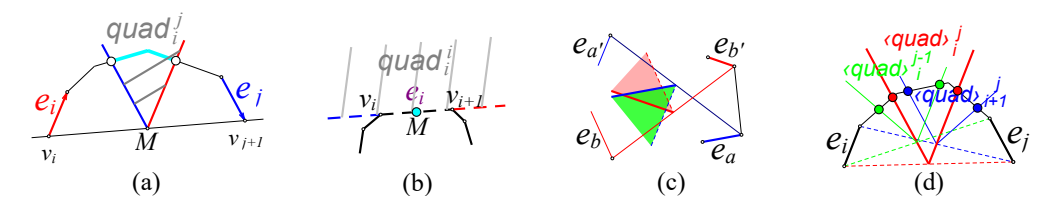


**Figure 10** Definition and two properties of the bounding-quadrants.

We state the following four properties of the bounding-quadrants below and prove them in Subsection 3.3. Recall that  $[v_i \circlearrowright v_{j+1}]$  is called an *inferior portion* when  $e_i \leq e_j$ .

▶ Lemma 15 (A peculiar property of quad). For any four edges  $e_a, e_{a'}, e_b, e_{b'}$  such that  $e_a \leq e_{a'}, e_b \leq e_{b'}$  and that  $e_a, e_{a'}, e_b, e_{b'}$  are not contained in any inferior portion, the intersection region  $\operatorname{quad}_b^{a'} \cap \operatorname{quad}_b^{b'}$  lies in the interior of P, as illustrated in Figure 10 (c).

For any boundary-portion  $\gamma$ , denote its starting and terminal point by  $\gamma.s$  and  $\gamma.t$ .

▶ Lemma 16 (Monotonicity of  $\langle \text{quad} \rangle$ ). See Figure 10 (d). Assume  $e_i \prec e_j$ . Let  $\rho = [v_i \circlearrowright v_{j+1}]$ . Recall that  $\leq_{\rho}$  denotes the clockwise order among the points in  $\rho$ . We claim that

$$(\langle \mathsf{quad} \rangle_i^{j-1}).s \leq_{\rho} (\langle \mathsf{quad} \rangle_i^j).s \leq_{\rho} (\langle \mathsf{quad} \rangle_{i+1}^j).s, (\langle \mathsf{quad} \rangle_i^{j-1}).t \leq_{\rho} (\langle \mathsf{quad} \rangle_i^j).t \leq_{\rho} (\langle \mathsf{quad} \rangle_{i+1}^j).t.$$

For unit pair (u, u') such that u is chasing u', we know  $forw(u) \leq back(u')$  and denote

$$\operatorname{quad}_{u}^{u'} = \operatorname{quad}_{forw(u)}^{back(u')}, \quad \langle \operatorname{quad} \rangle_{u}^{u'} = \langle \operatorname{quad} \rangle_{forw(u)}^{back(u')}. \tag{7}$$

- ▶ Lemma 17 (Connection between blocks and their corresponding bounding-quadrants). Assume unit u is chasing unit u'. Then,  $\mathsf{block}(u,u')$  is contained in  $\mathsf{quad}_u^{u'}$ . (Note that  $\mathsf{quad}_u^{u'}$  is always open and so the block cannot intersect the boundary of the quadrant.)
- ▶ Lemma 18 (Monotonicity of the borders of blocks). Recall that the borders of blocks are directional; see the illustrations in Figure 7. Suppose some point X travels along some border of  $\operatorname{block}(u,u')$  (in its positive direction) and suppose we stand both in P and in the opposite quadrant of  $\operatorname{quad}_{u'}^{u'}$ . Then, X travels in clockwise order (strictly) around us.

# **2.5** Sketched proofs for the six properties of f(T)

In this subsection, we sketch the proof of Theorem 2. The proof is given in Section 4 and 5. First, we sketch the proof of Block-disjointness and Interleavity-of-f. We point out that these two properties are strongly connected and their proofs are analogous.

Given  $(e_c, e_{c'})$  such that  $e_c \prec e_{c'}$ , this edge pair is said *extremal* if the inferior portion  $[v_c \circlearrowright v_{c'+1}]$  is **not** contained in other inferior portions. For extremal pair  $(e_c, e_{c'})$ , denote

$$\Delta(c,c') := \left\{ (u,u') \mid \begin{array}{c} \text{unit } u \text{ is chasing } u', \text{ and} \\ forw(u), back(u') \in \{e_c, e_{c+1}, \dots, e_{c'}\} \end{array} \right\}.$$

**Proof sketch of Block-disjointness**. Two blocks  $\mathsf{block}(u, u')$  and  $\mathsf{block}(v, v')$  is a **local pair** if the four edges forw(u), back(u'), forw(v), back(v') are contained in an inferior portion; and a **global pair** otherwise. The Block-disjointness follow from:

- (I) For a global pair block(u, u'), block(v, v'), the block intersection lies in the interior of P.
- (II) For a local pair block(u, u'), block(v, v'), the block intersection is always empty.

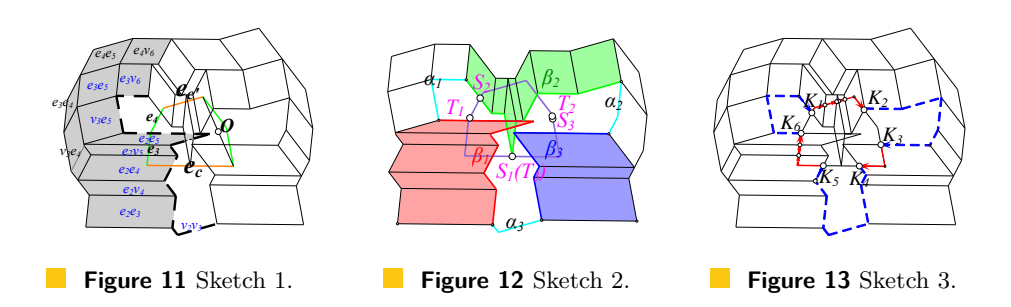
We employ the bounding-quadrants to prove (I). By Lemma 15, if the blocks is a global pair,  $\operatorname{\mathsf{quad}}_{forw(u)}^{back(u')}\cap\operatorname{\mathsf{quad}}_{forw(v)}^{back(v')}$  lies in the interior of P. Moreover, by Lemma 17,  $\operatorname{\mathsf{block}}(u,u')\cap\operatorname{\mathsf{block}}(v,v')\subset\operatorname{\mathsf{quad}}_u^{u'}\cap\operatorname{\mathsf{quad}}_v^{v'}=\operatorname{\mathsf{quad}}_{forw(u)}^{back(u')}\cap\operatorname{\mathsf{quad}}_{forw(v)}^{back(v')}$ . Together, we get (I). We can restated (II) as follows: For every extremal pair  $(e_c,e_{c'})$ , the blocks in  $\{\operatorname{\mathsf{block}}(u,u')\mid (u,u')\in\Delta(c,c')\}$  (see Figure 11) are pairwise-disjoint. Interesting, the monotonicity of the borders stated in Lemma 18 somehow implies this argument. The proof is based on an induction.  $\blacktriangleleft$ 

We say a directed curve  $\mathcal{D}$  interleaves  $\partial P$ , if it is disjoint with  $\partial P$  or the following holds. Starting from their first intersection point (according to the order among points in  $\mathcal{D}$ ), regardless of whether we travel along  $\mathcal{D}$  in its positive direction or along  $\partial P$  in clockwise, we would encounter the intersection points between  $\mathcal{D}$  and  $\partial P$  in the same order.

**Proof sketch of Interleavity-of-**f. As in the above proof, we have a local and a global case in this proof. Locally, we argue that every local fraction of  $\sigma P$  (see  $\sigma(c_i, c_i')$  below) interleaves  $\partial P$ . Globally, we argue that all these local fractions are well-scattered around  $\partial P$ . The proving technique is basically the same as above; the local case is taken care of by the monotonicity of the borders, whereas the global case by the properties of bounding-quadrants.

Let q be the number of extremal pairs. See Figure 12. First, we cut  $\sigma P$  into 2q well-defined fragments  $\beta_1, \alpha_1, \ldots, \beta_q, \alpha_q$  (see their definitions below) satisfying that

- (i) For  $1 \leq i \leq q$ , the concatenation of  $\alpha_{i-1}, \beta_i, \alpha_i$  interleaves  $\partial P$ .  $(\alpha_0 = \alpha_q)$ . Second, we find 2q (well-defined) points  $S_1, T_1, \ldots, S_q, T_q$  lying in clockwise order around  $\partial P$ , which "delimitate" the 2q fragments, by which we mean that
- (ii) For  $1 \le i \le q$ , the intersections between  $\beta_i$  and  $\partial P$  are contained in  $[S_i \circlearrowright T_i]$ ; and
- (iii) For  $1 \le i \le q$ , the intersections between  $\alpha_i$  and  $\partial P$  are contained in  $[S_i \circlearrowright T_{i+1}]$ .



Last, we argue that if there exist 2q fragments satisfying the above three properties, their concatenation interleaves  $\partial P$  (this is rather easy to prove). Therefore,  $\sigma P$  interleaves  $\partial P$ .

We define the 2q fragments as follows. For every extremal pair  $(e_c, e_{c'})$ , let  $\sigma(c, c')$  be the concatenation of the "bottom borders" of the "frontier blocks" (see their definitions in Section 3.4 where we define  $\sigma P$ ) in  $\{\operatorname{block}(u, u') \mid (u, u') \in \Delta(c, c')\}$ ; this is illustrated by the dotted polygonal curve in Figure 11. Let  $(e_{c_1}, e_{c'_1}), \ldots, (e_{c_q}, e_{c'_q})$  be an enumeration of all extremal pairs in clockwise order. We define  $\alpha_i$  to be  $\sigma(c_i, c'_i) \cap \sigma(c_{i+1}, c'_{i+1})$ ; and  $\beta_i$  to be  $\sigma(c_i, c'_i) - \alpha_{i-1} - \alpha_i$ . Note that the concatenation of  $\alpha_{i-1}, \beta_i, \alpha_i$  equals  $\sigma(c_i, c'_i)$ . Following this definition, (i) easily follow from the monotonicity of the borders in Lemma 18.

The 2q points  $S_1, T_1, \ldots, S_q, T_q$  are chosen from particular endpoints of the portions in  $\{\langle \mathsf{quad} \rangle_i^j \}$  so that (ii) and (iii) may be deduced from the monotonicity of these portions.

**Proof sketch of Reversiblity-of**-f. For each unit pair (u, u') such that u is chasing u', let  $\mathcal{T}(u, u') = \{(X_1, X_2, X_3) \in \mathcal{T} \mid X_3 \in u, X_1 \in u'\}$  and call it a *component* of  $\mathcal{T}$ . It can easily be proved that (X) f is a bijection from  $\mathcal{T}(u, u')$  to  $\mathsf{block}(u, u') = f(\mathcal{T}(u, u'))$ .

For two elements in  $\mathcal{T}^*$ , if they belong to the same component, their images under f differ according to (X); Otherwise, there images differ because otherwise there exist two blocks intersecting on the boundary of P, which contradicts the BLOCK-DISJOINTNESS.

**Proof sketch of Monotonicity-of-**f . See Figure 13. Let  $K_1, \ldots, K_m$  denote all the intersections between  $\sigma P$  and  $\partial P$ , and assume that they lie in clockwise order around  $\partial P$ . Points  $K_1, \ldots, K_m$  divide  $\partial P$  into m portions; and we call each of them a K-portion. We state:

- (i) The outer boundary of  $f(\mathcal{T})$  is a simple closed curve whose interior contains P.
- (ii) Points  $f_2^{-1}(K_1), \ldots, f_2^{-1}(K_m)$  lie in clockwise order around  $\partial P$ .
- (iii) Function  $f_2^{-1}$ () is monotone on any K-portion that lies in  $f(\mathcal{T})$ .
  - (i) and (ii) are easy and their proofs are not sketched here. To prove (iii), we consider the reverse function of  $f: \mathcal{T}(u,u') \to \mathsf{block}(u,u')$ , which can be defined due to (X) and is denoted by  $f_{u,u'}^{-1}$ . We prove a monotonicity of the second dimension of  $f_{u,u'}^{-1}$ , which implies that  $f_2^{-1}()$  is monotone on any boundary-portion inside  $\mathsf{block}(u,u')$ , which implies (iii).

Combining (i) with the INTERLEAVITY-OF-f, we see that a K-portion either lies in or lies entirely outside  $f(\mathcal{T})$ . Now, imagine that a point X is traveling around  $f(\mathcal{T}) \cap \partial P$  in clockwise; argument (iii) assures that  $f_2^{-1}(X)$  is monotone inside each K-portion, and (ii) assures that it is monotone between the K-portions. This is illustrated in Figure 13.

Since  $\operatorname{sector}(w) \cap \partial P = \{Y \in f(\mathcal{T}) \cap \partial P \mid \mathbf{u}(f_2^{-1}(Y)) = w\}$ , the Sector-monotonicity is a simple consequence of the Monotonicity-of-f. See the proof in Section 4.

The interconnections between the first five properties are illustrated in Figure 14.

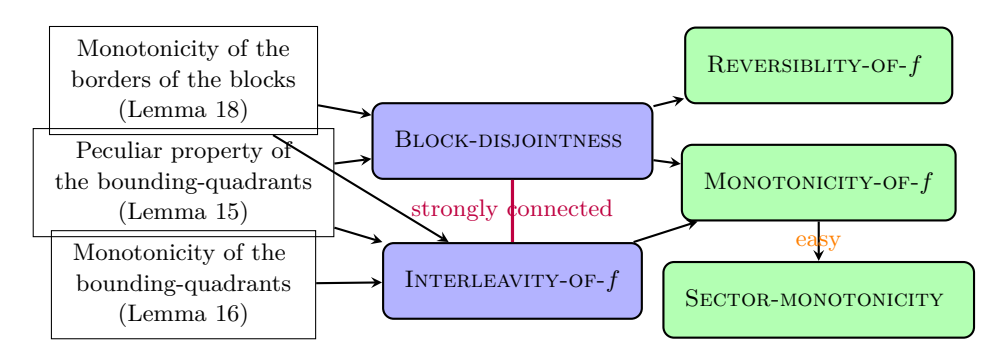


**Figure 14** Interconnections between the five properties. The last property Sector-Continuity is independent with the other five and is not drawn here.

# Sketch: Proof of Sector-continuity

Assume V is a fixed vertex of P. In the following, we depict the shape of sector(V) and define its two boundaries, and then sketch the proof of Sector-Continuity.

We first state a new formula of sector(V). Recall " $\oplus$ " in the remark of (4). Applying definition (3) into (5), which states  $sector(V) := f(\{(X_1, X_2, X_3) \in \mathcal{T} \mid X_2 \in V\})$ , we get

$$\mathsf{sector}(V) = 2\text{-scaling of}\left(\bigcup_{u \text{ is chasing } u', \text{ and } \zeta(u, u') \text{ contains } V} u \oplus u'\right) \text{ w.r.t } V. \tag{8}$$

Denote  $\Lambda_V := \{(u, u') \mid u \text{ is chasing } u', \text{ and } \zeta(u, u') \text{ contains } V\}$ . Based on (8), it is important to study the structure of  $\Lambda_V$  in order to study sector(V). We introduce some symbols in the next and then describe the simple structure of  $\Lambda_V$  in (iii).

There are two key symbols,  $e_{sV}$  and  $e_{tV}$ , called **delimiting edges**, which are well-defined for the fixed V. In this sketch, however, we omit their definitions (given in Section 5.1; useless for getting the main idea) but only state the following facts. Abbreviate  $s_V, t_V$  as s, t.

- (i)  $e_s \leq e_t$ . Moreover, the inferior portion  $[v_s \circlearrowright v_{t+1}]$  does not contain V.
- (ii) If  $(u, u') \in \Lambda_V$ , units u, u' both lie in  $[v_s \circlearrowright v_{t+1}]$ . (This suggests the name "delimiting".)

In addition, there is a symbol  $\Delta_V$  associated with s,t. Notice that there is an order '<' (short for  $<_{s,t}$ ) among the units in  $[v_s \circlearrowright v_{t+1}]$  conforming to the clockwise order. Denote  $\Delta_V = \{(u,u') \mid u,u' \in [v_s \circlearrowright v_{t+1}], u < u', \text{and they are not incident}\}.$ 

By (ii),  $\Lambda_V$  is a subset of  $\Delta_V$ . This is further strengthened to (iii) (stated in Fact 49).

- (iii)  $(u, u') \in \Lambda_V$  if and only if  $(u, u') \in \Delta_V$  and  $u \oplus u' \subseteq \mathsf{mid}_V$  and u is chasing u', where  $\mathsf{mid}_V$  is a union of some regions in  $\{u \oplus u' \mid (u, u') \in \Delta_V\}$  defined below.
- roads & routes. See Figure 15 (a). Since  $e_s \leq e_t$ , the regions in  $\{u \oplus u' \mid (u, u') \in \Delta_V\}$  are pairwise-disjoint. See Figure 15 (b). For any  $(e_i, v_j) \in \Delta_V$ , we assume segment  $e_i \oplus v_j$  has the same direction as  $e_i$ ; for any  $(v_i, e_j) \in \Delta_V$ , we assume segment  $v_i \oplus e_j$  has the opposite direction to  $e_j$ ; and we refer to these segments as **roads**. See Figure 15 (c). By concatenating several roads, we can obtain directional polygonal curves starting from the mid point of  $v_s, v_{t+1}$  until some point in  $[v_s \circlearrowright v_{t+1}]$ ; such curves are called **routes**.
- $\mathcal{L}_V, \mathcal{R}_V$ . Denote  $\rho = [v_{t+1} \circlearrowright v_s]$ . For any edge pair  $(e_i, e_j)$  in  $\Delta_V$ , we mark region  $e_i \oplus e_j$  by '-' if  $Z_i^j <_{\rho} V$ ; '+' if  $V <_{\rho} Z_i^j$ ; and '0' if  $V = Z_i^j$ . By the bi-monotonicity of the Z-points (Lemma 6 in [15]; Fact 22), there exists a unique route,  $\mathcal{L}_V$ , which separates the regions marked by '-' from the regions marked by '+' from the regions marked by '-'0'.
- $\operatorname{\mathsf{mid}}_V$ . According to the definitions of  $\mathcal{L}_V, \mathcal{R}_V$  and bi-monotonicity of the Z-points, the region bounded by  $\mathcal{L}_V, \mathcal{R}_V$  and  $\partial P$  is well-defined (see Figure 15 (f)) and is denoted by  $\operatorname{\mathsf{mid}}_V$ . To be more clear, we consider  $\operatorname{\mathsf{mid}}_V$  contains its two boundaries  $\mathcal{L}_V$  and  $\mathcal{R}_V$ .

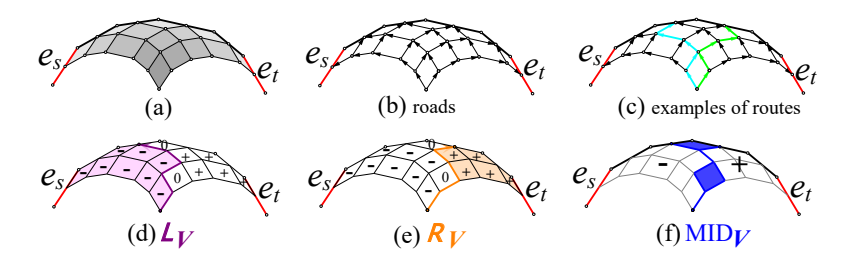


**Figure 15** Illustration of the definition of curves  $\mathcal{L}_V$ ,  $\mathcal{R}_V$  and region  $\mathsf{mid}_V$ .

Note: (i), (ii), and (iii) are formally stated in Fact 44, Fact 45, and Fact 49.

**Note:** For the special case s = t, we define  $\mathcal{L}_V = \mathcal{R}_V = \mathsf{mid}_V = v_s \oplus v_{t+1}$ .

Now, denote the 2-scaling of  $\operatorname{mid}_V, \mathcal{L}_V, \mathcal{R}_V$  with respect to V by  $\operatorname{mid}_V^{\star}, \mathcal{L}_V^{\star}, \mathcal{R}_V^{\star}$  respectively. Combining (8) and (iii), we see  $\operatorname{sector}(V)$  is (roughly) the same as  $\operatorname{mid}_V^{\star}$ . More rigorously, the closed set of  $\operatorname{sector}(V)$  equals  $\operatorname{mid}_V^{\star}$ . Therefore, regions  $\operatorname{mid}_V^{\star}$  and  $\operatorname{sector}(V)$  have the same boundaries, so  $\mathcal{L}_V^{\star}, \mathcal{R}_V^{\star}$  are boundaries of  $\operatorname{sector}(V)$ . (See details in Lemma 50.)

Furthermore, we observe that either of  $\mathcal{L}_V^\star, \mathcal{R}_V^\star$  has at most one intersection with  $\partial P$ , and thus prove  $\mathsf{mid}_V^\star = [\mathcal{L}_V^\star \cap \partial P \circlearrowleft \mathcal{R}_V^\star \cap \partial P]$ . Further since the closed set of  $\mathsf{sector}(V)$  equals  $\mathsf{mid}_V^\star$ , we get that  $\mathsf{sector}(V) \cap \partial P$  is a boundary-portion which starts at  $\mathcal{L}_V^\star \cap \partial P$  and terminates at  $\mathcal{R}_V^\star \cap \partial P$ , thus prove the Sector-continuity. (See details in Lemma 51.)

▶ Remark. Although the particular values of s, t are of no use for understanding the high-level idea of the proof and the general shape of  $\operatorname{sector}(V)$ , the formal definitions of s, t omitted above are cornerstones for the proof. Arguments (i)-(iii) depend directly on these definitions.

# 2.6 Sketched algorithms for computing the information (6)

In this subsection, we sketch how we prove the following result. Details are given in Section 6.

- ▶ **Theorem 19.** In  $O(n \log^2 n)$  time, we can compute the information (6).
- 1. Compute the endpoints of  $\operatorname{sector}(V) \cap \partial P$  for a given vertex V. According to the proof sketch of Sector-Continuity above, it reduces to computing  $\mathcal{L}_V^{\star} \cap \partial P$  and  $\mathcal{R}_V^{\star} \cap \partial P$ . Recall that either of  $\mathcal{L}_V^{\star}, \mathcal{R}_V^{\star}$  is a polygonal curve and has at most one intersection with  $\partial P$ , as shown in Figure 8. Moreover, it is not difficult to generate an arbitrary edge of  $\mathcal{L}_V^{\star}$  (or  $\mathcal{R}_V^{\star}$ ), and in  $O(\log n)$  time decide whether it lies inside, outside, or intersects P. Therefore, we can compute  $\mathcal{L}_V^{\star} \cap \partial P$  (or  $\mathcal{R}_V^{\star} \cap \partial P$ ) by a binary search in  $O(\log^2 n)$  time.
- 2. Compute the units that intersect  $\operatorname{sector}(V)$  for a given vertex V. By Sector-Continuity, the units that intersect  $\operatorname{sector}(V)$  are (almost in every case) the units from  $u_L$  to  $u_R$  in clockwise order (a degenerated case is discussed in Section 6), where  $u_L, u_R$  are respectively the unit containing  $\mathcal{L}_V^* \cap \partial P$  and the unit containing  $\mathcal{R}_V^* \cap \partial P$ , which can be easily computed when we compute  $\mathcal{L}_V^* \cap \partial P$  and  $\mathcal{R}_V^* \cap \partial P$ .
- 3. Compute the respective sectors that contain each vertex. We introduce two groups of event-points: the points in  $\{\mathcal{L}_V^{\star} \cap \partial P, \mathcal{R}_V^{\star} \cap \partial P \mid V \text{ is a vertex of } P\}$ , and the intersections between  $\sigma P$  and  $\partial P$ . Notice that all the event-points lie in  $\partial P$ . Then, two tags, current-tag and future-tag, are assigned to each event-point; the former one denotes the sector containing this event-point; the latter one denotes the sector containing the boundary-portion that starts at this event-point and terminates at its (clockwise) next event-point. By a sweeping around  $\partial P$ , we determine the sector containing each vertex by using these tags.
- **4.** Compute the block containing V for a given vertex V. Assume V lies in sector(w) and w is known. Let  $block(u_1^*, u_2^*)$  denote the block containing V; we shall compute  $(u_1^*, u_2^*)$ .

```
Let [X \circlearrowleft X'] denote [X \circlearrowleft X'] - \{X'\}, and (X \circlearrowleft X'] denote [X \circlearrowleft X'] - \{X\}.
```

First, we compute two **delimiting edges**  $e_{p_V}$ ,  $e_{q_V}$  (well-defined on V) ( $p_V$ ,  $q_V$  are abbreviated as p,q). By their definitions (see Section 6.3), we can prove that

- (i)  $e_p \prec e_q$ . Moreover, the boundary-portion  $(v_p \circlearrowright v_{q+1})$  contains V.
- (ii)  $u_1^* \in [v_p \circlearrowright V)$ , and  $u_2^* \in (V \circlearrowright v_{q+1}]$ . (This suggests the name "delimiting".)

For any unit pair (u, u') such that u is chasing u', we regard it as *alive*, if it satisfies (ii); in other words, if  $u \in [v_p \circlearrowright V)$  and  $u' \in (V \circlearrowleft v_{q+1}]$ .

Moreover, for any alive pair (u, u'), we regard it as active if  $\zeta(u, u')$  intersects w.

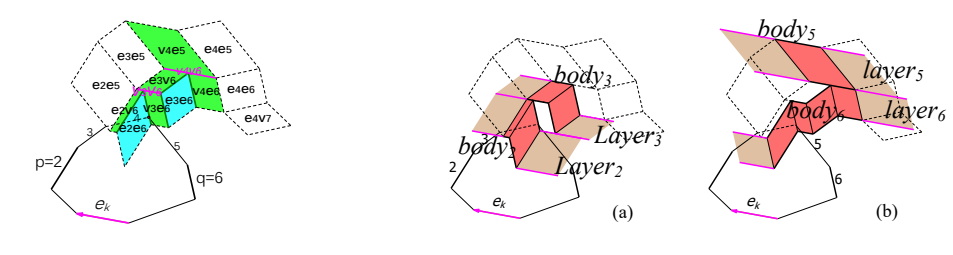


Figure 16 "active" and cells.

**Figure 17** Illustration of layers.

For an illustration, Figure 16 draws all alive pairs, in which the active ones are colored. By (ii) and the assumption that  $V \in \operatorname{sector}(w)$ , we know  $(u_1^*, u_2^*)$  is active, so we only need to search  $(u_1^*, u_2^*)$  among the active pairs. Next, we discuss two cases depending on whether w is an edge or a vertex. The edge case is more typical; assume now  $w = e_k$ . To describe the algorithm, two types of regions, *cells* and *layers*, are introduced here.

**Cells.** For each active pair (u, u'), define a region  $\operatorname{cell}(u, u') := \operatorname{block}(u, u') \cap \operatorname{sector}(w)$ .

**Layers.** For each edge  $e_j$  in  $(v_p \circlearrowright v_{q+1})$ , we define a region layer<sub>j</sub>, which contains all the cells parallel to  $e_j$ , and two more infinite strip region parallel to  $e_k$  as shown Figure 17.

Algorithm for computing  $u_1^*, u_2^*$  (overview). We prove a monotonicity between the cells within the same layer and a monotonicity between the different layers. Based on these monotonicities, in  $O(\log n)$  time we can determine the relative position between any layer and V. So, in  $O(\log^2 n)$  time we find the layer that contains V. Then, in another  $O(\log n)$  time we find the cell containing V, which must be  $\text{cell}(u_1^*, u_2^*)$ . Thus we obtain  $(u_1^*, u_2^*)$ .

▶ Remark. This last module for computing the block containing V is highly **symmetric** to the first module for computing the endpoints of  $sector(V) \cap \partial P$ . First, the "cells" and "layers" are counterparts of the "roads" and "routes". (In fact, the roads have two different types and so do the layers.) Second, both run in  $O(\log^2 n)$  time. Third, the biggest challenges in designing these modules both lie in defining the delimiting edges  $e_s, e_t$  and  $e_p, e_q$ , and all the indices s, t, p, q can be computed in  $O(\log n)$  time. This symmetry suggests that if one module can be optimized to  $O(\log n)$  time, the other may also be optimized.

The delimiting edges  $e_s$ ,  $e_t$  are used to delimit those pairs of units (u, u') for which  $\zeta(u, u')$  may contain V, whereas  $e_p$ ,  $e_q$  delimit those pairs for which  $\mathsf{block}(u, u')$  may contain V. The tricky definitions of s, t and p, q are given in Section 5.1 and Section 6.3. To define p, q, we have to apply the bounding quadrants of the blocks and their properties stated in Section 2.4.

# 2.7 Summary

▶ **Theorem 20** (Main result). Given an n-sided convex polygon P, all the LMAPs in P can be computed in  $O(n \log^2 n)$  time. Moreover, there number of LMAPs is bounded by O(n).

**Proof.** The first claim is a corollary of Theorem 13 and Theorem 19. The number of LMAPs is O(n) because each of the three routines outputs O(n) parallelograms (see the details in Section 7). (Note that [15] proves an interesting property of the LMAPs in P, which states that all of them interleave each other, which immediately implies the second claim.)

A summary of our algorithmic technique. In this paper, we elucidate a subquadratic time algorithm that is based on  $\Theta(n^2)$  bounds in Lemma 6. One one side, we identify  $\Theta(n)$ -space key information (6) hidden in these bounds, by which we can compute all the LMAPs in  $O(n \log n)$  (or even in  $\Theta(n)$ ) time. On the other side, the inner structure of the  $\Theta(n^2)$  bounds

(implied by the structural properties of  $f(\mathcal{T})$ ) enables us to extract the key information in  $O(n\log^2 n)$  time without checking every bound. The general principle of this algorithmic optimization technique may find applications in other related problems.

A summary of  $\operatorname{Nest}(P)$ . We show that each convex polygon P is accompanied with a "subdivision"  $\operatorname{Nest}(P)$ , who has a nice interaction with P as demonstrated by Theorem 2. (Rigorously,  $\operatorname{Nest}(P)$  is **not** a subdivision over the plane, because it may intersect itself as shown in Figure 1, but is a subdivision over the exterior of P due to the BLOCK-DISJOINTNESS.) This structure is **not** applied directly in our algorithm, yet is helpful for understanding its high-level picture, which in one word says that our geometric optimization problem on P is reduced to answering some point-location (or intersection-location) queries on  $\operatorname{Nest}(P)$ .

A slightly modification of Nest(P). Recall that Nest(P) is the union of the boundaries of all blocks and  $\mathcal{L}_{v_1}^{\star}, \ldots, \mathcal{L}_{v_n}^{\star}$  and  $\mathcal{R}_{v_1}^{\star}, \ldots, \mathcal{R}_{v_n}^{\star}$  (given in Section 5), where  $\mathcal{L}_{V}^{\star}, \mathcal{R}_{V}^{\star}$  are 2-scalings of  $\mathcal{L}_{V}, \mathcal{R}_{V}$  with respect to V, and where  $\mathcal{L}_{V}, \mathcal{R}_{V}$  consist of several roads (see Subsection 2.5). Previously we assume road  $e_i \oplus v_j$  has the same direction as  $e_i$ , whereas road  $v_i \oplus e_j$  has the **opposite** direction to  $e_j$ . This is convenient for proving the Sector-Continuity. However, when defining Nest(P), it is more reasonable to assume that  $v_i \oplus e_j$  has the **same** direction as  $e_i$ . Only in this way, the last property of Nest(P) claimed above Figure 2 holds.

**Summary and open problems.** The bottleneck of our algorithm lies in the preprocessing procedure, in particular, in its first and forth modules. However, this procedure is amendable for being parallelized – we can use n processors to solve the  $\Theta(n)$  location queries. In the future, it remains to study whether these two modules can be improved to  $O(\log n)$  time.

In our opinion, the discovery of Nest(P) and the proof of its properties are our major contributions. Some previous reviewers also commented that Nest(P) is as beautiful and interesting as some well-known geometric structures like the Voronoi Diagrams and Zonotopes. A natural problem is that can it find more applications (perhaps in some other disciplines like turbine design, art design, or physics)? In addition, can we construct a space subdivision associated with a three dimensional convex polyhedron similar to Nest(P)?

Organization the following paper. Section 3 investigates the Z-points, blocks, bounding-quadrants of blocks, and inner boundary  $\sigma P$ . Section 4 proves the first five properties of  $f(\mathcal{T})$ . Section 5 proves the last one - the Section-Continuity. Section 6 presents the preprocessing procedure for computing (6). Section 7 presents the main algorithm for computing the LMAPs. The last two sections are independent and can be read in any order.

## Frequently used notation.

- Denote by  $e_i \not\prec e_j$  if  $e_i$  is not chasing  $e_j$ .
- $\blacksquare$  Denote by M(A, B) the mid point of A, B.
- Denote by  $D_i$  the unique vertex of P with largest distance to  $\ell_i$ . The uniqueness follows from the pairwise-nonparallel assumption of edges.
- Denote by  $I_{i,j}$  the intersection of  $\ell_i$  and  $\ell_j$ .
- When a point X lies in  $\partial P$ , we define its backward and forward edge of X:

$$back(X) := back(\mathbf{u}(X)); \quad forw(X) := forw(\mathbf{u}(X)).$$

■ In most cases, the Greek symbols are applied for denoting the boundary-portions of P. Recall that the starting and terminal point of  $\rho$  are denoted by  $\rho$ .s and  $\rho$ .t, respectively.

20

# **3** Z-points, blocks, bounding-quadrants, and the inner boundary $\sigma P$

In this section, we prove basic properties of the Z-points, blocks (as well as borders of the blocks), and bounding-quadrants, and establish various connections between these objects. Moreover, we define  $\sigma P$  (i.e. the inner boundary of  $f(\mathcal{T})$ ) explicitly and introduce a function  $g: \sigma P \to \partial P$ . All of these are preliminaries for the proof of Theorem 2.

Recall the Z-points in Definition 1.

- ▶ Fact 21 ([15]). 1. Point  $Z_i^j$  lies in  $[\mathsf{D}_i \circlearrowright \mathsf{D}_j]$  and  $(v_{j+1} \circlearrowright v_i)$ .
- **2.** If  $Z_i^j$  lies in some edge  $e_k$ , it lies at the mid point of  $I_{i,k}$  and  $I_{j,k}$ .
- ▶ Fact 22 ([15] Bi-monotonicity of the Z-points). Given  $e_s, e_t$  such that  $e_s \leq e_t$ . Let

$$S = \{(e_i, e_j) \mid e_i \prec e_j, \text{ and } e_i, e_j \text{ both belong to } \{e_s, e_{s+1}, \dots, e_t\}\}.$$

We claim that all the Z-points in set  $\{Z_i^j \mid (e_i, e_j) \in S\}$  lie in boundary-portion  $\rho = [v_{t+1} \circlearrowright v_s]$  and they obey the following bi-monotonicity: For  $(e_i, e_j) \in S$  and  $(e_{i'}, e_{j'}) \in S$ ,

if 
$$e_i \leq e_{i'}$$
 and  $e_j \leq e_{j'}$ , then  $Z_i^j \leq_{\rho} Z_{i'}^{j'}$ .

- ▶ **Lemma 23** ([15] Computational aspect of the Z-points).
- **1.** Given  $e_i, e_j$  such that  $e_i \prec e_j$ , the position of  $Z_i^j$  can be computed in O(1) time provided that the unit containing this point is given. (A unit means a vertex or an edge of P.)
- **2.** Assume  $e_i \prec e_j$  and  $v_k$  lies in  $(v_{j+1} \circlearrowright v_i)$ . Notice that  $Z_i^j$  lies in  $(v_{j+1} \circlearrowleft v_i)$  by Fact 21. So, the position of  $Z_i^j$  have the following three cases: (i) equals  $v_k$ ; (ii) lies in  $(v_{j+1} \circlearrowleft v_k)$ ; or (iii) lies in  $(v_k \circlearrowleft v_i)$ . Given i, j, k, we can distinguish these cases in O(1) time.
- 3. Given m pairs of edges  $(a_1,b_1),\ldots,(a_m,b_m)$  such that  $a_i \prec b_i$  for  $1 \leq i \leq m$ , and that  $a_1,\ldots,a_m$  lie in clockwise order around  $\partial P$  and  $b_1,\ldots,b_m$  lie in clockwise order around  $\partial P$ , we can compute the positions of  $Z_{a_1}^{b_1},\ldots,Z_{a_m}^{b_m}$  altogether in O(m+n) time.

## 3.1 Geometric definition of the blocks and their borders

Denote

$$\mathcal{T}(u, u') := \{ (X_1, X_2, X_3) \in \mathcal{T} \mid X_3 \in u, X_1 \in u' \}$$

$$= \{ (X_1, X_2, X_3) \mid X_3 \in u, X_2 \in \zeta(u, u'), X_1 \in u' \}.$$

$$(9)$$

We now give the intuitive geometric definition of  $\mathsf{block}(u, u')$ , which was previously defined as  $f(\mathcal{T}(u, u'))$  in (4). Here, we define not only the blocks, but also their borders and the direction of each border. These borders are surprisingly important in the proof of Theorem 2.

Recall that M(X, X') denotes the mid point of X, X' and

$$u \oplus u' := \{ \mathsf{M}(X, X') \mid X \in u, X' \in u' \}. \tag{10}$$

The shape of  $u \oplus u'$  is a parallelogram, a segment, or a point. More specific,  $e_i \oplus e_j$  is an open parallelogram, whose four corners are respectively  $\mathsf{M}(v_i,v_j)$ ,  $\mathsf{M}(v_i,v_{j+1})$ ,  $\mathsf{M}(v_{i+1},v_j)$ ,  $\mathsf{M}(v_{i+1},v_j)$ ,  $\mathsf{M}(v_{i+1},v_j)$ ,  $\mathsf{M}(v_i,v_j)$ . See Figure 7.

Two formulas of block(u, u').

$$\mathsf{block}(u, u') = \bigcup_{X \in u \oplus u'} \mathsf{the \ reflection \ of} \ \zeta(u, u') \ \mathsf{with \ respect \ to} \ X. \tag{11}$$

$$\mathsf{block}(u,u') = \bigcup_{X \in \zeta(u,u')} \mathsf{the} \ 2\mathsf{-scaling} \ \mathsf{of} \ u \oplus u' \ \mathsf{with} \ \mathsf{respect} \ \mathsf{to} \ X. \tag{12}$$

Proof of (11) and (12).

$$\begin{aligned} \operatorname{block}(u,u') &= f(\mathcal{T}(u,u')) \\ &= \bigcup_{X_3 \in u, X_1 \in u', X_2 \in \zeta(u,u')} f(X_1,X_2,X_3) \\ &= \bigcup_{X_3 \in u, X_1 \in u'} \bigcup_{X_2 \in \zeta(u,u')} \operatorname{the \ reflection \ of} \ X_2 \ \operatorname{around} \ \mathsf{M}(X_3,X_1) \\ &= \bigcup_{X_3 \in u, X_1 \in u'} \operatorname{the \ reflection \ of} \ \zeta(u,u') \ \operatorname{around} \ \mathsf{M}(X_3,X_1) \\ &= \bigcup_{X \in u \oplus u'} \operatorname{the \ reflection \ of} \ \zeta(u,u') \ \operatorname{around \ point} \ X \end{aligned}$$
 
$$\operatorname{block}(u,u') = f(\mathcal{T}(u,u')) \\ &= \bigcup_{X_3 \in u, X_1 \in u', X_2 \in \zeta(u,u')} f(X_1,X_2,X_3) \\ &= \bigcup_{X_2 \in \zeta(u,u')} \bigcup_{X_3 \in u, X_1 \in u'} \operatorname{the \ 2-scaling \ of} \ \mathsf{M}(X_3,X_1) \ \operatorname{with \ respect \ to} \ X_2 \\ &= \bigcup_{X_2 \in \zeta(u,u')} \operatorname{the \ 2-scaling \ of} \ u \oplus u' \ \operatorname{with \ respect \ to} \ X_2 \end{aligned}$$

We now give a geometric definition of blocks. This definition is consistent with the original definition in (4) according to (11) and (12).

Recall that the directions of the boundary-portions conforms to the clockwise order. In particular, the direction of edge  $e_i$  is from  $v_i$  to  $v_{i+1}$ . Assume u is chasing u'.

Case 1  $(u, u') = (e_i, e_i)$ . See Figure 7 (a).

The 2-scaling of  $e_i \oplus e_j$  with respect to point  $Z_i^j$  is a parallelogram whose sides are congruent to either  $e_i$  or  $e_j$ . We define this parallelogram as  $\mathsf{block}(e_i, e_j)$ .

Each side of this parallelogram is called a *border* of  $\mathsf{block}(e_i, e_j)$ . For those two borders that are congruent to  $e_i$ , we assume that they have the same direction as  $e_i$ . For those two borders that are congruent to  $e_i$ , we assume that they have the same direction as  $e_i$ .

Case 2  $(u, u') = (v_i, v_j)$ . See Figure 7 (d).

The reflection of  $\zeta(v_i, v_j)$  around  $\mathsf{M}(v_i, v_j)$  is a polygonal curve, and we define it as  $\mathsf{block}(v_i, v_j)$ . We regard this curve as the only border of  $\mathsf{block}(v_i, v_j)$ , and assume that its direction is from the reflection of  $Z_{i-1}^{j-1}$  to the reflection of  $Z_i^j$ .

Case 3  $(u, u') = (v_i, e_i)$ . See Figure 7 (b).

In this case,  $block(v_i, e_j)$  is the region bounded by the following curves:

the 2-scaling of segment  $v_i \oplus e_j$  with respect to  $Z_{i-1}^j$ ;

the 2-scaling of segment  $v_i \oplus e_i$  with respect to  $Z_i^j$ .

the reflection of  $\zeta(v_i, e_j)$  around the mid point of  $v_i, v_j$ ;

the reflection of  $\zeta(v_i, e_i)$  around the mid point of  $v_i, v_{i+1}$ .

We call each of these curves a border of  $\mathsf{block}(v_i, e_j)$ . The first two borders have the same direction as  $e_j$ ; the other two go from the reflection of  $Z_{i-1}^j$  to the reflection of  $Z_i^j$ .

Case 4  $(u, u') = (e_i, v_i)$ . See Figure 7 (c).

We define  $block(e_i, v_i)$  and its related notation symmetric to  $block(v_i, e_i)$ .

**Note:** Every border is an arrangement of some boundary-portion of P. Moreover, the direction of each border always conforms that of the original boundary-portion of this border.

## 3.2 Local-reversibility and Local-monotonicity of f

In the following we state two properties of  $\mathcal{T}(u, u')$  under function f. They are referred to as Local-reversibility and Local-monotonicity of f, respectively, and are applied to prove the Reversibility and Monotonicity of f later in Section 4.

▶ Fact 24. Assume u, u' are distinct units. For any point O in  $u \oplus u'$ , there exists only one pair of points (X, X') such that M(X, X') = O and that X, X' lie in u, u' respectively.

This fact is trivial and proof omitted. (See a proof in Section 4 of [15].)

▶ **Lemma 25** (LOCAL-REVERSIBILITY of f). Assume unit u is chasing unit u'. Then, f is a bijection from  $\mathcal{T}(u, u')$  to  $\mathsf{block}(u, u')$ .

**Proof.** For distinct tuples  $A = (A_1, A_2, A_3)$  and  $B = (B_1, B_2, B_3)$  from  $\mathcal{T}(u, u')$ , we shall prove that  $f(A) \neq f(B)$ . According to the definition of  $\mathcal{T}(u, u')$  (see (9)), we have

(i) 
$$A_3 \in u, A_1 \in u'$$
; (ii)  $B_3 \in u, B_1 \in u'$ ; and (iii)  $A_2, B_2 \in \zeta(u, u')$ .

For convenience, denote by r(X, O) the reflection of X around O.

- Case 1:  $A_2 = B_2$ . Since A, B are distinct, we have  $(A_1, A_3) \neq (B_1, B_3)$  in this case. According to (i), (ii) and Fact 24,  $M(A_3, A_1) \neq M(B_3, B_1)$ . Therefore,  $f(A) = r(A_2, M(A_3, A_1)) = r(B_2, M(A_3, A_1)) \neq r(B_2, M(B_3, B_1)) = f(B)$ .
- Case 2:  $A_2 \neq B_2$ . By (iii), points  $A_2, B_2$  both lie in  $\zeta(u, u')$ . This means  $\zeta(u, u')$  is not a single point, so there is at least one vertex among u, u'. When u, u' are both vertices,  $\mathsf{M}(A_1, A_3) = \mathsf{M}(u', u) = \mathsf{M}(B_1, B_3)$ , and so  $r(A_2, \mathsf{M}(A_1, A_3)) \neq r(B_2, \mathsf{M}(B_1, B_3))$ , i.e.  $f(A) \neq f(B)$ . Now, assume that u, u' are an edge and a vertex, e.g.  $(u, u') = (v_i, e_j)$ . In order to show that  $f(A) \neq f(B)$ , we argue that their distances to line  $\ell_j$  differ. By Fact 21,  $\zeta(v_i, e_j) = [Z_{i-1}^j \circlearrowright Z_j^i] \subseteq [v_{j+1} \circlearrowleft \mathsf{D}_j]$ . This implies that all points on  $\zeta(v_i, e_j)$  have different distances to  $\ell_j$ . In particular,  $A_2, B_2$  have different distances to  $\ell_j$ . However,  $\mathsf{M}(A_1, A_3)$  and  $\mathsf{M}(B_1, B_3)$  both lie in  $v_i \oplus e_j$  and thus have the same distance to  $\ell_j$ . So,  $f(A) = r(A_2, \mathsf{M}(A_1, A_3))$  and  $f(B) = r(B_2, \mathsf{M}(B_1, B_3))$  have different distances to  $\ell_j$ .
  - ▶ **Definition 26** (Local reverse function  $f_{u,u'}^{-1}()$ ) and  $f_{u,u'}^{-1,2}()$ ). Assume u is chasing u'. By the LOCAL-REVERSIBILITY OF f (Lemma 25), there is a reverse function of f on  $\operatorname{block}(u,u')$ , denoted by  $f_{u,u'}^{-1}(\cdot)$ . Equivalently, for any point X in  $\operatorname{block}(u,u')$ , denote by  $f_{u,u'}^{-1}(X)$  the unique preimage of X in  $\mathcal{T}(u,u')$  under f. Further, notice that  $f_{u,u'}^{-1}(X)$  is a tuple of three points, we denote the second point by  $f_{u,u'}^{-1,2}(X)$ .
  - ▶ Lemma 27 (LOCAL-MONOTONICITY of f). Assume unit u is chasing unit u'. Suppose a point X travels along some boundary-portion of P within  $\mathsf{block}(u,u')$  (in clockwise). We claim that point  $f_{u,u'}^{-1,2}(X)$  travels along  $\partial P$  in clockwise (non-strictly, which means that it may sometimes stay at the same position).
  - **Proof.** For convenience, let  $(J_X, K_X, L_X) = f_{u,u'}^{-1}(X)$  for any point X in  $\mathsf{block}(u, u')$ . Assume  $\rho$  is a boundary-portion of P that lies in  $\mathsf{block}(u, u')$  and point X travels (in  $\mathsf{clockwise}$ ) along  $\rho$ . We shall prove that  $K_X$  goes along  $\partial P$  in  $\mathsf{clockwise}$  non-strictly. Since  $(J_X, K_X, L_X) \in \mathcal{T}(u, u')$ , we have

$$J_X \in u', K_X \in \zeta(u, u')$$
 and  $L_X \in u$ .

Case 1: Both u, u' are edges. Since  $K_X \in \zeta(u, u')$  and  $\zeta(u, u') = Z_u^{u'}, K_X$  is invariant.

Case 2: u, u' are a vertex and an edge. Without loss of generality, assume that  $(u, u') = (v_i, e_j)$ . Denote by d(X) the distance from point X to  $\ell_j$ . We first state three arguments.

- (i) When point X travels along  $\rho$  in clockwise, d(X) (non-strictly) decreases.
- (ii) For any point X in  $\mathsf{block}(v_i, e_i) \cap \partial P$ , quantity  $d(X) + d(K_X)$  is a constant.
- (iii) Suppose that point Y is in a movement in which its position is restricted on  $\zeta(v_i, e_j)$ , and we observe that d(Y) (non-strictly) increases during the movement of Y. We can conclude that point Y moves in clockwise (non-strictly) along  $\zeta(v_i, e_j)$ .

Altogether, we can obtain our result. Recall that X travels along  $\rho$ . So, d(X) non-strictly decreases due to (i). So,  $d(K_X)$  non-strictly increases due to (ii). Finally, applying (iii) for  $Y = K_X$ , point  $K_X$  travels along  $\zeta(v_i, e_j)$  in clockwise non-strictly.

*Proof of (i):* To prove this argument, we only need to combine the following two arguments.

- (i.1) When X travels along  $[v_i \circlearrowright v_{i+1}]$  in clockwise, d(X) non-strictly decreases.
- (i.2) The boundary-portion  $\rho$  lies in  $[v_i \circlearrowright v_{j+1}]$ .

Because  $v_i$  is chasing  $e_j$ , we get  $e_i \prec e_j$ , which implies (i.1). The proof of (i.2) is as follows. See Figure 7 (b). Let H denote the half-plane delimited by the extended line of  $\overline{v_iv_{j+1}}$  and not containing  $e_i$ . By Fact 21,  $Z_i^j$  and  $Z_{i-1}^j$  both lie in  $(v_{j+1} \circlearrowright v_i)$ . Therefore,  $\zeta(v_i,e_j)=[Z_i^j \circlearrowright Z_{i-1}^j]$  is contained in H. Since  $\zeta(v_i,e_j) \subset H$  whereas  $v_i \oplus e_j$  lies in the opposite half-plane of H, applying (11),  $\mathsf{block}(v_i,e_j)$  lies in the opposite half-plane of H. So,  $\mathsf{block}(v_i,e_j) \cap \partial P \subseteq [v_i \circlearrowright v_{j+1}]$ . Further since  $\rho \subset \mathsf{block}(v_i,e_j) \cap \partial P$ , we get (i.2).

Proof of (ii): Because  $f(J_X, K_X, L_X) = X$ , we have  $\mathsf{M}(X, K_X) = \mathsf{M}(J_X, L_X)$ . Because  $J_X \in u'$  and  $L_X \in u$ , point  $\mathsf{M}(J_X, L_X)$  lies in  $u \oplus u' = v_i \oplus e_j$ . Therefore,  $\mathsf{M}(X, K_X)$  lies in  $v_i \oplus e_j$ , and hence  $d(\mathsf{M}(X, K_X))$  is a constant. Further, since  $X, K_X$  both lie in  $\partial P$ , they lie on the same side of  $\ell_j$ , so  $d(X) + d(K_X) = 2d(\mathsf{M}(X, K_X))$  is a constant.

Proof of (iii): By Fact 21,  $\zeta(v_i, e_j) = [Z_{i-1}^j \circlearrowleft Z_i^j] \subseteq [v_{j+1} \circlearrowleft \mathsf{D}_j]$ , which implies that d(Y) strictly increases when Y travels along  $\zeta(v_i, e_j)$ . This simply implies (iii).

Case 3 u, u' are both vertices. In this case  $\mathsf{block}(u, u')$  is a curve and there is no boundary-portion lying in  $\mathsf{block}(u, u')$  under our assumption that edges are pairwise-nonparallel. Note that the result holds even if there is a boundary-portion lying in  $\mathsf{block}(u, u')$ ; the proof is similar to that of Case 2 and is omitted.

## 3.3 Proofs of the properties of the bounding-quadrants

Recall the bounding-quadrants defined in Subsection 2.4 and the four observations - Lemma 15, Lemma 16, Lemma 17, and Lemma 18. We prove these observations in this subsection.

The following notation are frequently applied in this subsection.

For edge pair  $(e_i, e_j)$  such that  $e_i \leq e_j$ , denote by  $\mathsf{hp}_i^j$  the **open** half-plane delimited by the extended line of  $\overrightarrow{v_{j+1}v_i}$  and lies on the right side of  $\overrightarrow{v_{j+1}v_i}$ . See Figure 18 for illustrations. **Note**:  $\mathsf{hp}_i^j$  always contain  $\mathsf{quad}_i^j$ . This is according to Definition 14; see Figure 10.

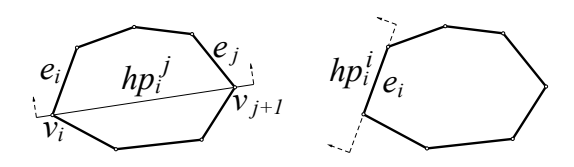


**Figure 18** Definition of  $\{hp_i^j \mid e_i \leq e_i\}$ .

•

Given point X and edge  $e_i$ , denote by  $p_i(X)$  the unique line at X that is parallel to  $e_i$ . Recall the inferior portions introduced in Section 1.2.

**Restatement of Lemma 15.** For any four edges  $e_a, e_{a'}, e_b, e_{b'}$  such that

 $e_a \leq e_{a'}, e_b \leq e_{b'}$  and that  $e_a, e_{a'}, e_b, e_{b'}$  are not contained in any inferior portion,

the intersection region  $quad_a^{a'} \cap quad_b^{b'}$  lies in the interior of P.

**Proof.** First, we discuss some trivial cases in which  $quad_a^{a'}$  would be disjoint with  $quad_b^{b'}$ .

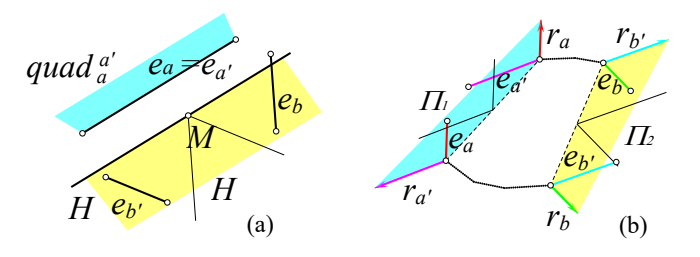


Figure 19 Trivial cases of the peculiar property of quad

Case 1 a=a'. Since  $e_a, e_{a'}, e_b, e_{b'}$  are not contained in any inferior portion, we know  $e_a \prec e_b$  and  $e_{b'} \prec e_a$ . See Figure 19 (a). Let M denote the apex of  $\mathsf{quad}_b^{b'}$ , which equals  $\mathsf{M}(v_b, v_{b'+1})$ . Because M is the mid point of  $v_b, v_{b'+1}$ , it lies in or on the right of  $e_a$ . Denote by H the half plane delimited by  $\mathsf{p}_a(M)$  and on the right of  $e_a$ . By this definition, (1) H is disjoint with  $\mathsf{quad}_a^{a'}$ . Moreover, we claim that (2) H contains  $\mathsf{quad}_b^{b'}$ . Since  $e_a \prec e_b$ , the boundary of  $\mathsf{quad}_b^{b'}$  that is parallel to  $e_b$  lies in H. Since  $e_{b'} \prec e_a$ , the boundary of  $\mathsf{quad}_b^{b'}$  that is parallel to  $e_{b'}$  also lies in H. So, two boundaries of quadrat  $\mathsf{quad}_b^{b'}$  both lie in H, which implies (2). Combining (1) and (2), the subregion  $\mathsf{quad}_b^{b'}$  of H is disjoint with  $\mathsf{quad}_a^{a'}$ .

Case 2 b = b'. This case is symmetric to Case 1.

Case 3  $e_a, e_{a'}, e_b, e_{b'}$  are distinct edges and lie in clockwise order on  $\partial P$ . See Figure 19 (b). We make four rays. Ray  $r_a$  locates at  $v_{a'+1}$  and has the same direction as  $e_a$ . Ray  $r_{a'}$  locates at  $v_a$  and has the opposite direction to  $e_{a'}$ . Ray  $r_b$  locates at  $v_{b'+1}$  and has the same direction as  $e_b$ . Ray  $r_{b'}$  locates at  $v_b$  and has the opposite direction to  $e_{b'}$ . Let  $\Pi_1$  denote the region bounded by  $r_{a'}, \overline{v_a v_{a'+1}}, r_a$  and containing  $\operatorname{quad}_a^{a'}$ . Let  $\Pi_2$  denote the region bounded by  $r_{b'}, \overline{v_b v_{b'+1}}, r_b$  and containing  $\operatorname{quad}_b^{b'}$ . Assume that  $\Pi_1, \Pi_2$  do not contain the boundaries. Since  $e_a, e_{a'}, e_b, e_{b'}$  are not containing in any inferior portion, we have  $e_{b'} \prec e_a$  while  $e_{a'} \prec e_b$ . This directly implies that  $\Pi_1, \Pi_2$  are disjoint. Therefore,  $\operatorname{quad}_a^{a'}, \operatorname{quad}_b^{b'}$  are disjoint, since they are respectively subregions of  $\Pi_1, \Pi_2$ .

In the preceding cases,  $quad_a^{a'} \cap quad_b^{b'}$  is empty and hence it lies in the interior of P.

When none of the preceding cases occur, two cases remain:

Case 4  $e_a \prec e_b \leq e_{a'} \prec e_{b'} \prec e_a$ .

Case 5  $e_b \prec e_a \leq e_{b'} \prec e_{a'} \prec e_b$ .

Assume that Case 4 occurs; the other case is symmetric.

See Figure 20. Let  $C = v_{b'+1}, D = v_a, E = v_b, F = v_{a'+1}$ . Let G denote the intersection of CE and DF. Obviously,  $\triangle EFG \subseteq P$ . So, to prove that  $\operatorname{\mathsf{quad}}_a^{a'} \cap \operatorname{\mathsf{quad}}_b^{b'}$  lies in the interior of P reduces to prove that it lies in the interior of P reduces to prove that P reduces to prove.

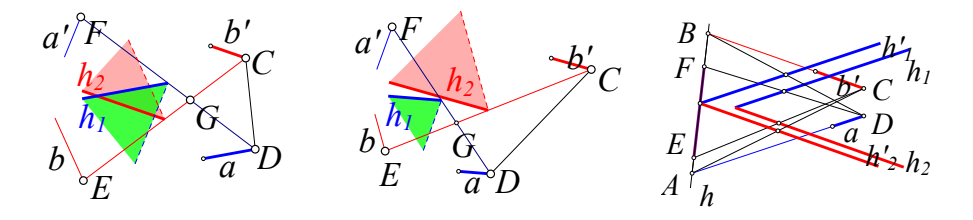


Figure 20 Nontrivial cases of the peculiar property of quad

- $\begin{array}{ll} \mathrm{i.} & \mathsf{quad}_a^{a'} \cap \mathsf{quad}_b^{b'} \ \mathrm{lies} \ \mathrm{in} \ \mathsf{hp}_a^{a'}. \\ \mathrm{ii.} & \mathsf{quad}_a^{a'} \cap \mathsf{quad}_b^{b'} \ \mathrm{lies} \ \mathrm{in} \ \mathsf{hp}_b^{b'}. \\ \mathrm{iii.} & \mathsf{quad}_a^{a'} \cap \mathsf{quad}_b^{b'} \ \mathrm{lies} \ \mathrm{in} \ \mathrm{half-plane} \ h, \ \mathrm{where} \ h \ \mathrm{denotes} \ \mathrm{the} \ \mathrm{open} \ \mathrm{half-plane} \ \mathrm{bounded} \ \mathrm{by} \ \mathrm{the} \end{array}$ extended line of  $\overline{EF}$  and containing G. (So, h is the complementary half-plane of  $hp_h^{a'}$ .)
- (i) and (ii) are trivial. As mentioned under the definition of hp, we have  $quad_a^{a'} \subseteq hp_a^{a'}$ and  $quad_b^{b'} \subseteq hp_b^{b'}$ . They respectively imply (i) and (ii). We prove (iii) in the following.

One of the two (open) half-planes defining  $quad_a^{a'}$  is parallel to  $e_a$ , denoted by  $h_1$ . One of the two (open) half-planes defining quad b' is parallel to  $e_{b'}$ , denoted by  $h_2$ . Clearly,  $\operatorname{\mathsf{quad}}_a^{a'} \cap \operatorname{\mathsf{quad}}_b^{b'} \subseteq h_1 \cap h_2$ . So proving (iii) reduces to proving that  $h_1 \cap h_2 \subseteq h$ .

See the right picture of Figure 20. Assume that the extended line of  $\overline{EF}$  intersects  $\ell_a, \ell_{b'}$  at A, B respectively. Denote by  $h'_1$  the open half-plane bounded by  $p_a(\mathsf{M}(D,B))$  and containing  $e_a$ , and  $h'_2$  the open half-plane bounded by  $p_{b'}(M(A,C))$  and containing  $e_{b'}$ .

Because P is convex, points E, F both lie in  $\overline{AB}$ . Since F lie in  $\overline{AB}$ , we know  $\mathsf{M}(D, F)$ lies in or on the boundary of  $h'_1$ , which implies  $h_1 \subseteq h'_1$  because  $h_1$  is parallel to  $h'_1$  and has M(D,F) on its boundary. Since E lie in  $\overline{AB}$ , we know M(C,E) lies in or on the boundary of  $h'_2$ , which implies  $h_2 \subseteq h'_2$  because  $h_2$  is parallel to  $h'_2$  and has M(C, E) on its boundary.

It remains to show that  $h'_1 \cap h'_2 \subseteq h$ . By the definition of  $h'_1, h'_2$ , their boundaries pass through M(A, B). Combining this with the facts that  $h'_1$  is parallel to  $e_a$  and  $h'_2$  is parallel to  $e_{b'}$ , as well as  $e_{b'} \prec e_a$ , we easily get  $h'_1 \cap h'_2 \subseteq h$ .

The following lemma is a full version of Lemma 16.

▶ **Lemma 28.** Given  $e_i, e_j$  such that  $e_i \prec e_j$ . See Figure 21. Let  $\rho = [v_i \circlearrowright v_{j+1}]$ . Then,

$$(\langle \mathsf{quad} \rangle_i^{j-1}).s \leq_{\rho} (\langle \mathsf{quad} \rangle_i^j).s \leq_{\rho} (\langle \mathsf{quad} \rangle_{i+1}^j).s, \tag{13}$$

$$(\langle \mathsf{quad} \rangle_i^{j-1}).t \leq_{\rho} (\langle \mathsf{quad} \rangle_i^j).t \leq_{\rho} (\langle \mathsf{quad} \rangle_{i+1}^j).t. \tag{14}$$

Moreover, consider m boundary-portions in a list  $\langle \mathsf{quad} \rangle_{u_1}^{u_1'}, \ldots, \langle \mathsf{quad} \rangle_{u_m}^{u_m'}$ , where

- (1)  $u_1, \ldots, u_m$  are units lying in clockwise order around  $\partial P$ , and
- (2)  $u'_1, \ldots, u'_m$  are units lying in clockwise order around  $\partial P$ , and
- (3)  $u_k$  is chasing  $u'_k$  for  $1 \le k \le m$ .

We claim that the starting points of these portions lie in clockwise order around  $\partial P$ , and so do their terminal points. (Note: to be rigorous, when we say points  $X_1, \ldots, X_m$  lie in clockwise order around  $\partial P$ , we allow some points, e.g.  $X_k, \ldots, X_l$ , lie in the same position.)

**Proof.** When j = i + 1, the following facts directly imply (13) and (14). See Figure 21 (c).

- (i)  $\langle \mathsf{quad} \rangle_i^{j-1}$  contains a single point, which is the midpoint of  $e_i$ .
- (ii)  $\langle \mathsf{quad} \rangle_{i+1}^j$  contains a single point, which is the midpoint of  $e_j$ .
- (iii)  $\langle \mathsf{quad} \rangle_i^j$  starts at the midpoint of  $e_i$  and terminates at the midpoint of  $e_j$ .

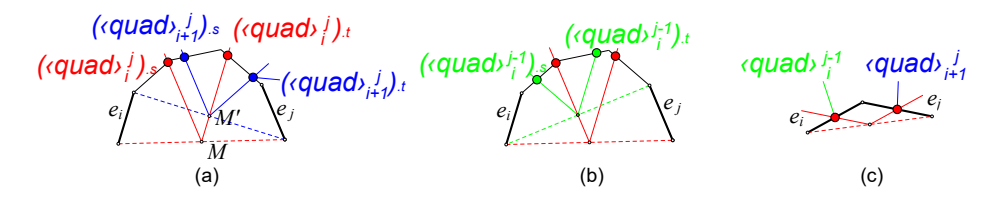


**Figure 21** Illustration of the monotonicity of (quad).

Now, assume  $j \neq i + 1$ . See Figure 21 (a). Let  $M = M(v_i, v_{j+1}), M' = M(v_{i+1}, v_{j+1})$ .

First, let us compare  $(\langle \mathsf{quad} \rangle_i^j).s$  and  $(\langle \mathsf{quad} \rangle_{i+1}^j).s$ . Clearly, their distance to  $\ell_j$  are respectively equal to the distance from M, M' to that line. Moreover, since  $e_i \prec e_j$  while MM' is parallel to  $e_i$ , point M is further to  $\ell_j$  than M'. Therefore,  $(\langle \mathsf{quad} \rangle_i^j).s$  is further to  $\ell_j$  than  $(\langle \mathsf{quad} \rangle_{i+1}^j).s$ . This means  $(\langle \mathsf{quad} \rangle_i^j).s \leq_{\rho} (\langle \mathsf{quad} \rangle_{i+1}^j).s$ .

Then, let us compare  $(\langle \mathsf{quad} \rangle_i^j).t$  and  $(\langle \mathsf{quad} \rangle_{i+1}^j).t$ . Consider segments  $M'(\langle \mathsf{quad} \rangle_i^j).t$ and  $M'(\langle \mathsf{quad} \rangle_{i+1}^j).t$ . They are parallel to  $e_i, e_{i+1}$  respectively. Moreover, we know  $e_i \prec e_{i+1}$ . Therefore, it follows that  $(\langle \mathsf{quad} \rangle_i^j).t \leq_{\rho} (\langle \mathsf{quad} \rangle_{i+1}^j).t$ .

Symmetrically,  $(\langle \mathsf{quad} \rangle_i^{j-1}).s \leq_{\rho} (\langle \mathsf{quad} \rangle_i^{j}).s$  and  $(\langle \mathsf{quad} \rangle_i^{j-1}).t \leq_{\rho} (\langle \mathsf{quad} \rangle_i^{j}).t$ . See Figure 21 (b) for an illustration. Altogether, we get (13) and (14).

Next, we prove the claim on list  $\langle \mathsf{quad} \rangle_{u_1}^{u_1'}, \ldots, \langle \mathsf{quad} \rangle_{u_m}^{u_m'}$ . For  $1 \leq k \leq m$ , denote  $a_k = forw(u_k)$  and  $a_k' = back(u_k')$ . Clearly, lists  $\{a_k\}$  and  $\{a_k'\}$ have the following properties: (i)  $a_k \leq a'_k$  for  $1 \leq k \leq m$ ; (ii)  $a_1, \ldots, a_m$  lie in clockwise order; (iii)  $a'_1, \ldots, a'_m$  lie in clockwise order. According to these properties and applying (13) and (14), the starting points of  $\langle \mathsf{quad} \rangle_{a_1}^{a'_1}, \ldots, \langle \mathsf{quad} \rangle_{a_m}^{a'_m}$  lie in clockwise order around  $\partial P$ , and the terminal points of  $\langle \mathsf{quad} \rangle_{a_1}^{a_1'}, \ldots, \langle \mathsf{quad} \rangle_{a_m}^{a_m'}$  lie in clockwise order around  $\partial P$ .

We complete the proof by recalling (7), which defines  $\langle \mathsf{quad} \rangle_{u_k}^{u_k'} := \langle \mathsf{quad} \rangle_{a_k}^{a_k'}$ .

#### Connections between Z-points and bounding-quadrants.

In the following we employ the opposite quadrant of quad<sup>j</sup> to bound point  $Z_i^j$  and  $\zeta(v_i, v_{j+1})$ . Applying these bounds, we can then prove the connection between blocks and their boundingquadrants (as stated in Lemma 17). Since  $quad_i^j$  is open, for consistency we regard its opposite quadrant **open** as well; so it does not contain its boundary.

▶ Fact 29. For any edge pair  $e_i, e_j$  such that  $e_i \prec e_j$ , point  $Z_i^j$  lies in or on the boundary of the opposite quadrant of quad<sup>j</sup><sub>i</sub>. (Note that  $Z_i^j$  may lie on the boundary sometimes.)

**Proof.** See Figure 22 (a). Let  $M = M(v_i, v_{i+1})$ . Let  $H_1$  denote the closed half-plane bounded by  $p_i(M)$  and containing  $v_{j+1}$ , and let  $H_2$  denote the closed half-plane bounded by  $p_j(M)$ and containing  $v_i$ . We shall prove that  $Z_i^j$  lies in  $H_1 \cap H_2$ . Denote  $e_b = back(Z_i^j)$ . Because  $Z_i^j$  has the largest distance-product to  $(\ell_i, \ell_j)$  in P, it has a larger distance-product to  $(\ell_i, \ell_j)$ than all the other points on  $e_b$ . Then, by the concavity of  $\operatorname{disprod}_{\ell_i,\ell_i}()$  on segment  $\overline{I_{j,b}I_{i,b}}$ (See Lemma 3 in [15]), we have  $|\mathsf{I}_{i,b}Z_i^j| \geq \frac{1}{2}|\mathsf{I}_{j,b}\mathsf{I}_{i,b}|$ , which implies that  $d_{\ell_i}(Z_i^j) \geq \frac{1}{2}d_{\ell_i}(\mathsf{I}_{j,b})$ . Further since  $\frac{1}{2}d_{\ell_i}(\mathsf{I}_{j,b}) \geq \frac{1}{2}d_{\ell_i}(v_{j+1}) = d_{\ell_i}(M)$ , we have  $d_{\ell_i}(Z_i^j) \geq d_{\ell_i}(M)$ . This inequality implies that  $Z_i^j \in H_1$ . Symmetrically,  $Z_i^j \in H_2$ . Therefore,  $Z_i^j \in H_1 \cap H_2$ .

**Fact 30.** For two vertices  $v_i, v_{i+1}$  such that  $v_i$  is chasing  $v_{i+1}$ , the boundary-portion  $\zeta(v_i, v_{j+1})$  is contained in the opposite quadrant of quad<sub>i</sub>.

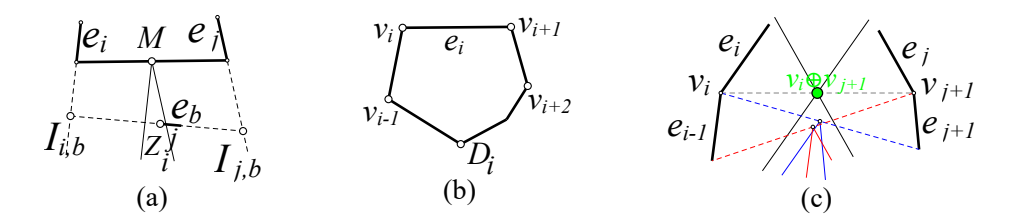


Figure 22 Illustration of the proof of Fact 29 and Fact 30

**Proof.** Recall that  $D_i$  is the unique vertex that is furthest to the extended line of  $e_i$ .

Case 1: i=j. See Figure 22 (b). By Fact 21,  $Z_{i-1}^i$  lies in  $[v_{i+1} \circlearrowleft \mathsf{D}_i]$  and it does not equal to  $v_{i+1}$ , whereas  $Z_i^{i+1}$  lies in  $[D_i \circlearrowright v_i]$  and it does not equal to  $v_i$ . This means  $[Z_{i-1}^i \circlearrowright Z_i^{i+1}] \subset (v_{i+1} \circlearrowright v_i)$ , i.e.  $\zeta(v_i, v_{i+1}) \subset (v_{i+1} \circlearrowright v_i)$ . Moreover,  $(v_{i+1} \circlearrowright v_i)$  is contained in the opposite quadrant of quad<sub>i</sub>. So,  $\zeta(v_i, v_{i+1})$  is also contained by this quadrant.

Case 2:  $i \neq j$ . See Figure 22 (c). Let  $\gamma$  be the intersection of  $\partial P$  and the opposite quadrant of  $quad_i^j$ , which is a boundary-portion of P. We state that

- (i)  $Z_{i-1}^j$  and  $Z_i^{j+1}$  both lie in  $\gamma$ .

(ii)  $Z_{i-1}^{j} \leq_{\rho} Z_{i}^{j+1}$ , where  $\rho = [v_{j+1} \circlearrowright v_{i}]$ . Clearly,  $\gamma$  is contained in  $\rho$ . So (i) and (ii) together imply that  $Z_{i-1}^{j} \leq_{\gamma} Z_{i}^{j+1}$ . This means  $\zeta(v_i, v_{j+1}) = [Z_{i-1}^j \circlearrowleft Z_i^{j+1}]$  lies in  $\gamma$  and hence in the opposite quadrant of  $\operatorname{\mathsf{quad}}_i^j$ .

Proof of (i). We only consider point  $Z_{i-1}^j$ . The other point  $Z_i^{j+1}$  is symmetric. Since  $v_i$  is chasing  $v_{j+1}$ , we get  $e_{i-1} \prec e_j$ . This implies that point  $M(v_{i-1}, v_{j+1})$ , which is the apex of the opposite quadrant of  $quad_{i-1}^j$ , lies in the opposite quadrant of  $quad_i^j$ . Therefore, the opposite quadrant of  $quad_{i-1}^j$  and its boundary are contained in the opposite quadrant of  $quad_i^j$ . Moreover, By Fact 29,  $Z_{i-1}^j$  lies in or on the boundary of the opposite quadrant of  $\operatorname{\mathsf{quad}}_{i-1}^j$ . Therefore,  $Z_{i-1}^j$  lies in the opposite quadrant of  $\operatorname{\mathsf{quad}}_i^j$  and thus lies in  $\gamma$ .

Proof of (ii). This follows from the bi-monotonicity of Z-points (Fact 22).

# Connections between blocks and bounding-quadrants

Henceforth in this subsection, assume u, u' are given units such that u is chasing u'.

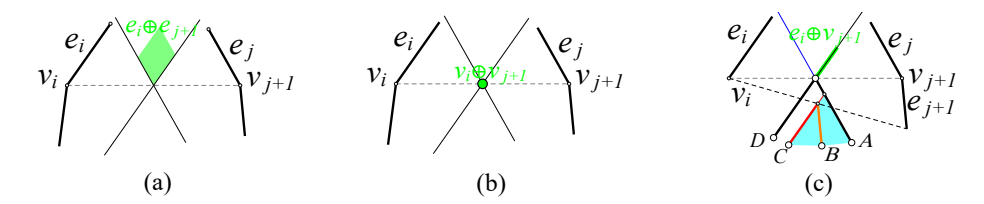
Recall Section 3.1 for the geometric definition of the blocks and their borders. We now prove the two underlying observations of the block stated in Lemma 17 and 18.

**Restatement of Lemma 17.**  $\operatorname{block}(u,u')$  is contained in  $\operatorname{quad}_u^{u'}$ , i.e.  $\operatorname{block}(u,u') \subset \operatorname{quad}_u^{u'}$ . (Remind that  $\mathsf{quad}_u^{u'}$  is open; so the block cannot intersect the boundary of the quadrant.)

**Restatement of Lemma 18.** Suppose some point X travels along some border of block(u, u')(in its positive direction) and suppose we stand both in P and in the opposite quadrant of  $\operatorname{\mathsf{quad}}_{u}^{u'}$ . Then, X travels in clockwise order (strictly) around us.

**Proof of Lemma 17.** Recall that  $quad_u^{u'} := quad_{forw(u)}^{back(u')}$  in (7). We shall prove:

$$\begin{aligned} \operatorname{block}(e_i,e_j) \subset \operatorname{quad}_i^j, & \operatorname{block}(v_i,v_{j+1}) \subset \operatorname{quad}_i^j, \\ \operatorname{block}(e_i,v_{j+1}) \subset \operatorname{quad}_i^j, & \operatorname{block}(v_i,e_j) \subset \operatorname{quad}_i^j. \end{aligned}$$



- Figure 23 Illustration of the proof of Lemma 17
- $\mathsf{block}(e_i, e_i) \subset \mathsf{quad}_i^j$ . See Figure 23 (a). Point  $Z_i^j$  lies in or on the boundary of the opposite quadrant of quad<sup>j</sup> (by Fact 29), whereas  $e_i \oplus e_j$  is clearly contained in  $quad_i^j$ . Therefore, the 2-scaling of  $e_i \oplus e_j$  with respect to  $Z_i^j$ , which equals  $\mathsf{block}(e_i, e_j)$  due to (12), is contained in  $\mathsf{quad}_i^j$ .
- $\mathsf{block}(v_i, v_{i+1}) \subset \mathsf{quad}_i^j$ . See Figure 23 (b). By Fact 30,  $\zeta(v_i, v_{i+1})$  lies in the opposite quadrant of quad<sup>j</sup>. So, its reflection around the apex  $M(v_i, v_{j+1})$ , which equals  $block(v_i, v_{j+1})$  due to (11), is contained in  $quad_i^j$ .
- $\mathsf{block}(e_i, v_{i+1}) \subset \mathsf{quad}_i^j$ . See Figure 23 (c). Denote by  $H_1$  the closed half-plane delimited by line  $p_j(M(v_i, v_{j+1}))$  and not containing  $e_j$ , and  $H_2$  the closed half-plane delimited by line  $p_i(M(v_i, v_{j+2}))$  and not containing  $e_i$ .  $(H_1 \cap H_2 \text{ is the colored region in Figure 23 (c).})$  We state (i)  $\zeta(e_i, v_{j+1})$  lies in  $H_1 \cap H_2$ . According to (i), for each point  $X \in e_i \oplus v_{j+1}$ , the reflection of  $\zeta(e_i, v_{j+1})$  around X is contained in  $\mathsf{quad}_i^j$ . Therefore,  $\left(\bigcup_{X\in e_i\oplus v_{j+1}}$  the reflection of  $\zeta(e_i,v_{j+1})$  around  $X\right)$ , which equals  $\mathsf{block}(e_i, v_{j+1})$  due to (11), is contained in  $\mathsf{quad}_i^j$ .

We now prove (i). Notice that the intersection between  $\partial P$  and the opposite quadrant of  $quad_i^j$  is a boundary-portion, denoted by  $(A \circlearrowright D)$ . Similarly, the intersection between  $\partial P$  and the opposite quadrant of quad<sub>i</sub><sup>j+1</sup> is a boundary-portion, denoted by  $(B \circlearrowright C)$ .

- (i.1)  $[B \circlearrowright C] \subset [A \circlearrowright D]$ .
- (i.2)  $Z_i^j \in [A \circlearrowright D]$  and  $Z_i^{j+1} \in [B \circlearrowright C]$ . (i.3)  $Z_i^j \leq_{\gamma} Z_i^{j+1}$ , where  $\gamma = [A \circlearrowright D]$ .

Following (i.1), (i.2), and (i.3), we get  $[Z_i^j \circlearrowright Z_i^{j+1}] \subseteq [A \circlearrowright C]$ , which implies (i).

*Proof of (i.1):* Since  $e_i$  is chasing  $v_{i+1}$ , we know  $e_i \prec e_{i+1}$ , which implies (i.1).

Proof of (i.2): These inequalities are applications of Fact 29.

*Proof of (i.3):* This is an application of the bi-monotonicity of Z-points (Fact 22).

 $\mathsf{block}(v_i, e_i) \subset \mathsf{quad}_i^{\jmath}$ . This one is symmetric to the preceding one. Proof omitted.

**Proof of Lemma 18.** Take an arbitrary point O that lies in P and in the opposite quadrant of quad u. We shall prove that (i) when a point X travels along any border of block(u, u')(in its positive direction), it travels in clockwise around O.

We discuss cases depending on whether u, u' are edges, vertices, or an edge and a vertex. Case 1: both u, u' are edges. Since  $\mathsf{block}(u, u') \subset \mathsf{quad}_u^{u'}$ , all points in the opposite quadrant of  $quad_u^{u'}$ , including O, are on the right of each border of block(u, u'). This can be easily observed in Figure 24 (a), so details are omitted. This implies (i).

Case 2: both u, u' are vertices. Let O' denote the reflection of O around  $\mathsf{M}(u, u')$ . Since the unique border of block(u, u') equals the reflection of  $\zeta(u, u')$  around M(u, u'). It reduces to prove that (ii) when X travels along  $\zeta(u, u')$ , it travels in clockwise around O'

Without loss of generality, assume  $(u, u') = (v_i, v_{j+1})$ . We consider two subcases.

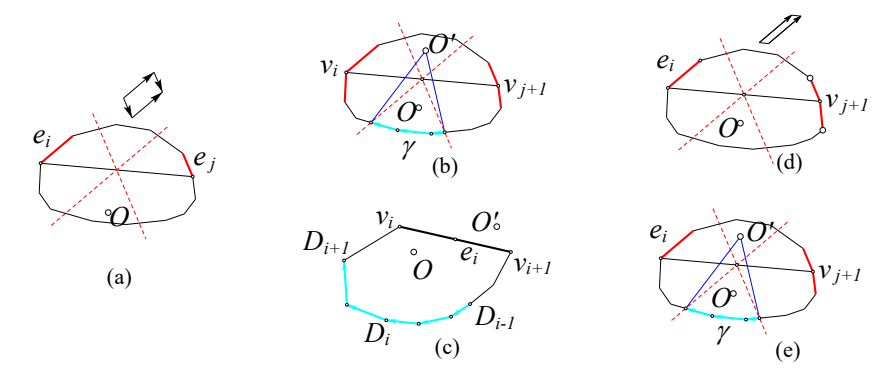


Figure 24 Illustration of the proof of Lemma 18

- Case 2.1:  $j \neq i$ . See Figure 24 (b). Let  $\gamma$  denote the intersection between  $\partial P$  and the opposite quadrant of  $\operatorname{\mathsf{quad}}_u^{u'}$ . The following statements imply (ii).
  - (I)  $\zeta(u, u')$  is contained in boundary-portion  $\gamma$ .
- (II) When point X travels along  $\gamma$ , it travels in clockwise around O'.
  - (I) follows from Fact 30. We prove (II) in the following.

Pick any edge  $e_k$  that intersects  $\gamma$ . Because P is convex and  $e_k$  intersects  $\gamma$ , we know  $\ell_k$  interests both boundaries of the opposite quadrant of  $\mathsf{quad}_u^{u'}$ , and this implies that  $\mathsf{quad}_u^{u'}$  lies on the right of  $e_k$ . Notice that  $O' \in \mathsf{quad}_u^{u'}$  because O lies in the opposite quadrant of  $\mathsf{quad}_u^{u'}$ . So, O' lies on the right of  $e_k$ . Therefore, if X travels along  $e_k$ , it travels in clockwise around O'. This implies (II) because  $\gamma$  is the concatenation of such edges.

- **Case 2.2:** j = i. See Figure 24 (c). The following statements imply (ii).
- (ii.1)  $\zeta(u, u') \subseteq [\mathsf{D}_{i-1} \circlearrowright \mathsf{D}_{i+1}].$
- (ii.2) When X travels along  $[D_{i-1} \circlearrowright D_i]$ , it travels in clockwise around O'.
- (ii.3) When X travels along  $[D_i \circlearrowright D_{i+1}]$ , it travels in clockwise around O'. (ii.1) follows from Fact 21; we prove (ii.2) in the next; (ii.3) is symmetric. Pick any edge  $e_k$  in  $[D_{i-1} \circlearrowleft D_i]$ . We shall prove that when X travels along  $e_k$ , it travels

in clockwise around O'. In other words, for any edge  $e_k$  in  $[D_{i-1} \circlearrowright D_i]$ , O' lies on the right of  $e_k$ . Let d(X) denote the signed distance from point X to  $\ell_k$ , so that the points on the right of  $e_k$  have positive values. It reduces to prove that d(O') > 0.

Since  $e_k$  lies in  $[D_{i-1} \circlearrowright D_i]$ , point  $v_i$  has the largest distance to  $\ell_k$  in P. Moreover,  $O \neq v_i$  since O lies in the opposite quadrant of  $\mathsf{quad}_u^{u'}$ . Therefore,  $d(v_i) > d(O)$ . Because P is convex,  $d(v_{i+1}) \geq 0$ . Furthermore, since O' is the reflection of O around  $\mathsf{M}(v_i, v_{i+1})$ , we get  $d(O') = 2d(\mathsf{M}(v_i, v_{i+1})) - d(O) = d(v_i) + d(v_{i+1}) - d(O)$ . Altogether, d(O') > 0.

Case 3: u, u' are a vertex and an edge, e.g.  $u = e_i, u' = v_{j+1}$ . In this case block(u, u') has four borders; two of which are congruent to the only edge in u, u' and the other two are reflections of  $\zeta(u, u')$ . The statement about the former two can be proved similar to Case 1. See Figure 24 (d). The statement about the latter two can be proved similar to Case 2. See Figure 24 (e). We show the second statement more clearly in the following. Consider the region  $\phi$  consists by the opposite quadrant of  $\operatorname{quad}_u^{u'} = \operatorname{quad}_i^j$  and its boundary. Its intersection with  $\partial P$  is a boundary-portion; denoted by  $\gamma$ . (Compare to Case 2, here  $\gamma$  must contain its endpoints.) Let O' denote the reflection of O around  $\operatorname{M}(v_i, v_{j+1})$ . We argue that for this case claims (I) and (II) still hold, and so does (ii).

Proof of (I): Recall the proof of  $\mathsf{block}(e_i, v_{j+1}) \subset \mathsf{quad}_i^j$  in the proof of Lemma 17, where we have shown that  $\zeta(e_i, v_{j+1})$  is contained in  $\phi$ . So,  $\zeta(e_i, v_{j+1}) \subset \gamma$ .

Proof of (II): This is the same as the proof in Case 2.1.

# **3.4** The Inner boundary of $f(\mathcal{T})$

We see region  $f(\mathcal{T})$  is an annular region with two boundaries in Figure 8. In this subsection, we define explicitly an oriented and polygonal closed curve to be the *inner boundary* of  $f(\mathcal{T})$ , denoted by  $\sigma P$ . Moreover, we define a function  $g: \sigma P \to \partial P$ , which is related to  $f_{u,u'}^{-1,2}()$  - the second dimension of the local reverse function of f introduced in Definition 26.

**Outline.** To define  $\sigma P$ , we first define two terms - the *frontier blocks* and the *bottom borders* of the *frontier blocks*. Briefly, frontier blocks are those blocks that lie at the inner side of  $f(\mathcal{T})$ . The bottom border of each frontier block is a specific border or the concatenation of two borders of this block. We state an intrinsic order between the frontier blocks, and argue that the concatenation of the bottom borders is a closed curve. Thus we define  $\sigma P$ .

#### Definition of the frontier blocks

To define the frontier blocks, we shall define a circular list of unit pairs, called *frontier-pair-list*. Then, block(u, u') a *frontier block* if and only if (u, u') belongs to this list.

The frontier-pair-list is defined as  $\mathsf{FPL}$  generated by Algorithm 1.

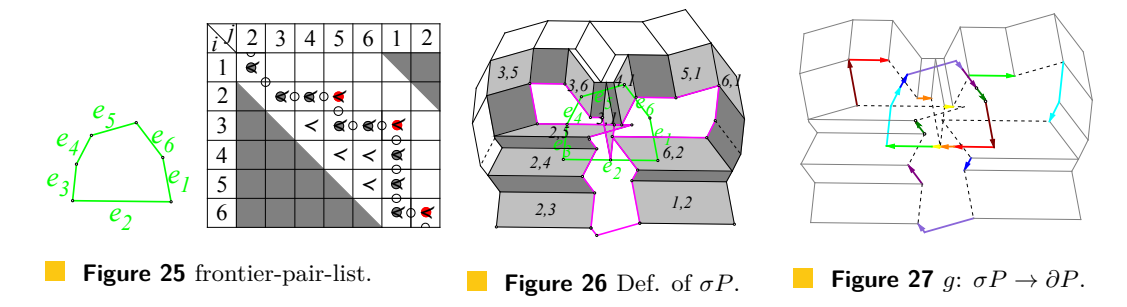
```
1 Let FPL be empty, let i = 1, and let e_i be the previous edge of D_1;
2 repeat
       Add unit pair (e_i, e_j) to the tail of FPL;
3
       if e_i \prec e_{j+1} then
           Add unit pair (e_i, v_{i+1}) to the tail of FPL and increase j by 1;
5
6
           if i+1 \neq j then
              Add unit pair (v_{i+1}, e_i) to the tail of FPL and increase i by 1;
 8
           else Add unit pair (v_{i+1}, v_{j+1}) to the tail of FPL and increase i, j both by 1;;
9
       end
10
11 until i = 1 and e_j is the previous edge of D_1;
```

Algorithm 1: An algorithm for defining FPL

See Figure 25 for an illustration. The left picture shows P. The table exhibits the "chasing" relation between the edges of P, where the solid circles indicate edge pairs in the frontier-pair-list, and the hollow circles indicate other unit pairs in this list.

According to the frontier-pair-list, we can find out all the frontier blocks. The frontier blocks of this example are the grey blocks shown in Figure 26.

All the bottom borders (defined below) are colored pink in Figure 26.



31

#### Definition of lower borders and bottom borders

Recall the geometric definition of the blocks and their borders in 3.1.

▶ **Definition 31.** First, we define lower border of each block. See Figure 7.

The left lower border of block $(e_i, e_j)$  refers to the 2-scaling of  $v_i \oplus e_j$  w.r.t  $Z_i^j$ .

The right lower border of block $(e_i, e_j)$  refers to the 2-scaling of  $e_i \oplus v_{j+1}$  w.r.t  $Z_i^j$ .

The lower border of block $(v_i, e_j)$  refers to the reflection of  $\zeta(v_i, e_j)$  around  $M(v_i, v_{i+1})$ .

The lower border of block $(e_i, v_i)$  refers to the reflection of  $\zeta(e_i, v_i)$  around  $M(v_i, v_i)$ .

The **bottom border** of block(u, u') for (u, u') in FPL is defined as follows.

- If u, u' are vertices, block (u, u') has a single border (which is the block itself) and this border is called the *bottom border* of block(u, u').
- If u, u' comprise an edge and a vertex, we define the bottom border of  $\mathsf{block}(u, u')$  to be the lower border of  $\mathsf{block}(u, u')$ .
- If u, u' are edges, e.g.  $u = e_i, u' = e_j$ , we define the bottom border of  $\mathsf{block}(u, u')$  to be

```
if (e_{i-1}, e_j) \in FPL, (e_i, e_{j+1}) \in FPL.
its right lower border,
its left lower border,
                                                                      if (e_{i-1}, e_i) \in \mathsf{FPL}, (e_i, e_{i+1}) \notin \mathsf{FPL};
                                                                     if (e_{i-1}, e_i) \notin FPL, (e_i, e_{i+1}) \in FPL;
                   tion of its two lower borders, if (e_{i-1}, e_j) \notin \mathsf{FPL}, (e_i, e_{j+1}) \notin \mathsf{FPL};
```

By the geometric definition of the blocks, we obtain the following fact. (Proof omitted)

▶ Fact 32. The bottom borders of the frontier blocks are end-to-end connected — the starting point of the bottom border of  $block(u_{i+1}, u'_{i+1})$  is the terminal point of the bottom border of  $block(u_i, u'_i)$ , where  $(u_i, u'_i)$ ,  $(u_{i+1}, u'_{i+1})$  indicate two adjacent pairs in the frontier-pair-list.

We define the concatenation of the bottom borders (based on the above order) as  $\sigma P$ .

▶ **Note 1.** According to the definition, when  $(e_{i-1}, e_j) \notin \mathsf{FPL}$  and  $(e_i, e_{j+1}) \notin \mathsf{FPL}$ , the bottom border of  $block(e_i, e_i)$  excludes the "corner point" – the common endpoint of its two lower borders — because these lower borders are open segments. So, in Figure 26, the lowermost corner of block(3,1), the leftmost corner of block(6,2), and the rightmost corner of block(2,5) are not contained in the bottom borders. Therefore, none of these "corner points" are contained in  $\sigma P$ . This fact is very important for understanding some theorems (e.g. interleavity-of-f in Theorem 2) and will be mentioned later.

# Extension of $f_{u,u'}^{-1,2}(\cdot)$ and the definition of g.

Recall  $f_{u,u'}^{-1,2}(\cdot)$  in Definition 26. It was only defined on  $\mathsf{block}(u,u')$  but not on its lower border. (The lower border(s) in general do not belong to the block, unless both u, u' are vertices.) Nevertheless, it can be naturally extended to the lower border(s) as follows.

Assume point X lies in the lower border of block(u, u').

- Case 1:  $u = e_i, u' = e_j$ . We define  $f_{u,u'}^{-1,2}(X) = Z_i^j$ .
- Case 2:  $u = e_i, u' = v_j$ . In this case, X must be the reflection of some point X' in  $\zeta(v_i, v_j)$  around  $M(v_i, v_j)$ ; and we define  $f_{u,u'}^{-1,2}(X) = X'$ .
- Case 3:  $u = v_i, u' = e_j$ . In this case, X must be the reflection of some point X' in  $\zeta(v_i, e_j)$  around  $\mathsf{M}(v_i,v_{j+1});$  and we define  $f_{u,u'}^{-1,2}(X)=X'.$  Case 4:  $u=v_i,u'=v_j.$  For this case  $f_{u,u'}^{-1,2}(X)$  is already defined.
- - ▶ **Definition 33** (g). For any point X in  $\sigma P$ , assuming it comes from the bottom border of frontier block block (u, u'), we define  $g(X) = f_{u,u'}^{-1,2}(X)$ . Figure 27 explains this definition.

# 4 Proofs of the first five properties of $\mathcal{T}$ under function f

This section proves the first five properties of  $f(\mathcal{T})$  stated in Theorem 2. Recall the sketch of this proof in Subsection 2.5.

**Outline.** The main difficulty of this section lies in the proof of the first two properties, Block-disjointness and Interleavity-of-f. Subsection 4.1 presents some preliminaries for these two properties. The following subsections prove the properties of  $f(\mathcal{T})$  one by one.

# 4.1 Preliminary: extremal pairs and some observations

▶ **Definition 34.** Edge pair  $(e_c, e_{c'})$  is *extremal*, if  $e_c \prec e_{c'}$  and the inferior portion  $[v_c \circlearrowright v_{c'+1}]$  is not contained in any other inferior portions. Equivalently, if  $e_c \prec e_{c'}, e_{c-1} \not\prec e_{c'}, e_c \not\prec e_{c'+1}$ . For example, in Figure 25, the edge pairs indicated by red solid circles are extremal.

Obviously, the extremal pairs are always contained in the frontier-pair-list.

▶ Fact 35. There exist at least three extremal pairs.

**Proof.** Apparently there must be at least one extremal pair. This claim can be made slightly stronger as follows. Let  $(e_i, e_j)$  be any pair of edges such that  $e_i$  is chasing  $e_j$ . Then, there is an extremal edge pair  $(e_{i'}, e_{j'})$  such that  $[v_{i'} \circlearrowright v_{j'+1}]$  contains  $e_i$  and  $e_j$ .

Now, assume that  $(e_i, e_j)$  is extremal. Pick  $e_k$  to be any edge that does not lie in the corresponding inferior portion  $[v_i \circlearrowright v_{j+1}]$ . Then, we have

$$e_i \prec e_j$$
,  $e_i \prec e_k$  and  $e_k \prec e_i$ .

Starting from  $(e_k, e_i)$ , we can find an extremal pair  $(e_a, e_b)$  so that  $[v_a \circlearrowright v_{b+1}]$  contains  $e_k, e_i$ . Notice that  $[v_a \circlearrowright v_{b+1}]$  is inferior and thus cannot contain  $e_j$ . Starting from  $(e_j, e_k)$ , we can find an extremal pair  $(e_c, e_d)$  so that  $[v_c \circlearrowright v_{d+1}]$  contains  $e_j, e_k$ . Notice that  $[v_c \circlearrowright v_{d+1}]$  is inferior and thus cannot contain  $e_i$ . Therefore, we obtain three different extremal pairs.

For each extremal pair  $(e_c, e_{c'})$ , denote

$$\Delta(c,c') := \left\{ (u,u') \mid \begin{array}{c} \text{unit } u \text{ is chasing } u', \text{ and} \\ forw(u), back(u') \in \{e_c, e_{c+1}, \dots, e_{c'}\} \end{array} \right\},\tag{15}$$

For any set S of unit pairs, denote  $BLOCK[S] = \{ block(u, u') \mid (u, u') \in S \}.$ 

- ▶ **Lemma 36.** Assume  $(e_c, e_{c'})$  any extremal pair and consider the blocks in  $BLOCK[\Delta(c, c')]$ .
- 1. None of these blocks intersects the opposite quadrant of  $\operatorname{\mathsf{quad}}^{c'}_c$ .
- 2. When point X travels along any border of any block in  $BLOCK[\Delta(c,c')]$ , it travels in clockwise order around point  $O = M(v_c, v_{c'+1})$ .

**Proof.** Take any unit pair (u, u') in  $\Delta(c, c')$ , we shall prove:

- (i)  $\mathsf{block}(u,u')$  is disjoint with the opposite quadrant of  $\mathsf{quad}_c^{c'}$ ;
- (ii) When X travels along a border of  $\mathsf{block}(u, u')$ , it travels in clockwise order around O. Let  $e_i = forw(u)$  and  $e_j = back(u')$ . Because  $(u, u') \in \Delta(c, c')$ , according to (15),

$$e_i, e_j$$
 belong to  $\{e_c, \dots, e_{c'}\}$  and  $e_i \leq e_j$ . (16)

Recall the definition of  $hp_i^j$  in Subsection 3.3 (as shown in Figure 18).

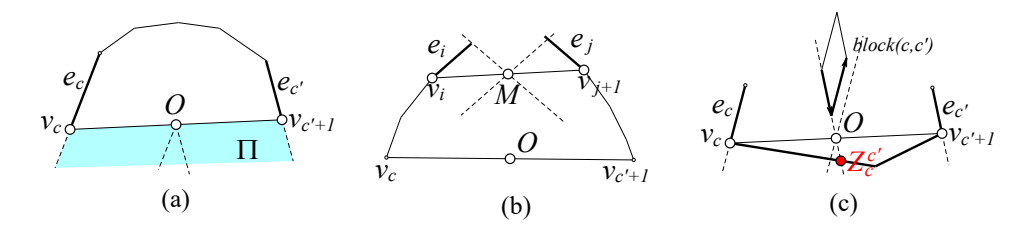


**Figure 28** Illustration of the proof of Lemma 36.

Proof of (i): See Figure 28 (a). Let  $\Pi$  denote the region that lies on the right of  $e_c$ ,  $e_{c'}$  and  $\overrightarrow{v_cv_{c'+1}}$ . According to (16) and the definition of  $\mathsf{hp}^i_j$ , the half-plane  $\mathsf{hp}^j_i$  is disjoint with  $\Pi$ . Moreover, since  $\mathsf{block}(u,u') \subset \mathsf{quad}^{u'}_u = \mathsf{quad}^j_i \subseteq \mathsf{hp}^j_i$ , region  $\mathsf{block}(u,u')$  is disjoint with  $\Pi$ . Furthermore, since the opposite quadrant of  $\mathsf{quad}^{c'}_c$  is a subregion of  $\Pi$ , we get (i).

Proof of (ii): First of all, assume that  $(u, u') \neq (e_c, e_{c'})$ .

When  $(u, u') \neq (e_c, e_{c'})$ , we claim  $(i, j) \neq (c, c')$ . Suppose to the contrary that (i, j) = (c, c'). Then,  $(u, u') \in \{(e_c, e_{c'}), (e_c, v_{c'+1}), (v_c, e_{c'}), (v_c, v_{c'+1})\}$ . Since  $(e_c, e_{c'})$  is extremal,  $e_c$  is not chasing  $v_{c'+1}$ ,  $v_c$  is not chasing  $e_{c'}$ , and  $v_c$  is not chasing  $v_{c'+1}$ . But we know u is chasing u'. Therefore, (u, u') can only be  $(e_c, e_{c'})$ . This contradicts the assumption.

See Figure 28 (b). Let  $M = M(v_i, v_{j+1})$ . Recall that  $d_l(X)$  denotes the distance from X to l. Now, consider the distance to  $l_j$ . Because (16),

$$d_{\ell_j}(v_c) \ge d_{\ell_j}(v_i)$$
 and  $d_{\ell_j}(v_{c'+1}) \ge d_{\ell_j}(v_{j+1})$ .

At least one of these inequalities is unequal since  $(i, j) \neq (c, c')$ . So,

$$d_{\ell_i}(v_c) + d_{\ell_i}(v_{c'+1}) > d_{\ell_i}(v_i) + d_{\ell_i}(v_{j+1}).$$

The left and right sides equal to  $2 \cdot d_{\ell_j}(O)$  and  $2 \cdot d_{\ell_j}(M)$ , respectively. So  $d_{\ell_j}(O) > d_{\ell_j}(M)$ . Symmetrically,  $d_{\ell_i}(O) > d_{\ell_i}(M)$ . These two inequalities imply that O lies in the opposite quadrant of  $\mathsf{quad}_u^{u'}$ . Further since  $O \in P$ , applying the monotonicity of the borders (Lemma 18), we get (ii).

When  $(u, u') = (e_c, e_{c'})$ , statement (ii) still holds. However, if X travels along the two lower borders of  $\mathsf{block}(e_c, e_{c'})$  (see Definition 31), it is possible that the orientation of OX keeps invariant during the traveling process. This occurs when  $Z_c^{c'}$  lies on the boundary of the opposite quadrant of  $\mathsf{quad}_c^{c'}$  as shown in Figure 28 (c). (See Fact 29 for more information.)

▶ Note 2. In most cases, X in Lemma 36.2 travels in clockwise order around O strictly (which means that the orientation of OX strictly increases during the traveling process). This is true for almost all borders; the only exceptions are lower borders of  $block(e_c, e_{c'})$ .

## 4.2 Proof of Block-disjointness

The first property of  $f(\mathcal{T})$  states that blocks intersect only in the interior of P.

Two blocks block(u, u') and block(v, v') are a **local pair**, if forw(u), back(u'), forw(v), back(v') are contained in an inferior portion; otherwise a **global pair**.

To prove Block-disjointness, we combine the following two arguments.

- (I) When  $\mathsf{block}(u, u')$ ,  $\mathsf{block}(v, v')$  are a global pair, their intersection lies in the interior of P.
- (II) When block(u, u'), block(v, v') are a local pair, their intersection is empty!

Argument (I) easily follows from the peculiar property of the bounding-quadrants. (However, the idea to employ the bounding-quadrants for this proof is not straightforward.)

**Proof of (I).** Applying the peculiar property of quad (Lemma 15),

$$\mathsf{quad}_{forw(u)}^{back(u')}\cap\mathsf{quad}_{forw(v)}^{back(v')} \text{ lies in the interior of } P.$$

On the other side, by Lemma 17,

$$\mathsf{block}(u,u') \cap \mathsf{block}(v,v') \subset \mathsf{quad}_u^{u'} \cap \mathsf{quad}_v^{v'} = \mathsf{quad}_{forw(u)}^{back(u')} \cap \mathsf{quad}_{forw(v)}^{back(v')}$$

Together, the intersection of these two blocks lies in the interior of P.

Argument (II) is equivalent to the following fact. (Recall  $\Delta(c,c')$  in (15).)

▶ Fact 37. For extremal pair  $(e_c, e_{c'})$ , the blocks in  $BLOCK[\Delta(c, c')]$  are pairwise-disjoint.

As claimed in Subsection 2.5, we prove Fact 37 by using the monotonicity of the borders (Lemma 18 and its successor Lemma 36). First, we prove the following intermediate fact.

▶ Fact 38. For  $(e_a, e_{a'})$  in  $\Delta(c, c')$ , all blocks in BLOCK[U(a, a')] are pairwise-disjoint, where

$$\mathsf{U}(a,a') = \{(u,u') \mid u \text{ is chasing } u', \text{ and } u,u' \text{ lie in } (v_a \circlearrowright v_{a'+1})\}.$$

In the following two proofs, we use a new term "tiling" and a new notation  $SWEPT_O(X, Y)$ . Suppose S is a set of unit pairs. We call BLOCK[S] a tiling if all the blocks in BLOCK[S] are pairwise-disjoint. For distinct points O, X, Y, imaging that a ray originated at O rotates from OX to OY in clockwise, we denote by  $SWEPT_O(X, Y)$  the region swept by this ray.

**Proof of Fact 38.** We prove it by using induction on the number of edges k in  $(v_a \circlearrowright v_{a'})$ . *Initial:* k=2, i.e., a'=a+1.

 $BLOCK[\mathsf{U}(a,a')]$  contains exactly one block,  $\mathsf{block}(e_a,e_{a+1})$ , so the claim is trivial. Induction: k>2. Divide the unit pairs in  $\mathsf{U}(a,a')$  into four parts distinguished by whether  $\mathsf{U}(a,a'-1), \mathsf{U}(a+1,a')$  contain them. (See Figure 29.) Formally,

$$U_{10} = U(a, a'-1) - U(a+1, a'),$$
  $U_{01} = U(a+1, a') - U(a, a'-1),$   $U_{11} = U(a, a'-1) \cap U(a+1, a'),$   $U_{00} = U(a, a') - U(a, a'-1) - U(a+1, a').$ 

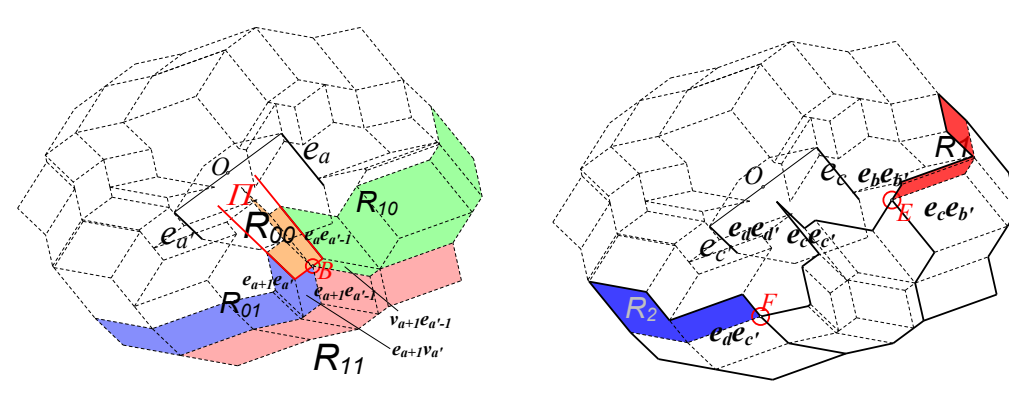


Figure 29 Proof of Fact 38

Figure 30 Proof of Fact 37

By the induction hypothesis,  $BLOCK[U_{01}]$ ,  $BLOCK[U_{10}]$ ,  $BLOCK[U_{11}]$  are tilings. Moreover, since  $U_{00} = \{(e_a, e_{a'}), (v_{a+1}, e_{a'}), (e_a, v_{a'}), (v_{a+1}, v_{a'})\}$  only contains four unit pairs, by the geometric definition of blocks, it can be simply checked that  $BLOCK[U_{00}]$  is also a tiling (details omitted). So, we only need to prove that  $R_{00}, R_{01}, R_{10}, R_{11}$  are pairwise-disjoint, where  $R_{00}, R_{01}, R_{10}, R_{11}$  denotes the regions occupied by  $BLOCK[U_{00}], BLOCK[U_{01}], BLOCK[U_{11}], BLOCK[U_{11}],$  respectively.

It reduces to prove the following four statements.

- (i)  $R_{11}$ ,  $R_{10}$  are disjoint.
- (ii)  $R_{11}, R_{01}$  are disjoint.
- (iii)  $R_{01}, R_{10}$  are disjoint. (Note: this is the kernel of the proof.)
- (iv)  $R_{00}$  is disjoint with the other three regions.

The first statement holds because BLOCK[U(a, a'-1)] is a tiling. The second holds because BLOCK[U(a+1, a')] is a tiling. We prove the other two in the following. See Figure 29.

Proof of (iii): Let  $O = M(v_a, v_{a'+1})$ . Let A be an arbitrary point in the opposite quadrant of  $quad_c^{c'}$ , and let B be the terminal point of the lower border of  $block(v_{a+1}, e_{a'-1})$ ; or equivalently, let B be the starting point of the lower border of  $block(e_{a+1}, v_{a'})$ . (Recall the definition of lower borders in Definition 31.) The key observations are the following:

 $R_{10} \subset \mathsf{SWEPT}_O(A, B) \text{ and } R_{01} \subset \mathsf{SWEPT}_O(B, A).$ 

The first observation is due to two reasons. 1. All borders of the blocks in  $BLOCK[U_{10}]$  are directed, and a point (X) can eventually reach to B by tracking down these borders. 2. While tracking down these borders, OX always rotates in clockwise by Lemma 36.

The second observation is due to symmetric reasons.

Further, since  $SWEPT_O(B, A)$  is disjoint with  $SWEPT_O(A, B)$ , we obtain (iii).

Proof of (iv): Let  $\Pi$  denote the region bounded by:  $\mathcal{C}_1$  - the right lower border of  $\mathsf{block}(e_a, e_{a'-1})$ ,  $\mathcal{C}_2$  - the left lower border of  $\mathsf{block}(e_{a+1}, e_{a'})$ , and  $\mathcal{C}_3$  - the lower border of  $\mathsf{block}(v_{a+1}, v_{a'})$ . We point out that (iv.1)  $R_{00}$  is contained in  $\Pi$ ; and (iv.2) the united region of  $R_{10}, R_{01}, R_{11}$  is also bounded by  $\mathcal{C}_1, \mathcal{C}_2$  and  $\mathcal{C}_3$  and hence is disjoint with  $\Pi$ . Together, we get (iv). The proofs of (iv.1) and (iv.2) are too burdensome and hence omitted.

**Proof of Fact 37.** For convenience, let  $(e_b, e_{b'}), (e_d, e_{d'})$  respectively denote the previous and next extremal pair of  $(e_c, e_{c'})$  in the frontier-pair-list. We divide  $\Delta(c, c')$  into three parts:

$$U_1 = (\Delta(c,c') - \mathsf{U}(c,c')) \cap \mathsf{U}(b,b'), \quad U_2 = (\Delta(c,c') - \mathsf{U}(c,c')) \cap \mathsf{U}(d,d'), \quad U_3 = \mathsf{U}(c,c').$$

It is obvious that  $\Delta(c, c') = U_1 \cup U_2 \cup U_3$ . See Figure 30 for an illustration, where  $R_1, R_2$  respectively indicate the regions occupied by  $BLOCK[U_1]$ ,  $BLOCK[U_2]$ .

By Fact 38, BLOCK[U(b,b')], BLOCK[U(c,c')], BLOCK[U(d,d')] are tilings. Therefore,  $BLOCK[U_1]$ ,  $BLOCK[U_2]$ ,  $BLOCK[U_3]$  are tilings. So, we only need to prove:

- (a) Each block in  $BLOCK[U_1]$  is disjoint with each in  $BLOCK[\Delta(c,c')-U_1]$ .
- (b) Each block in  $BLOCK[U_2]$  is disjoint with each in  $BLOCK[\Delta(c,c') U_2]$ . We only show the proof of (a); the proof of (b) is symmetric. Clearly, (a) follows from
- (a1) Each block in  $BLOCK[U_1]$  is disjoint with each in  $BLOCK[\Delta(c,c') U(b,b')]$ .
- (a2) Each block in  $BLOCK[U_1]$  is disjoint with each in  $BLOCK[U(b,b')-U_1]$ .

Proof of (a1): Let  $O = M(v_c, v_{c'+1})$  and let E be the common endpoint of the two lower borders of  $\mathsf{block}(e_c, e_{b'})$ . Similar to the key observations used in the proof of Fact 38, by applying Lemma 36, we have: the blocks in  $BLOCK[U_1]$  lie in  $\mathsf{SWEPT}_O(A, E)$  while the blocks in  $BLOCK[\Delta(c, c') - \mathsf{U}(b, b')]$  lie in  $\mathsf{SWEPT}_O(E, A)$ . Thus we obtain (a1).

Proof of (a2): Since BLOCK[U(b,b')] is a tiling and  $U_1 \subseteq U(b,b')$ , we have (a2).

# 4.3 Proof of Interleavity-of-f

## Step 1. A preliminary lemma.

Recall the definition of interleave between two oriented closed curve above Theorem 2. The following lemma proposes a general method to prove that some directed closed curve interleaves  $\partial P$ . It is used to prove the Interleaves  $\partial P$  interleaves  $\partial P$  below.

▶ Note 3. To understand the Interleavity-of-f correctly, we need to recall Note 1, which points out that when  $(e_c, e_{c'})$  is an extremal pair, a "corner point" of  $block(e_c, e_{c'})$  cannot be (and it is not) included in  $\sigma P$ . Otherwise the Interleavity-of-f would not hold. For example, in Figure 26, the lowermost corner of block(3,1) lies exactly on  $\partial P$ . If this point was counted as an intersection of  $\partial P \cap \sigma P$ , the Interleavity-of-f is wrong.

Before stating the following lemma, we need to recall moreover the definition of interleave between a directed curve  $\mathcal{D}$  and  $\partial P$ . We say  $\mathcal{D}$  interleaves  $\partial P$ , if it is disjoint with  $\partial P$  or the following holds. Starting from their first intersection point (according to the order among points in  $\mathcal{D}$ ), regardless of whether we travel along  $\mathcal{D}$  in its positive direction or along  $\partial P$  in clockwise, we would encounter the intersection points between  $\mathcal{D}$  and  $\partial P$  in the same order.

▶ **Lemma 39.** Given a directed closed curve C. Assume that it is cut into 2q  $(q \ge 3)$  fragments:  $\beta_1, \alpha_1, \ldots, \beta_q, \alpha_q$ , such that

for 
$$1 \le i \le q$$
, the concatenation of  $\alpha_{i-1}, \beta_i, \alpha_i$  interleaves  $\partial P$ .  $(\alpha_0 = \alpha_q)$ . (17)

Further assume that we can find 2q points  $S_1, T_1, \ldots, S_q, T_q$  lying in clockwise order around  $\partial P$  which "delimitate" the 2q fragments, by which we mean that

for  $1 \leq i \leq q$ , the intersections between  $\beta_i$  and  $\partial P$  are contained in  $[S_i \circlearrowright T_i]$ , and (18) for  $1 \leq i \leq q$ , the intersections between  $\alpha_i$  and  $\partial P$  are contained in  $[S_i \circlearrowright T_{i+1}]$ . (19)

Then, the given curve C interleaves  $\partial P$ . See the illustration in Figure 31.

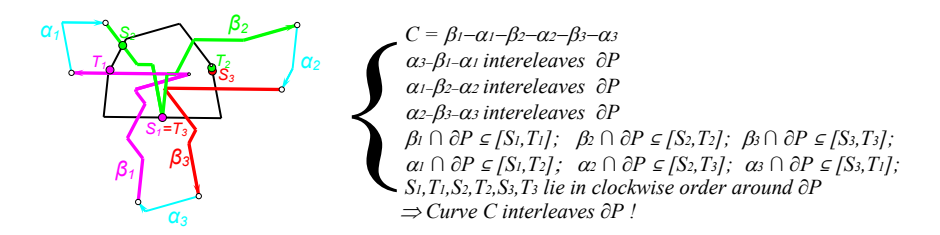


Figure 31 Illustration of Lemma 39.

**Proof.** Index  $\beta_1, \alpha_1, \ldots, \beta_q, \alpha_q$  the 1st, 2nd, etc., the 2q-th fragment.

Assume that at least one fragment in  $\alpha_1, \ldots, \alpha_q$  intersects  $\partial P$  (otherwise the consequence is much easier and actually trivial). Without loss of generality, assume that  $\alpha_q$  intersects  $\partial P$ .

Let  $(C - \alpha_q)$  denote the concatenation of the first 2q - 1 fragments. We state:

- (i) The curve  $\alpha_q$  interleaves  $\partial P$ .
- (ii) The curve  $(\mathcal{C} \alpha_q)$  interleaves  $\partial P$ .
- (iii) We can find two points A, B on  $\partial P$  such that the points in  $\alpha_q \cap \partial P$  are restricted in  $[A \circlearrowright B]$  while the points in  $(\mathcal{C} \alpha_q) \cap \partial P$  are restricted in  $[B \circlearrowleft A]$ .

Notice that C is the concatenation of  $\alpha_q$  and  $(C - \alpha_q)$ , statements (i), (ii), and (iii) together imply our result, which states that C interleaves  $\partial P$ .

**Proof of (i)**: This one simply follows from (17).

**Proof of (ii):** We need some notation here. Regard  $S_1$  as the starting point of the closed curve  $\partial P$ . For two points A, A' on  $\partial P$ , we say that A lies behind A' if A = A' or, A is encountered later than A' traveling around  $\partial P$  starting from  $S_1$ . We say that fragment  $\gamma$  lies behind fragment  $\gamma'$ , if all of the points in  $\gamma \cap \partial P$  lie behind all of the points in  $\gamma' \cap \partial P$ . Since each fragment interleaves  $\partial P$  according to (17), it reduces to prove that

for 1 < k < 2q, the k-th fragment lies behind the first k - 1 fragments.

Case 1: k = 2. By (19, 18), the points in  $\alpha_1 \cap \partial P$  and the points in  $\beta_1 \cap \partial P$  are contained in  $[S_1 \circlearrowright T_2]$ . Moreover, by (17), the concatenation of  $\beta_1, \alpha_1$  interleaves  $\partial P$ . Together,  $\alpha_1$  lies behind  $\beta_1$ , i.e. the 2-nd fragment lies behind the 1-st fragment.

Case 2: k>2 and k is odd. Assume the k-th fragment is  $\beta_i$ . Similar to Case 1,  $\beta_i$  lies behind the (k-1)-th fragment  $\alpha_{i-1}$ . By (19, 18), the first k-2 fragments have their intersections with  $\partial P$  lying in  $[S_1 \circlearrowright T_{i-1}]$  while  $\beta_i \cap \partial P$  lie in  $[S_i \circlearrowright T_i]$ , so the k-th fragment  $\beta_i$  lies behind the first k-2 fragments. Together, the k-th fragment lies behind all the first k-1 fragments.

Case 3: k > 2 and k is even. Assume the k-th fragment is  $\alpha_i$ . Similar to Case 1,  $\alpha_i$  lies behind the (k-1)-th and (k-2)-th fragments  $\beta_i, \alpha_{i-1}$ . Similar to Case 2,  $\alpha_i$  also lies behind the first k-3 fragments. Together, the k-th fragment lies behind all the first k-1 fragments.

**Proof of (iii)**: Points A, B are defined as the first and last points of  $\alpha_q \cap \partial P$ . (Recall that  $\alpha_q \cap \partial P \neq \emptyset$ ; so A, B are well defined.) Assume that  $A \neq B$ , otherwise it is trivial.

Clearly,  $\alpha_q \cap \partial P$  are contained in  $[A \circlearrowright B]$ . We only need to prove that  $(\mathcal{C} - \alpha_q) \cap \partial P \subset [B \circlearrowright A]$ , i.e. for each fragment beside  $\alpha_q$ , its intersections with  $\partial P$  lie in  $[B \circlearrowleft A]$ .

First, consider the four fragments  $\alpha_1, \beta_1, \alpha_{q-1}, \beta_q$ . By (17), the concatenation of  $\alpha_q, \beta_1, \alpha_1$ , or  $\alpha_{q-1}, \beta_q, \alpha_q$  interleaves  $\partial P$ . So, for these four fragments, their intersections with  $\partial P$  do not lie in  $(A \circlearrowright B)$ , and hence can only lie in  $[B \circlearrowleft A]$ .

Then, consider any fragment  $\gamma$  other than  $\alpha_q$  and does not belong to the four mentioned above. Applying (19, 18), the points in  $\gamma \cap \partial P$  lie in  $[S_2 \circlearrowright T_{q-1}]$ . Therefore, it reduces to prove that  $[S_2 \circlearrowright T_{q-1}] \subseteq [B \circlearrowright A]$ . The proof is as follows.

Applying (19),  $\alpha_q \cap \partial P$  are contained in  $[S_q \circlearrowright T_1]$ , and so  $[A \circlearrowright B] \subseteq [S_q \circlearrowright T_1]$ . Since  $S_1, T_1, \ldots, S_q, T_q$  lie in clockwise order around  $\partial P$ ,  $[S_q \circlearrowright T_1] \subseteq [T_{q-1} \circlearrowright S_2]$ . Together,  $[A \circlearrowleft B] \subseteq [T_{q-1} \circlearrowleft S_2]$ . Equivalently,  $[S_2 \circlearrowleft T_{q-1}] \subseteq [B \circlearrowleft A]$ .

#### Step 2. Definition of q, the 2q fragments, and the 2q points $S_1, T_1, \ldots, S_q, T_q$ .

To prove the Interleavity-of-f by applying the general method in Lemma 39, we now define  $q, \alpha, \beta, S, T$  explicitly.

We choose q to be the number of extremal pairs (see Definition 34). Fact 35 states that  $q \geq 3$ . Let us denote the q extremal pairs in clockwise order by  $(e_{c_1}, e_{c'_1}), \ldots, (e_{c_q}, e_{c'_q})$ .

Recall  $\Delta(c, c')$  in (15) and recall the bottom borders of frontier blocks in Section 3.4. For any extremal pair  $(e_c, e_{c'})$ , denote

$$\sigma(c,c') = \begin{array}{c} \text{the concatenation of the bottom borders of the} \\ \text{frontier blocks in } \{\mathsf{block}(u,u') \mid (u,u') \in \Delta(c,c')\}. \end{array} \tag{20}$$

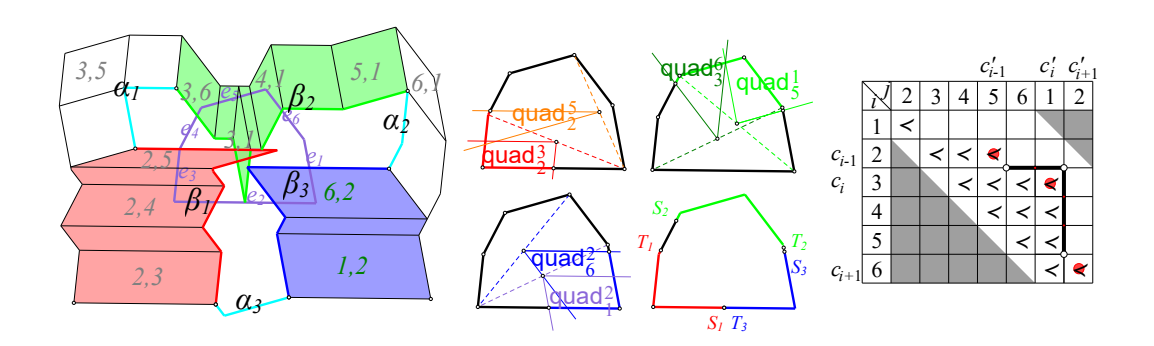


**Figure 32** Illustration of the proof of the Interleavity-of-f.

Notice that  $\sigma(c,c')$  is a directional curve and is a fraction of  $\sigma P$ . The dotted line in Figure 11 indicates  $\sigma(c,c')$ . Moreover, for each  $1 \le i \le q$ , we define two fragments:

$$\alpha_i$$
 = the fragment of  $\sigma P$  that is contained in both  $\sigma(c_i, c'_i)$  and  $\sigma(c_{i+1}, c'_{i+1})$ . (21)

$$\beta_i$$
 = the fragment that belongs to  $\sigma(c_i, c_i')$  but does not belong to  $\alpha_{i-1}$  or  $\alpha_i$ . (22)

See Figure 32 for an illustration of  $\beta_1, \alpha_1, \ldots, \beta_q, \alpha_q$ .

▶ Fact 40. Fragment  $\beta_i$  begins with the bottom border of block $(e_{a_i}, e_{a'_i})$  and ends with the bottom border of block $(e_{b_i}, e_{b'})$ , where

$$(a_i, a_i') = (c_i, c_{i-1}' + 1), (b_i, b_i') = (c_{i+1} - 1, c_i').$$
 (23)

This fact simply follows the definition and is illustrated in the right picture of Figure 32. Recall  $\langle \mathsf{quad} \rangle$  in (7). Use the notation  $a_i, a_i', b_i, b_i'$  given in Fact 40, we define the delimiting points  $S_1, \ldots, S_q, T_1, \ldots, T_q$  as follows. See the middle of Figure 32 for illustration.

$$S_i = \text{the starting point of } \langle \mathsf{quad} \rangle_{a_i}^{a_i'}$$

$$T_i = \text{the terminal point of } \langle \mathsf{quad} \rangle_{b_i}^{b_i'}.$$
(24)

#### Step 3. Verify the delimiting points lying in order and prove (17), (18), and (19).

In the following, we prove that  $S_1, T_1, \ldots, S_q, T_q$  lie in clockwise order around  $\partial P$  and prove three conditions (17), (18), and (19) in Lemma 39. These proofs together with Lemma 39 constitute a proof for the Interleavity-of-f.

Prove that  $S_1, T_1, \ldots, S_q, T_q$  lie in clockwise order around  $\partial P$ . Consider any pair of neighboring extremal pairs  $(e_{c_i}, e_{c'_i}), (e_{c_{i+1}}, e_{c'_{i+1}})$ . A key observation is that

edges 
$$b_i, b'_i, a_{i+1}, a'_{i+1}$$
 are not in any inferior portion

which follows Definition 34 and (23). According to this observation and applying the peculiar property of the bounding-quadrants (Lemma 15), for any i,  $\langle \mathsf{quad} \rangle_{b_i}^{b_i'}$  and  $\langle \mathsf{quad} \rangle_{a_{i+1}}^{a_{i+1}'}$  are disjoint (although their endpoints may coincide). Combining this with (24) and the monotonicity of the  $\langle \mathsf{quad} \rangle$  (Lemma 16), the q portions  $(S_1 \circlearrowright T_1), \ldots, (S_q \circlearrowright T_q)$  are pairwise-disjoint and lie in clockwise order.  $\blacksquare$ 

**Proof of (17).** Notice that the concatenation of  $\alpha_{i-1}, \beta_i, \alpha_i$  is exactly  $\sigma(c_i, c'_i)$ . We shall prove that for each extremal pair  $(e_c, e_{c'})$ , the curve  $\sigma(c, c')$  interleaves  $\partial P$ .

For ease of discussion, assume that  $\sigma(c, c')$  and  $\partial P$  have a finite number of intersections. Denote the intersections by  $I_1, \ldots, I_x$ , and assume that

(i) they are sorted by the priority on  $\sigma(c,c')$ .

Denote  $O = \mathsf{M}(v_c, v_{c'+1})$ . Since (i) and by applying Lemma 36, rays  $OI_1, \ldots, OI_x$  are in clockwise order. Further, because O lies in P, we get

(ii) points  $I_1, \ldots, I_x$  lie in clockwise order around  $\partial P$ .

Due to (i) and (ii) and since that  $I_1, \ldots, I_x$  are all the intersections between  $\sigma(c, c')$  and  $\partial P$ , we get: starting from  $I_1$ , regardless of traveling along  $\sigma(c, c')$  or  $\partial P$ , we meet their intersections in identical order. This means that  $\sigma(c, c')$  interleaves  $\partial P$ .

**Proof of (18).** Notice that  $\beta_i$  is the concatenation of bottom borders of some frontier blocks. Consider any frontier block whose bottom border is a fraction of  $\beta_i$ , e.g.  $\mathsf{block}(u, u')$ , we shall prove that (X) the intersections between its bottom border and  $\partial P$  lie in  $[S_i \circlearrowright T_i]$ .

Denote by  $\overline{\langle \mathsf{quad} \rangle_u^{u'}}$  the closed set of  $\langle \mathsf{quad} \rangle_u^{u'}$ , which contains  $\langle \mathsf{quad} \rangle_u^{u'}$  and its endpoints. By Lemma 17,  $\mathsf{block}(u,u') \subset \mathsf{quad}_u^{u'}$ . So, the bottom border of  $\mathsf{block}(u,u')$  lie in the closed set of  $\mathsf{quad}_u^{u'}$ . Therefore, the intersections between  $\partial P$  and the bottom border of  $\mathsf{block}(u,u')$  are contained in  $\overline{\langle \mathsf{quad} \rangle_u^{u'}}$ . Moreover, by the monotonicity of the  $\langle \mathsf{quad} \rangle$  (Lemma 16) and the definition (24) of  $S_i, T_i$ , we get  $\overline{\langle \mathsf{quad} \rangle_u^{u'}} \subseteq [S_i \circlearrowright T_i]$ . Together, we get (X).

(19) can be proved the same way as (18); proof omitted.

#### 4.4 Proof of Reversibility-of- f

The Reversiblity-of-f states that f is a bijection from  $\mathcal{T}^*$  to  $f(\mathcal{T}^*)$ . This property immediately follows from the Block-disjointness and Local-Reversibility of f.

**Proof.** Recall  $\mathcal{T}(u, u')$  in (9) and recall that the LOCAL-REVERSIBILITY OF f (Lemma 25) states that f is a bijection from  $\mathcal{T}(u, u')$  to  $\mathsf{block}(u, u')$ .

For each unit pair (u, u') such that u is chasing u', we call  $\mathcal{T}(u, u')$  a component of  $\mathcal{T}$ . Notice that each element of  $\mathcal{T}$  belongs to exactly one component.

Now, consider two elements of  $\mathcal{T}^*$ . If they belong to the same component, their images under function f are distinct according to the Local-reversibility of f. If they belong to distinct components, their images under f do not coincide, since otherwise there would be two distinct blocks with an intersection on the boundary of P, which contradicts the Block-disjointness. Therefore, f is a bijection from  $\mathcal{T}^*$  to  $f(\mathcal{T}^*)$ .

### **4.5** Proof of Monotonicity-of-*f*

Here we prove that  $f_2^{-1}()$  is circularly monotone. (See its rigorous definition in Theorem 2.)

K-points and K-portions. See Figure 33. Let  $K_1, \ldots, K_m$  denote all the intersections between  $\sigma P$  and  $\partial P$ , and assume that they lie in clockwise order around  $\partial P$ . Points  $K_1, \ldots, K_m$  divide  $\partial P$  into m portions; and we call each of them a K-portion.

**Figure 33** Illustration of MONOTONICITY of f. **Figure 34** Illustration of the outer boundary.

**Top borders.** Recall the lower border of blocks in Definition 31. (See Figure 7.) For each i, notice that  $\mathsf{block}(v_i, v_{i+1})$  is a curve, we define this curve as the  $top\ border$  of  $\mathsf{block}(v_i, v_{i+1})$ .  $\mathsf{block}(e_i, e_{i+1})$  is a parallelogram with four borders, we define the  $top\ border$  of  $\mathsf{block}(e_i, e_{i+1})$  to be the concatenation of those two borders that are opposite to its lower borders.

**Outer boundary of**  $f(\mathcal{T})$ . See Figure 34. The *outer boundary* of  $f(\mathcal{T})$  is defined to be the concatenation of the top borders of  $\mathsf{block}(e_1, e_2), \mathsf{block}(v_2, v_3), \ldots, \mathsf{block}(e_n, e_1), \mathsf{block}(v_1, v_2)$ .

- ▶ Fact 41. 1. All the top borders defined above lie outside P.
- **2.** The outer boundary of  $f(\mathcal{T})$  is a simple closed curve whose interior contains P.
- **3.** For every K-portion, it either lies entirely in  $f(\mathcal{T})$ , or lies entirely outside  $f(\mathcal{T})$ .
- **Proof.** 1. The top border of  $\mathsf{block}(v_i, v_{i+1})$  is  $\mathsf{block}(v_i, v_{i+1})$  itself, and by Lemma 17 it lies in  $\mathsf{quad}_i^i$  and hence lies outside P. The top border of  $\mathsf{block}(e_i, e_{i+1})$  is the concatenation of two borders; one is parallel to  $e_i$  and the other is parallel to  $e_{i+1}$ . Because  $\mathsf{block}(e_i, e_{i+1})$  lies in  $\mathsf{quad}_i^{i+1}$ , the former border lies on the left of  $e_i$  while the latter one lies on the left of  $e_{i+1}$ ; so both borders lie outside P. Therefore, all top borders lie outside P.
- 2. By definition, the outer boundary is the concatenation of the top borders. It is easy to see that the concatenation is a closed curve. (See Figure 34.) Moreover, by BLOCK-DISJOINTNESS, the top borders do not intersect in the exterior of P. Combine this with Claim 1, we see that the closed curve is simple and contains P in its interior.
- 3. Notice that  $f(\mathcal{T})$  has an annular shape which is bounded by its inner and outer boundaries. So, Claim 3 immediately follows from Claim 2 and the INTERLEAVITY-OF-f.
- ▶ Fact 42.  $K_1, \ldots, K_m$  are not contained in  $f(\mathcal{T})$ .

**Proof.** Consider any K-point  $K_i$ . Since  $K_i \in \sigma P$ , we can assume without loss of generality that  $K_i$  comes from the bottom border of the frontier block  $\mathsf{block}(u, u')$ .

We first argue that u, u' cannot both be vertices. For a contradiction, suppose that they are vertices. Then, u' must be the clockwise next vertex of u since  $\mathsf{block}(u, u')$  is a frontier block. This can be observed easily from Algorithm 1. Then, by Fact 41.1,  $\mathsf{block}(u, u')$  lies outside P, so its bottom border (which is the block itself) has no intersection with  $\partial P$ . This means  $K_i$  cannot come from the bottom border of  $\mathsf{block}(u, u')$ . Contradictory.

Therefore, u, u' comprise at least one edge. Then, according to Definition 31, we can check that the lower and bottom border of  $\mathsf{block}(u, u')$  is not contained  $\mathsf{block}(u, u')$ . (Some details are omitted for simplicity.) This further implies that  $K_i$  is not contained in  $f(\mathcal{T})$ .

# Extend the definition of $f_2^{-1}$ .

Recall  $f_2^{-1}()$  in Theorem 2. So far, it is defined on  $f(\mathcal{T}) \cap \partial P$ , but **not** on the K-points. This is implied by Fact 42. However, to prove the monotonicity of  $f_2^{-1}()$ , it is convenient to also define  $f_2^{-1}$  on the K-points. In fact, there is a natural way to extend the definition of  $f_2^{-1}$  on to those K-points, and this extension is given in the following.

Consider any K-point  $K_i$ . Assuming it comes from the bottom border of  $\mathsf{block}(u,u')$ , and recall the extended definition of  $f_{u,u'}^{-1,2}()$  above Definition 33, we define

$$f_2^{-1}(K_i) = f_{u,u'}^{-1,2}(K_i).$$

**Proof of the Monotonicity-of-**f . We state two observations first.

- (i) The value of  $f_2^{-1}$ () is continuous at the K-points.
- (ii) Function g is circularly monotone on curve  $\sigma P$ . (Recall g in Definition 33.)

The way we extend  $f_{u,u'}^{-1,2}()$  onto the lower border of  $\mathsf{block}(u,u')$  assures (i). Also according to this extension,  $f_{u,u'}^{-1,2}()$  is monotone on the lower border of  $\mathsf{block}(u,u')$ , which implies (ii).

We then state two more observations.

- (iii)  $f_2^{-1}(K_1), \ldots, f_2^{-1}(K_m)$  lie in clockwise order around  $\partial P$ .
- (iv) Function  $f_2^{-1}()$  is monotone on any K-portion that lies in  $f(\mathcal{T})$ , i.e., when point X travels along such a K-portion,  $f_2^{-1}(X)$  goes in clockwise order around  $\partial P$  non-strictly.

Proof of (iii): Since  $K_1, \ldots, K_m$  lie in clockwise around  $\partial P$ , they lie in clockwise around  $\sigma P$  due to the Interleavity-of-f, and thus  $g(K_1), \ldots, g(K_m)$  lie in clockwise around  $\partial P$  according to (ii). Furthermore, notice that  $f_2^{-1}(K_i) = g(K_i)$ , we obtain (iii).

Proof of (iv): This follows from the LOCAL-MONOTONICITY OF f (Lemma 27); when X travels along a K-portion that lies in  $f(\mathcal{T})$ , it travels inside some blocks. (See Figure 33.)

We now complete the proof. By Fact 41.3, region  $f(\mathcal{T}) \cap \partial P$  consists of those K-portions who lie entirely in  $f(\mathcal{T})$ . Imagine that a point X travels around  $f(\mathcal{T}) \cap \partial P$  in clockwise; (iv) assures that  $f_2^{-1}(X)$  is monotone inside each K-portion, whereas (i) and (iii) assure that  $f_2^{-1}(X)$  is monotone between the K-portions. See Figure 33 for an illustration.

### 4.6 Proof of Sector-monotonicity

The Sector-Monotonicity states that  $\operatorname{sector}(v_1) \cap \partial P$ ,  $\operatorname{sector}(e_1) \cap \partial P$ , ...,  $\operatorname{sector}(v_n) \cap \partial P$ ,  $\operatorname{sector}(e_n) \cap \partial P$  are pairwise-disjoint and lie in clockwise order around  $\partial P$ . It immediately follows from Monotonicity-of-f.

**Proof.** For any unit w,

$$\begin{split} \operatorname{sector}(w) \cap \partial P &= \left\{ f(X_1, X_2, X_3) \mid (X_1, X_2, X_3) \in \mathcal{T}^*, X_2 \in w \right\} \\ &= \left\{ Y \in f(\mathcal{T}) \cap \partial P \mid f_2^{-1}(Y) \in w \right\} \\ &= \left\{ Y \in f(\mathcal{T}) \cap \partial P \mid \mathbf{u}(f_2^{-1}(Y)) = w \right\}. \end{split}$$

Consider the points in  $f(\mathcal{T}) \cap \partial P$ . Clearly,  $\mathbf{u}(f_2^{-1}())$  is a function on these points that maps them to the 2n units of P. Follows from the Monotonicity-off,  $\mathbf{u}(f_2^{-1}())$  is circularly monotone on these points. So,  $\mathbf{u}(f_2^{-1}())$  implicitly divides  $f(\mathcal{T}) \cap \partial P$  into 2n parts which are pairwise-disjoint and lie in clockwise order around  $\partial P$ . Moreover, according to the above equation, these 2n parts are precisely  $\mathsf{sector}(v_1) \cap \partial P$ ,  $\mathsf{sector}(e_1) \cap \partial P$ , ...,  $\mathsf{sector}(v_n) \cap \partial P$ ,  $\mathsf{sector}(e_n) \cap \partial P$ . Therefore, we obtain the Sector-Monotonicity .

# 5 Proof of the Sector-continuity

Assume that V is a fixed vertex of P throughout this section. Recall that

$$\begin{split} & \mathsf{sector}(V) &:= & f(\{(X_1, X_2, X_3) \in \mathcal{T} \mid X_2 \in V\}), \text{ and} \\ & \mathsf{sector}(V) &= & 2\text{-scaling of}\left(\bigcup_{u \text{ is chasing } u', \text{ and } \zeta(u, u') \text{ contains } V} u \oplus u'\right) \text{ w.r.t } V. \end{split}$$

The second equation is stated in (8) and is proved below.

$$\begin{split} &\operatorname{sector}(V) = &f\left(\left\{(X_1, X_2, X_3) \in \mathcal{T} \mid X_2 = V\right\}\right) \quad \text{(By definition (5))} \\ &= &f\left(\bigcup_{u \text{ is chasing } u'} \left\{(X_1, X_2, X_3) \mid X_1 \in u', X_2 = V, X_2 \in \zeta(u, u'), X_3 \in u\right\}\right) \\ &= &f\left(\bigcup_{u \text{ is chasing } u', V \in \zeta(u, u')} \left\{(X_1, V, X_3) \mid X_3 \in u, X_1 \in u'\right\}\right) \\ &= &\bigcup_{u \text{ is chasing } u', V \in \zeta(u, u')} f\left(\left\{(X_1, V, X_3) \mid X_3 \in u, X_1 \in u'\right\}\right) \\ &= &\bigcup_{u \text{ is chasing } u', V \in \zeta(u, u')} 2\text{-scaling of } \left(u \oplus u'\right) \text{ with respect to } V \\ &= &2\text{-scaling of } \left(\bigcup_{u \text{ is chasing } u', V \in \zeta(u, u')} u \oplus u'\right) \text{ with respect to } V. \quad \blacktriangleleft \end{split}$$

**Outline of this section.** Recall the sketch in Subsection 2.5.

1. Introduce two delimiting edges  $e_{s_V}$ ,  $e_{t_V}$  to study set  $\Lambda_V$ , where

$$\Lambda_V := \{(u, u') \mid u \text{ is chasing } u', \text{ and } \zeta(u, u') \text{ contains } V\}.$$
 (25)

- 2. Define a region  $\operatorname{mid}_V$  based on  $e_{s_V}$  and  $e_{t_V}$  and prove an equivalent description of  $\Lambda_V$  based on  $\operatorname{mid}_V$ . Also, define two boundaries  $\mathcal{L}_V$ ,  $\mathcal{R}_V$  of  $\operatorname{mid}_V$ . The 2-scaling of  $\operatorname{mid}_V$ ,  $\mathcal{L}_V$ ,  $\mathcal{R}_V$  with respect to V are respectively denoted by  $\operatorname{mid}_V^\star$ ,  $\mathcal{L}_V^\star$ ,  $\mathcal{R}_V^\star$ .
- 3. Prove the key observation:  $\operatorname{mid}_V^{\star}$  equals to the closed set of  $\operatorname{sector}(V)$ . Based on this observation, further obtain that  $\mathcal{L}_V^{\star}, \mathcal{R}_V^{\star}$  are boundaries of  $\operatorname{sector}(V)$ .
- **4.** Prove the Sector-continuity. Show that either of  $\mathcal{L}_V^{\star}$ ,  $\mathcal{R}_V^{\star}$  has at most one intersection with  $\partial P$ , and  $\operatorname{sector}(V) \cap \partial P$  is a boundary-portion from  $\mathcal{L}_V^{\star} \cap \partial P$  to  $\mathcal{R}_V^{\star} \cap \partial P$ .

# 5.1 Step 1 - Two delimiting edges $e_{s_V}, e_{t_V}$ for bounding $\Lambda_V$

We say that  $e_i$  is smaller than  $e_j$  or  $e_j$  is larger than  $e_i$  (with respect to V), if  $e_i$  would appear earlier than  $e_j$  when we enumerate all edges in clockwise order, starting from forw(V). We denote by  $e_i \leq_V e_j$  if  $e_i$  is smaller than or identical to  $e_j$ .

**Definition 43.** Recall that  $D_i$  is the furthest vertex to  $\ell_i$ . For any edge  $e_i$ , denote

$$\omega_{i}^{+} = \bigcup_{e_{j}: e_{i} \prec e_{j}} [v_{i+1} \circlearrowright Z_{i}^{j}] = [v_{i+1} \circlearrowright Z_{i}^{back(\mathsf{D}_{i})}], 
\omega_{i}^{-} = \bigcup_{e_{k}: e_{k} \prec e_{i}} [Z_{k}^{i} \circlearrowright v_{i}] = [Z_{forw(\mathsf{D}_{i})}^{i} \circlearrowright v_{i}].$$
(26)

Define  $e_{s_V}$  to be the smallest edge  $e_i$  such that  $\omega_i^+$  contains V. Define  $e_{t_V}$  to be the largest edge  $e_i$  such that  $\omega_i^-$  contains V. Figure 35 illustrates these definitions by an example.

Notice that portion  $\omega_{back(V)}^+$  always contains V. So, there is at least one element in  $\omega^+$  which contains V. Therefore,  $e_{s_V}$  is well defined. Denote  $s_V$  by s for short.

Notice that portion  $\omega_{forw(V)}^-$  always contains V. So, there is at least one element in  $\omega^-$  which contains V. Therefore,  $e_{t_V}$  is well defined. Denote  $t_V$  by t for short.

**Note:** The definition of  $e_s, e_t$  is essentially complicated and can hardly be simplified.

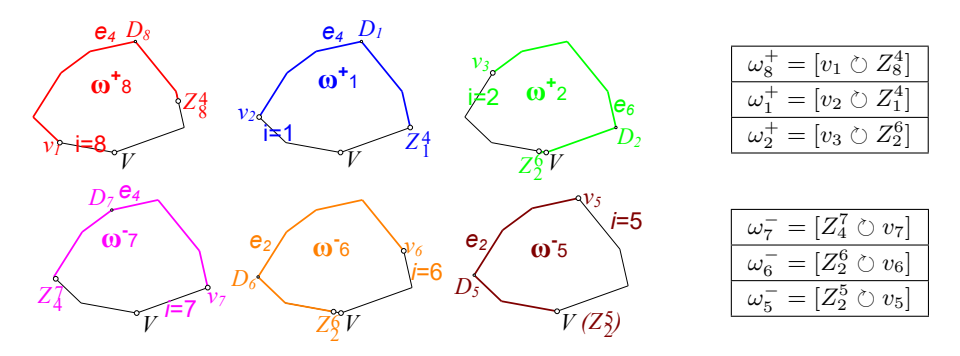


**Figure 35** Demonstration of the definitions of  $s_V$  and  $t_V$ . Here,  $s_V = 2, t_V = 5$ .

▶ Fact 44.  $e_s \leq e_t$  and the inferior portion  $[v_s \circlearrowright v_{t+1}]$  does not contain V.

**Proof.** Assume  $V = v_1$  for simplicity. This proof is divided into three parts.

1) We argue that  $e_s \leq_V e_t$ . To this end, we introduce two edges:  $e_{s^*} = forw(\mathsf{D}_n)$  and  $e_{t^*} = back(\mathsf{D}_1)$ , and we give the following observation. (i)  $e_s \leq_V e_{s^*}$  and  $e_{t^*} \leq_V e_t$ . Proof of (i): See Figure 36 (a). By Fact 21,  $Z_{s^*}^n$  lies in  $(V \circlearrowright v_{s^*})$ . Therefore,  $V \in [v_{s^*+1} \circlearrowright Z_{s^*}^n]$ . Moreover,  $[v_{s^*+1} \circlearrowright Z_{s^*}^n] \subseteq \omega_{s^*}^+$  by the definition of  $\omega_{s^*}^+$ . Therefore,  $V \in \omega_{s^*}^+$ , which implies  $e_s \leq_V e_{s^*}$  due to the definition of s. Symmetrically,  $V \in \omega_{t^*}^-$  and thus  $e_{t^*} \leq_V e_t$ .

We now discuss two cases to show that  $e_s \leq_V e_t$ .

Case 1  $D_1 \neq D_n$ . In this case  $e_{s^*} \leq_V e_{t^*}$ . Combining with (i), we get  $e_s \leq_V e_t$ .

Case 2  $D_1 = D_n$ . See Figure 36 (b). In this case  $Z_{t^*}^{s^*}$  is defined since  $e_{s^*}$  is the next edge of  $e_{t^*}$ .

Case 2.1  $Z_{t^*}^{s^*}$  lies in  $[V \circlearrowright \mathsf{D}_1]$ . In this subcase, we argue that  $e_s \leq_V e_{t^*}$ . Since  $V \in [\mathsf{D}_1 \circlearrowright Z_{t^*}^{s^*}]$ , whereas  $[\mathsf{D}_1 \circlearrowright Z_{t^*}^{s^*}] = [v_{t^*+1} \circlearrowright Z_{t^*}^{s^*}] \subseteq \omega_{t^*}^+$ , we get  $V \in \omega_{t^*}^+$ , which implies that  $e_s \leq_V e_{t^*}$  according to the definition of s. Then, combine  $e_s \leq_V e_{t^*}$  with  $e_{t^*} \leq_V e_t$  stated in (i), we get  $e_s \leq_V e_t$ .

Case 2.2  $Z_{t^*}^{s^*}$  lies in  $[D_1 \circlearrowright V]$ . In this subcase, we argue that  $e_{s^*} \leq_V e_t$ . The proof is symmetric to Case 2.1 and omitted. Then, combine  $e_{s^*} \leq_V e_t$  with  $e_s \leq_V e_{s^*}$  stated in (i), we get  $e_s \leq_V e_t$ .

**2)** We now prove that  $[v_s \circlearrowright v_{t+1}]$  does not contain V. By the definition of  $\omega^+$ , we get  $V \notin \omega^+_{forw(V)}$ , which means  $e_s \neq forw(V)$ , i.e.  $V \neq v_s$ . Symmetrically,  $V \neq v_{t+1}$ . In addition, applying  $e_s \leq_V e_t$ , we get  $V \notin (v_s \circlearrowright v_{t+1})$ . Altogether,  $V \notin [v_s \circlearrowright v_{t+1}]$ .

3) We now prove  $e_s \leq e_t$ . For a contradiction, suppose that  $e_t \prec e_s$ . See Figure 36 (c). Denote  $e_a = back(\mathsf{D}_s)$  and  $e_b = forw(\mathsf{D}_t)$ . If  $\mathsf{D}_s \neq \mathsf{D}_t$ , denote  $\rho = [\mathsf{D}_s \circlearrowleft \mathsf{D}_t]$ ; otherwise, let  $\rho$  denote the entire boundary of P and assume that it starts and terminates at  $\mathsf{D}_s$ . Consider points  $Z_s^a$  and  $Z_b^t$ , which lie in  $\rho$  according to Fact 22. The following inequalities contradict

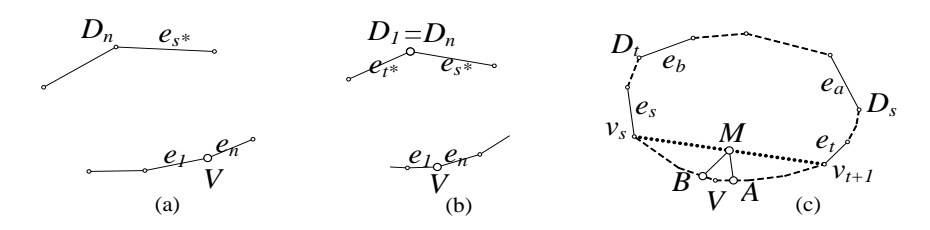


**Figure 36** Illustration of the proof of the relation between  $e_s, e_t$  and V

each other.

(I) 
$$Z_b^t \leq_{\rho} Z_s^a$$
, and (II)  $Z_s^a <_{\rho} Z_b^t$ .

Proof of (I). By definition of s, we have  $V \in \omega_s^+ = [v_{s+1} \circlearrowright Z_s^a]$ . This means  $V \leq_{\rho} Z_s^a$ . By definition of t, we have  $V \in \omega_t^- = [Z_b^t \circlearrowright v_t]$ . This means  $Z_b^t \leq_{\rho} V$ . Together, we get (I).

Proof of (II). Let  $M = M(v_s, v_{t+1})$ . Recall that  $p_i(X)$  denotes the unique line at point X that is parallel to  $e_i$ . Let A be the intersection of  $p_s(M)$  and  $[v_{t+1} \circlearrowright v_s]$ , and B the intersection of  $p_t(M)$  and  $[v_{t+1} \circlearrowright v_s]$ . We claim that  $Z_s^a <_{\rho} A <_{\rho} B <_{\rho} Z_b^t$ , which implies (II).

The inequality  $A <_{\rho} B$  follows from the assumption  $e_t \prec e_s$ . We prove  $Z_s^a <_{\rho} A$  in the following; the proof of  $B <_{\rho} Z_b^t$  is symmetric. Denote by h the open half-plane delimited by  $p_s(M)$  and containing  $v_{t+1}$ . Because  $D_s$  has a larger distance to  $\ell_s$  than  $v_{t+1}$ , the mid point of  $v_s$  and  $D_s$  is contained in h, which implies that the opposite quadrant of quads, together with its boundary, are contained in h. Moreover, by Fact 29,  $Z_s^a$  lies in or on the boundary of the opposite quadrant of quad<sup>a</sup><sub>s</sub>. So,  $Z_s^a$  lies in h, which implies that  $Z_s^a <_{\rho} A$ .

▶ Fact 45. Assume u is chasing u' and  $\zeta(u, u')$  contains V. Then u, u' both lie in  $[v_s \circlearrowright v_{t+1}]$ .

**Proof.** Let  $e_a = back(u), e_{a'} = back(u'), e_b = forw(u), e_{b'} = forw(u')$ . Notice that  $V \in$  $\zeta(u,u')=[Z_a^{a'}\circlearrowright Z_b^{b'}]\subseteq [v_{b+1}\circlearrowright Z_b^{b'}]\subseteq \omega_b^+$ . So,  $V\in\omega_b^+$ . This implies that  $e_s\leq_V e_b$  by the definition of s. Symmetrically,  $V \in \omega_{a'}^-$ , which implies that  $e_{a'} \leq_V e_t$  by the definition of t.

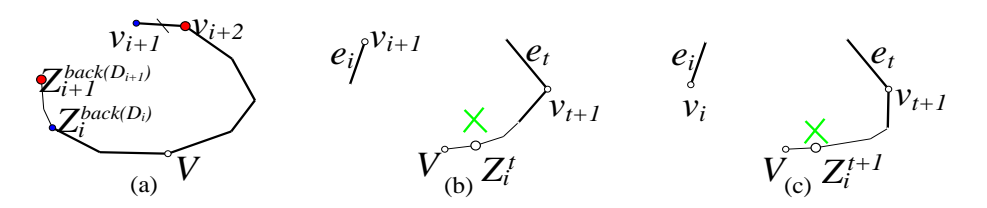
Since u is chasing u', we have  $forw(u) \leq back(u')$ . Together,  $e_s \leq_V forw(u) \leq$  $back(u') \leq_V e_t$ . Further since  $e_s \leq e_t$  (By Fact 44), we get  $e_s \leq_V forw(u) \leq_V back(u') \leq_V$  $e_t$ , which implies that u, u' both lie in the inferior portion  $[v_s \circlearrowright v_{t+1}]$ .

#### Two more observations of $e_s$ and $e_t$ that are useful in the next subsections.

- ▶ Fact 46. 1. For any edge  $e_i$ ,  $V \in \omega_i^+$  if and only if  $e_s \leq_V e_i$ .
- **2.** For any edge  $e_j$ ,  $V \in \omega_j^-$  if and only if  $e_j \leq_V e_t$ ,

**Proof.** We only give the proof of Claim 1. Claim 2 is symmetric.

The "only if" part follows from the definition of s. We shall prove that  $V \in \omega_i^+$  for  $e_i \in \{e_s, e_{s+1}, \dots, back(V)\}$ . We prove it by induction. Recall that  $\omega_i^+ = [v_{i+1} \circlearrowright Z_i^{back(\mathsf{D}_i)}]$ . Initially, let i = s. We know  $[v_{s+1} \circlearrowright Z_s^{back(\mathsf{D}_s)}]$  contains V by the definition of s. Next, consider  $\omega_{i+1}^+ = [v_{i+2} \circlearrowright Z_{i+1}^{back(\mathsf{D}_{i+1})}]$ . See Figure 37 (a). By the bi-monotonicity of the Z-points,  $Z_{i+1}^{back(\mathsf{D}_{i+1})}$  lies in  $[Z_i^{back(\mathsf{D}_i)} \circlearrowright v_{i+1}]$ . This implies that  $\omega_{i+1}^+$  contains V.



- **Figure 37** Illustrations of the proofs of Fact 46 and Fact 47.
- ▶ Fact 47. Denote  $\rho = [v_{t+1} \circlearrowright v_s]$ . Consider any edge  $e_i$  in  $[v_s \circlearrowright v_{t+1}]$ . We claim:
- 1. If  $e_i \prec e_t$  and  $Z_i^t <_{\rho} V$ , we have  $e_i \prec e_{t+1}$ .
- 2. If  $e_i \prec e_{t+1}$ , point  $Z_i^{t+1}$  lies in  $(V \circlearrowleft v_i)$ .

Consider any edge  $e_j$  in  $[v_s \circlearrowright v_{t+1}]$ . We claim:

- 3. If  $e_s \prec e_j$  and  $Z_s^j >_{\rho} V$ , we have  $e_{s-1} \prec e_j$ . 4. If  $e_{s-1} \prec e_j$ , point  $Z_{s-1}^j$  lies in  $(v_{j+1} \circlearrowright V)$ .
- **Proof.** We only prove Claim 1 and 2. Claims 3, 4 are symmetric to 1, 2, respectively.

Proof of 1: For a contradiction, suppose that  $e_i \not\prec e_{t+1}$ , as shown in Figure 37 (b). This means  $\mathsf{D}_i = v_{t+1}$ , which further implies  $\omega_i^+ = [v_{i+1} \circlearrowright Z_i^t]$ . Combining this equation with the assumption  $Z_i^t <_{\rho} V$ , we see  $\omega_i^+$  does not contain V, However, since  $e_i$  is an edge in  $[v_s \circlearrowright v_{t+1}]$ , we know  $e_s \leq_V e_i$  and so  $\omega_i^+$  contains V by Fact 46. Contradictory.

Proof of 2: For a contradiction, suppose that  $Z_i^{t+1}$  does not lie in  $(V \circlearrowright v_i)$ . Then, it must lie in  $[v_{t+1} \circlearrowright V]$  according to Fact 21.1, as shown in Figure 37 (c). So  $[Z_i^{t+1} \circlearrowright v_t]$  contains V. Moreover, noticing that  $[Z_i^{t+1} \circlearrowright v_t] \subseteq \omega_{t+1}^-$ , we get  $V \in \omega_{t+1}^-$ . This means  $e_t$  is not the largest edge such that  $\omega_t^-$  contains V, which contradicts the definition of  $e_t$ .

# 5.2 Step 2 - Definition of $mid_V$ and an equivalent description of $\Lambda_V$

The definition of  $\mathsf{mid}_V$  and its two boundaries  $\mathcal{L}_V, \mathcal{R}_V$  is presented in Subsection 2.5 and illustrated in Figure 15. Here, we add a fact which is implicitly applied in this definition. Recall  $\Delta_V = \{(u, u') \mid u, u' \in [v_s \circlearrowright v_{t+1}], u < u', \text{ and they are not incident}\}.$ 

▶ Fact 48. Regions in  $\{u \oplus u' \mid (u, u') \in \Delta_V\}$  (see Figure 15 (a)) are pairwise-disjoint.

**Proof.** A parallelogram is *degenerate* if all of its four corners lie in the same line. Otherwise, it is *non-degenerate*. First, we state that

(i) a non-degenerate parallelogram cannot be inscribed in any inferior portion of P.

For a contradiction, suppose that points A, B, C, D lie in clockwise order on a inferior portion  $\rho$  and that they constitute a non-degenerated parallelogram. See Figure 38. Consider forw(A) and back(D). Since  $\rho$  is an inferior portion,  $forw(A) \leq back(D)$ . However, since D, A are neighboring corners of a parallelogram,  $back(D) \prec forw(A)$ . Contradictory.

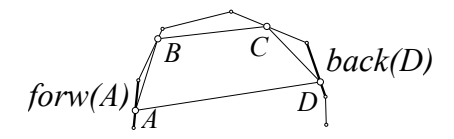


Figure 38 Non-degenerate parallelogram cannot be inscribed in an inferior portion.

Now, suppose to the opposite that  $(u_1, u_1'), (u_2, u_2')$  are distinct unit pairs in  $\Delta_V$  and that  $u_1 \oplus u_1'$  intersects  $u_2 \oplus u_2'$ . This means there exist four points A, A', B, B' such that  $A \in u_1, A' \in u_1', B \in u_2, B' \in u_2'$  and that  $\mathsf{M}(A, A') = \mathsf{M}(B, B')$ .

Because  $\mathsf{M}(A,A') = \mathsf{M}(B,B')$ , polygon ABA'B' is a parallelogram. Moreover, this parallelogram is non-degenerate. Suppose otherwise that A,B,A',B' lie in the same line. Then we can find  $e_i$  such that  $[v_i \circlearrowright v_{i+1}]$  contains A,B,A',B'. Since  $A,B \in [v_i \circlearrowright v_{i+1}]$ , units  $u_1,u_1'$  belong to  $\{v_i,e_i,v_{i+1}\}$ . However,  $u_1,u_1'$  are non-incident and  $u_1 < u_1'$  since  $(u_1,u_1') \in \Delta_V$ . So  $(u_1,u_1') = (v_i,v_{i+1})$ . Also,  $(u_2,u_2') = (v_i,v_{i+1})$ . So,  $(u_1,u_1') = (u_2,u_2')$ . Contradictory. Furthermore, we claim that ABA'B' is inscribed in the inferior portion  $[v_s \circlearrowright v_{t+1}]$ . This because  $u_1,u_1',u_2,u_2'$  lie in  $[v_s \circlearrowright v_{t+1}]$  by the assumption  $(u_1,u_1'),(u_2,u_2') \in \Delta_V$ .

Altogether, ABA'B' is a non-degenerate parallelogram inscribed in an inferior portion. This contradicts (i). Therefore, regions in  $\{u \oplus u' \mid (u, u') \in \Delta_V\}$  are pairwise-disjoint.

By introducing  $mid_V$ , we give the following description of  $\Lambda_V$ .

▶ Fact 49.  $(u, u') \in \Lambda_V$  if and only if  $[(u, u') \in \Delta_V, u \oplus u' \subseteq \mathsf{mid}_V, \text{ and } u \text{ is chasing } u']$ .

**Note:** Although  $e_s \leq e_t$ , set  $\Delta_V$  sometimes may contain unit pair (u, u') such that u is not chasing u'. For example,  $(v_s, v_{t+1}) \in \Delta_V$ , but it is possible that  $v_s$  is not chasing  $e_{t+1}$ .

**Proof.** According to (25) and Fact 45,  $\Lambda_V \subseteq \{(u, u') \mid (u, u') \in \Delta_V, u \text{ is chasing } u'\}$ . Thus it reduces to prove that for each unit pair  $(u, u') \in \Delta_V$  such that u is chasing u',

$$\zeta(u, u') \text{ contains } V \iff u \oplus u' \subseteq \mathsf{mid}_V.$$
 (27)

First, consider the trivial case s=t, where  $(v_s,v_{t+1})$  is the only unit pair in  $\Delta_V$  so that u is chasing u' (notice that  $v_i$  is always chasing  $v_{i+1}$ .) By definition of  $\mathsf{mid}_V$ , it equals  $v_s \oplus v_{t+1}$ . So it reduces to show that  $\zeta(v_s,v_{t+1})$  contains V. By Fact 47.2 and 47.4,  $Z_s^{t+1}$  lies in  $(V \circlearrowright v_s)$  whereas  $Z_{s-1}^t \in (v_{t+1} \circlearrowright V)$ . So,  $V \in [Z_{s-1}^t \circlearrowright Z_s^{t+1}]$ , namely,  $V \in \zeta(v_s,v_{t+1})$ .

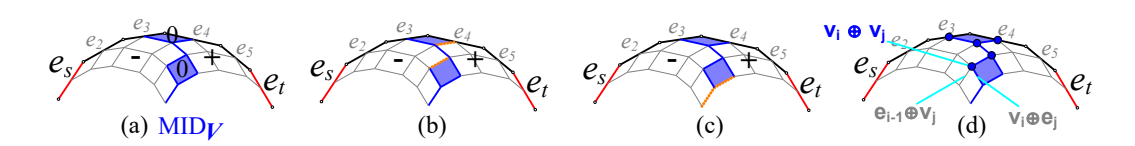


Figure 39 Illustration of Statement (27).

Assume now  $s \neq t$ . Let  $\rho = [v_{t+1} \circlearrowright v_s]$ . Take an arbitrary unit pair  $(u, u') \in \Delta_V$  such that u is chasing u'. We prove (27) by the following case by case discussion.

- Case 1: u, u' are both edges. By definition of  $\operatorname{mid}_V$ ,  $u \oplus u' \subseteq \operatorname{mid}_V \Leftrightarrow [u \oplus u']$  is marked by '0']  $\Leftrightarrow Z_u^{u'} = V$ . By definition of  $\zeta$  in (2),  $V \in \zeta(u, u') \Leftrightarrow Z_u^{u'} = V$ . Together, (27) holds.
- Case 2.1:  $(u, u') = (e_i, v_j)$  where  $j \neq t+1$ . See the dotted segments in Figure 39 (b). We have  $u \oplus u' \subseteq \mathsf{mid}_V \Leftrightarrow [e_i \oplus e_{j-1}]$  is marked by '0/-' whereas  $e_i \oplus e_j$  is marked by '0/+']  $\Leftrightarrow [Z_i^{j-1} \leq_{\rho} V \leq_{\rho} Z_j^i] \Leftrightarrow V \in \zeta(e_i, v_j)$ . In particular, the first " $\Leftrightarrow$ " is by the definition of  $\mathsf{mid}_V$ , the last " $\Leftrightarrow$ " is by the definition of  $\zeta$ .
- Case 2.2:  $(u,u')=(e_i,v_{t+1})$ . See the dotted segments in Figure 39 (c). We have  $u\oplus u'\subseteq \mathsf{mid}_V\Leftrightarrow [e_i\oplus e_t \text{ is marked by '0/-'}]\Leftrightarrow Z_i^t\leq_\rho V\Leftrightarrow V\in\zeta(u,u')$ . Here, the last " $\Leftrightarrow$ " is non-obvious and is proved in the following. Since  $u=e_i$  is chasing  $u'=v_{t+1}$ , we know  $e_i\prec e_{t+1}$ . Moreover, by Fact 47.2,  $Z_i^{t+1}\in (V\circlearrowright v_i)$ . This implies that  $Z_i^t\leq_\rho V\Leftrightarrow V\in\zeta(u,u')$ .
- Case 2.3: u is a vertex and u' is an edge. This is symmetric to Case 2.1 or Case 2.2.
- Case 3.1:  $(u, u') = (v_s, v_{t+1})$ . (This does not necessarily occur since  $v_s$  may not be chasing  $v_{t+1}$ .) Since u is chasing u', we have  $e_{s-1} \prec e_t$  and  $e_s \prec e_{t+1}$ . By Fact 47.2 and 47.4,  $Z_{s-1}^t$  lies in  $(v_{t+1} \circlearrowright V)$ , whereas  $Z_s^{t+1}$  lies in  $(V \circlearrowright v_s)$ . Therefore, V lies in  $[Z_{s-1}^t \circlearrowleft Z_s^{t+1}] = \zeta(v_s, v_{t+1})$ . Moreover,  $v_s \oplus v_{t+1}$  must be contained in mid $_V$ . Thus (27) holds.
- Case 3.2:  $(u, u') = (v_i, v_j)$  where  $i \neq s$  and  $j \neq t+1$ . See the dots in Figure 39 (d) for illustrations. We have  $v_i \oplus v_j \subseteq \mathsf{mid}_V \Leftrightarrow [e_{i-1} \oplus v_j \subseteq \mathsf{mid}_V \text{ or } v_i \oplus e_j \subseteq \mathsf{mid}_V] \Leftrightarrow [V \in \zeta(e_{i-1}, v_j) \text{ or } V \in \zeta(v_i, e_j)] \Leftrightarrow [V \in \zeta(v_i, v_j)]$ . The last second " $\Leftrightarrow$ " applies the results in Case 2. The last " $\Leftrightarrow$ " applies the fact that  $\zeta(v_i, v_j)$  is the concatenation of  $\zeta(e_{i-1}, v_j)$  and  $\zeta(v_i, e_j)$ .
- Case 3.3:  $[u = v_s \text{ and } u' \text{ is a vertex other than } v_{t+1}]$  or  $[u' = v_{t+1} \text{ and } u \text{ is a vertex other than } v_s]$ . The proof of this case is similar to those of Case 3.1 and Case 3.2 and is omitted.

# **5.3** Step 3 - $mid_V^*$ is the closed set of sector(V)

Recall  $\mathsf{sector}(V) = 2$ -scaling of  $\left(\bigcup_{(u,u') \in \Lambda_V} u \oplus u'\right)$  w.r.t V. For convenience, denote

$$\frac{1}{2} \operatorname{sector}(V) = \frac{1}{2} \operatorname{-scaling} \text{ of } \operatorname{sector}(V) \text{ w.r.t } V = \bigcup_{(u,u') \in \Lambda_V} u \oplus u'. \tag{28}$$

Consider all regions in  $\{u \oplus u' \mid (u,u') \in \Delta_V, u \text{ is chasing } u'\}$ . By the definition of  $\Lambda_V$  and  $\frac{1}{2}\mathsf{sector}(V)$ , such a region lies in  $\frac{1}{2}\mathsf{sector}(V)$  if and only if  $\zeta(u,u')$  contains V. On the other hand, Fact 49 shows that such a region lies in  $\mathsf{mid}_V$  if and only if  $\zeta(u,u')$  contains V. Therefore, we obtain the following close connection between  $\frac{1}{2}\mathsf{sector}(V)$  and  $\mathsf{mid}_V$ .

▶ **Lemma 50.** Let  $\epsilon_V = the \ union \ of \{u \oplus u' \mid (u, u') \in \Delta_V, u \ is \ not \ chasing \ u'\}, \ then$ 

$$\frac{1}{2}\mathsf{sector}(V) = \mathsf{mid}_V - \epsilon_V. \tag{29}$$

Moreover,  $\operatorname{mid}_V$  is the closed set of  $\frac{1}{2}\operatorname{sector}(V)$ . So  $\operatorname{mid}_V^{\star}$  is the closed set of  $\operatorname{sector}(V)$ .

**Proof.** We have shown that  $\frac{1}{2} \operatorname{sector}(V)$ ,  $\operatorname{mid}_V$ ,  $\epsilon_V$  are all unions of some regions in  $\{u \oplus u' \mid (u, u') \in \Delta_V\}$ , and that all regions in this set are pairwise-disjoint as claimed in Fact 48. Therefore, proving (29) reduces to prove that for any  $(u, u') \in \Delta_V$ ,

$$u \oplus u' \subseteq \frac{1}{2} \operatorname{sector}(V) \Leftrightarrow [u \oplus u' \subseteq \operatorname{mid}_V \text{ and } u \oplus u' \not\subseteq \epsilon_V]; \text{ equivalently,}$$

$$[u \text{ is chasing } u' \text{ and } V \in \zeta(u, u')] \Leftrightarrow [u \text{ is chasing } u' \text{ and } u \oplus u' \subseteq \operatorname{mid}_V].$$

which is proved in Fact 49. Next, we show that  $\mathsf{mid}_V$  is the closed set of  $\frac{1}{2}\mathsf{sector}(V)$ . For simplification, assume that  $s \neq t$ ; the case s = t is trivial. Denote

$$\epsilon_V^{(1)}$$
 = the union of  $\{u \oplus u' \mid (u, u') \in \Delta_V, u \text{ is not chasing } u', \text{ and } u = v_s\},$   
 $\epsilon_V^{(2)}$  = the union of  $\{u \oplus u' \mid (u, u') \in \Delta_V, u \text{ is not chasing } u', \text{ and } u' = v_{t+1}\}.$ 

Because  $e_s \leq e_t$ , when  $(u, u') \in \Delta_V$  and u is not chasing u', either  $u = v_s$  or  $u' = v_{t+1}$ . Therefore,  $\epsilon_V = \epsilon_V^{(1)} \cup \epsilon_V^{(2)}$ . In addition, we point out the following obvious facts.

- (I)  $\epsilon_V^{(1)} \subseteq \alpha$ , where  $\alpha$  denotes the unique route that terminates at the midpoint of  $e_s$ .
- (II)  $\epsilon_V^{(2)} \subseteq \beta$ , where  $\beta$  denotes the unique route that terminates at the midpoint of  $e_t$

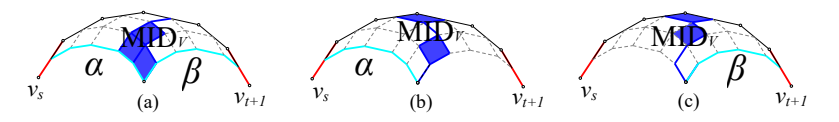


**Figure 40** mid<sub>V</sub> is the closed set of  $\frac{1}{2}$ sector(V).

Next, we discuss three different cases.

- Case 1:  $Z_s^t = V$ . See Figure 40 (a). In this case, by the definition of  $\mathsf{mid}_V$ , for any subregion R of  $\alpha \cup \beta$ , the closed set of  $\mathsf{mid}_V R$  equals  $\mathsf{mid}_V$ . In particular,  $\epsilon_V$  is a subset of  $\alpha \cup \beta$  by (I) and (II), so the closed set of  $\mathsf{mid}_V \epsilon_V$  (i.e. the closed set of  $\frac{1}{2}\mathsf{sector}(V)$ ) is  $\mathsf{mid}_V$ .
- Case 2:  $Z_s^t <_{\rho} V$ . By Fact 47.1,  $e_s \prec e_{t+1}$ . So every unit in  $[v_s \circlearrowright v_{t-1}]$  beside  $v_s$  is chasing  $v_{t+1}$ .  $(v_s \text{ may be chasing or not.})$  So,  $\epsilon_V^{(2)} \subseteq \epsilon_V^{(1)}$ . So,  $\epsilon_V = \epsilon_V^{(1)} \cup \epsilon_V^{(2)} = \epsilon_V^{(1)} \subseteq \alpha$ . Therefore, the closed set of  $\text{mid}_V \epsilon_V$  (i.e. the closed set of  $\frac{1}{2} \text{sector}(V)$ ) is  $\text{mid}_V$ . See Figure 40 (b).
- Case 3:  $V <_{\rho} Z_s^t$ . This case is symmetric to Case 2. See Figure 40 (c).

# 5.4 Step 4 - Proof of the enhanced version of Sector-continuity

Recall that the 2-scaling of  $\mathcal{L}_V$ ,  $\mathcal{R}_V$  with respect to V are respectively defined to be  $\mathcal{L}_V^{\star}$ ,  $\mathcal{R}_V^{\star}$ . (See Figure 8, where the blue and red curves indicate  $\mathcal{L}_{v_1}^{\star}$ , ...,  $\mathcal{L}_{v_n}^{\star}$  and  $\mathcal{R}_{v_1}^{\star}$ , ...,  $\mathcal{R}_{v_n}^{\star}$  respectively.) Since  $\mathcal{L}_V$ ,  $\mathcal{R}_V$  are boundaries of  $\mathsf{mid}_V$ , curves  $\mathcal{L}_V^{\star}$ ,  $\mathcal{R}_V^{\star}$  are boundaries of  $\mathsf{mid}_V^{\star}$ . Further applying Lemma 50,  $\mathcal{L}_V^{\star}$ ,  $\mathcal{R}_V^{\star}$  are also boundaries of  $\mathsf{sector}(V)$ .

To prove the Sector-Continuity, we prove a stronger statement:

- ▶ **Lemma 51.** If the common starting point of  $\mathcal{L}_V^{\star}$ ,  $\mathcal{R}_V^{\star}$  lies in P, then  $\mathcal{L}_V^{\star}$  has a unique intersection with  $\partial P$  and so does  $\mathcal{R}_V^{\star}$ . In this case  $\operatorname{sector}(V) \cap \partial P$  is a boundary-portion that starts at  $\mathcal{L}_V^{\star} \cap \partial P$  and terminates at  $\mathcal{R}_V^{\star} \cap \partial P$ . (This does not mean  $\operatorname{sector}(V) \cap \partial P = [\mathcal{L}_V^{\star} \cap \partial P \circlearrowleft \mathcal{R}_V^{\star} \cap \partial P]$ ; endpoints may not be contained.) Otherwise  $\operatorname{sector}(V) \cap \partial P$  is empty.
- **Proof.** Recall roads and routes in Subsection 2.5. For each road or route, call its 2-scaling with respect to V a scaled-road or scaled-route. Assume that each scaled-road (or scaled-route) has the same direction as its corresponding unscaled road (or route). We first state:
- (i) The 2-scaling of  $[v_s \circlearrowright v_{t+1}]$  with respect to V lies in the exterior of P.
- (ii) If we travel along a given scaled-route, we eventually get outside P and never return to P since then. Therefore, there is exactly one intersection between this scaled-route and  $\partial P$  if its starting point lies inside P; and no intersection otherwise.
- Proof of (i): This one follows from the relation  $V \notin [v_s \circlearrowright v_{t+1}]$  stated in Fact 44. Proof of (ii): Because all routes terminate at  $[v_s \circlearrowright v_{t+1}]$ , the scaled-routes terminate on the 2-scaling of  $[v_s \circlearrowright v_{t+1}]$  with respect to V. Applying (i), the scaled-routes terminate at the exterior of P. In other words, we will eventually get outside P traveling along any scaled-route. Moreover, consider any road  $e_i \oplus v_j$  where  $(e_i, v_j) \in \Delta_V$ . We claim that we do not return to P from outside P traveling along the 2-scaling of  $e_i \oplus v_j$ . This follows from (ii.1) and (ii.2) stated below. A similar claim holds for the roads in  $\{v_i \oplus e_j \mid (v_i, e_j) \in \Delta_V\}$ . Due to these claims and because the scaled-routes consist of the scaled-roads, we obtain (ii).
- (ii.1) The 2-scaling of  $e_i \oplus v_j$  w.r.t V is a translation of  $e_i$  that lies on the right of  $\overline{v_{t+1}v_i}$ .
- (ii.2) When we travel along any translation of  $e_i$  that lies on the right of  $\overrightarrow{v_{t+1}v_i}$ , we will not go back to P from outside P. (The translation of  $e_i$  has the same direction as  $e_i$ .)

  Proof of (ii.1):  $e_i \oplus v_j$  lies on the right of  $\overrightarrow{v_{t+1}v_i}$ , whereas V lies on its left; thus we get (ii.1). Proof of (ii.2): Since  $e_s \leq e_t$  and  $(e_i, v_j) \in \Delta_V$ , we get  $e_i \prec e_t$ , which implies (ii.2).
  - Let  $S_V^{\star}$  denote the common starting point of all scaled-routes (including  $\mathcal{L}_V^{\star}$  and  $\mathcal{R}_V^{\star}$ ). (Equivalently,  $S_V^{\star}$  is the 2-scaling of  $v_s \oplus v_{t+1}$  with respect to V.) The following statement follows from (i) and (ii).
  - (iii) If  $S_V^*$  lies in P, then  $\operatorname{mid}_V^* \cap \partial P = [\mathcal{L}_V^* \cap \partial P \circlearrowleft \mathcal{R}_V^* \cap \partial P]$ ; otherwise  $\operatorname{mid}_V^* \cap \partial P$  is empty. Proof of (iii): When  $S_V^*$  lies outside P, by (i) and (ii), all the boundaries that bound  $\operatorname{mid}_V^*$ , including  $\mathcal{L}_V^*$ ,  $\mathcal{R}_V^*$  and a fraction of the 2-scaling of  $[v_s \circlearrowleft v_{t+1}]$  with respect to V, lie in the exterior of P. Therefore  $\operatorname{mid}_V^*$  lies in the exterior of P, which implies that  $\operatorname{mid}_V^* \cap \partial P$  is empty. When  $S_V^*$  lies in P, the boundaries of  $\operatorname{mid}_V^*$  have exactly two intersections with  $\partial P$ . Therefore,  $\operatorname{mid}_V^* \cap \partial P$  either equals  $[\mathcal{L}_V^* \cap \partial P \circlearrowleft \mathcal{R}_V^* \cap \partial P]$ , or equals  $[\mathcal{R}_V^* \cap \partial P \circlearrowleft \mathcal{L}_V^* \cap \partial P]$ . We argue that it does not equal the latter one. Notice that region  $\operatorname{mid}_V^*$  is always on our right side when we travel along  $\mathcal{L}_V^*$ . This implies that  $\operatorname{mid}_V^* \cap \partial P \neq [\mathcal{R}_V^* \cap \partial P \circlearrowleft \mathcal{L}_V^* \cap \partial P]$ .

We complete the proof by combining (iii) with Lemma 50. By Lemma 50:  $\operatorname{sector}(V) \cap \partial P = (\operatorname{\mathsf{mid}}_V^\star - \epsilon_V^\star) \cap \partial P$  is a boundary-portion with the same endpoints as  $\operatorname{\mathsf{mid}}_V^\star \cap \partial P$ . Further according to (iii), we get the claim stated in this lemma.

# 6 Preprocess – solve the location queries

Recall that we have to preprocess for each vertex V of P,

which block and sector V lies in and which units are intersected by sector(V).

The preprocessing procedure is divided into four modules:

- **1.** Compute the two endpoints of  $sector(V) \cap \partial P$ .
- **2.** Determine the units intersected by sector(V).
- **3.** Compute the unique sector that contains V.
- **4.** Determine the unique block that contains V when V lies in a given sector.

Above all, we point out that the bottleneck of our algorithm lies in the first and forth preprocessing modules. These two are highly **symmetric**; see remarks in 2.6.

**Outline.** Subsection 6.1 presents the first module, 6.2 the second and third. The block locating module is the most nontrivial and is presented in the next two subsections.

# **6.1** Compute the endpoints of $sector(V) \cap \partial P$

Recall the two boundaries of  $\operatorname{sector}(V)$ ,  $\mathcal{L}_V^{\star}$  and  $\mathcal{R}_V^{\star}$ , and recall their properties introduced in Section 5. By Lemma 51, computing  $\operatorname{sector}(V) \cap \partial P$  reduces to computing two intersections  $\mathcal{L}_V^{\star} \cap \partial P$  and  $\mathcal{R}_V^{\star} \cap \partial P$ . In the following we compute  $\mathcal{L}_V^{\star} \cap \partial P$ ; the other one  $\mathcal{R}_V^{\star} \cap \partial P$  is symmetric. The idea is to use a binary search, as outlined in Subsection 2.6.

### An explicit definition for $\mathcal{L}_V$ .

To describe our algorithm, we shall give an explicit definition of  $\mathcal{L}_V$ . See Figure 41.

Recall the order  $\leq_V$ , s and t in Definition 43 and the marks '-/+/0' introduced in Subsection 2.5.  $\mathcal{L}_V$  divides all the regions marked by '-' from those marked by '+/0', and it must terminate at a midpoint of some edge  $e_l$ . First, we define  $e_l$  explicitly.

We denote by  $e_l$  the unique edge in  $[v_s \circlearrowright v_{t+1}]$  such that

- I For  $e_i$  such that  $e_s \leq_V e_i \leq_V e_{l-1}$ , region  $e_i \oplus e_{i+1}$  is marked by '-'.
- II For  $e_i$  such that  $e_l \leq_V e_i \leq_V e_{t-1}$ , region  $e_i \oplus e_{i+1}$  is marked by '+/0'.

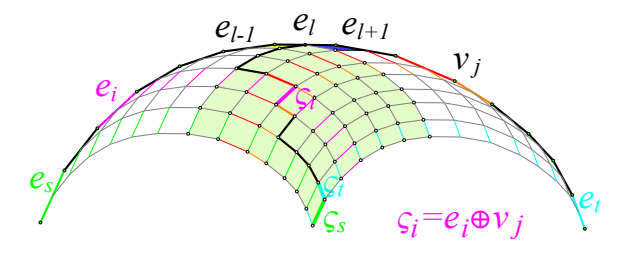


**Figure 41** Notations used in the algorithm for computing  $\mathcal{L}_V^{\star} \cap \partial P$ .

Explicitly,  $\mathcal{L}_V$  is the route that consists of all the A-type and B-type roads defined below.

- **A-type roads.** For any edge  $e_i$  in  $[v_s \circlearrowright v_l]$ , let  $e_j$  denote the smallest edge in  $[v_{l+1} \circlearrowright v_{t+1}]$  such that region  $e_i \oplus e_j$  is marked by '0/+' (or denote  $e_j = e_{t+1}$  if no such edge exists); we denote  $\varsigma_i = e_i \oplus v_j$  and call it an A-type road.
- **B-type roads.** For any edge  $e_j$  in  $[v_{l+1} \circlearrowright v_{t+1}]$ , let  $e_i$  denote the smallest edge in  $[v_s \circlearrowright v_l]$  such that region  $e_i \oplus e_j$  is marked by '0/+' (or denote  $e_i = e_l$  if no such edge exists); we denote  $\varsigma_j = v_i \oplus e_j$  and call it a *B-type road*.

The following observations of these roads are obvious.

- a) The order of the A-type roads in  $\mathcal{L}_V$  is determined, and equals to  $\varsigma_s, \varsigma_{s+1}, \ldots, \varsigma_{l-1}$ .
- b) The order of the B-type roads in  $\mathcal{L}_V$  is determined, and equals to  $\varsigma_t, \varsigma_{t-1}, \ldots, \varsigma_{l+1}$ .

#### The algorithm for computing $\mathcal{L}_V^{\star} \cap \partial P$ .

- ▶ **Lemma 52.** 1. We can compute s, t, l in  $O(\log n)$  time.
- 2. Given i such that road  $\varsigma_i$  is defined (in other words,  $e_i$  lies in  $[v_s \circlearrowright v_{t+1}]$  and  $e_i \neq e_l$ ), we can compute the endpoints of  $\varsigma_i$  in  $O(\log n)$  time. In addition, let  $\varsigma_i^*$  denote the 2-scaling of  $\varsigma_i$  with respect to V. We can distinguish the following in  $O(\log n)$  time:
  - $= \varsigma_i^* intersects \partial P.$

  - $= \varsigma_i^{\star}$  lies in the exterior of P.
- **3.** Let  $S_V^{\star}$  denote the starting point of  $\mathcal{L}_V^{\star}$ . We can compute  $S_V^{\star}$  in O(1) time. Moreover, if  $S_V^{\star}$  lies in P, we can compute  $\mathcal{L}_V^{\star} \cap \partial P$  in  $O(\log^2 n)$  time.

#### **Proof.** We suggest a recall of the proof of Lemma 51 here.

- 1. First, we show how we compute s; t can be computed symmetrically. We state two arguments. (The first one is Fact 46.1.)
- 1) For every edge  $e_i$ ,  $\omega_i^+$  contains V if and only if  $e_s \leq_V e_i$ .
- 2) Given an edge  $e_i$ , we can determine whether  $\omega_i^+$  contains V in O(1) time. Applying 1) and 2), s can be computed in  $O(\log n)$  time by a binary search.

Proof of 2). To determine whether  $\omega_i^+$  contains V is to determine the relation between  $Z_i^j$  and V, where  $e_j = back(\mathsf{D}_i)$ , which can be determined in O(1) time by Lemma 23.2.

Next, we show how we compute l. According to Lemma 23.2, we can determine whether  $e_i \oplus e_{i+1}$  is marked by '-', '0', or '+' in O(1) time. Therefore, based on properties I and II stated above, we can compute l in  $O(\log n)$  time by a binary search.

2. Then, we show how we compute road  $\varsigma_i$ . Assume that  $e_s \leq_V e_i \leq_V e_{l-1}$ ; otherwise  $e_{l+1} \leq_V e_i \leq_V e_t$  and it is symmetric. It reduces to find the edge  $e_j$  defined in "A-type roads" above. According to the bi-monotonicity of the Z-points (Fact 22),  $e_j$  is the unique edge such that  $e_i \oplus e_{j-1}$  is marked by '-' while  $e_i \oplus e_j$  is marked by '+/0'. We can compute each mark in O(1) time by Lemma 23.2 and thus binary search j in  $O(\log n)$  time.

When  $\varsigma_i$  has been computed, we can easily compute  $\varsigma_i^{\star}$ . We can then distinguish the relation between  $\varsigma_i^{\star}$  and  $\partial P$ . First, determine whether the endpoints of  $\varsigma_i^{\star}$  lie in P, which can be determined in  $O(\log n)$  time because P is convex. If both endpoints lie in P, then  $\varsigma_i^{\star}$  lies in P; if both of them lie outside P, then  $\varsigma_i^{\star}$  lies outside P; otherwise,  $\varsigma_i^{\star}$  intersects with  $\partial P$ .

3. Finally, we show how we compute the (potential) intersection  $\mathcal{L}_V^{\star} \cap \partial P$ .

First, notice that the starting point of  $\mathcal{L}_V$  locates at point  $\mathsf{M}(v_s, v_{t+1})$ . So,  $S_V^{\star}$  lies at the 2-scaling of  $\mathsf{M}(v_s, v_{t+1})$  with respect to V and thus can be computed in O(1) time.

Now, assume that  $S_V^{\star}$  lies in P, so that  $\mathcal{L}_V^{\star}$  has one intersection with  $\partial P$ .

We design two *subroutines*: one assumes that there is an A-type road whose 2-scaling (with respect to V) intersects  $\partial P$ , and it seeks for this road; the other is symmetric in that it assumes there is a B-type road whose 2-scaling (with respect to V) intersects  $\partial P$  and seeks for that road. Since one assumption is true, one subroutine would success.

According to observations a) and b) stated above, the A-type roads are in order on  $\mathcal{L}_V$ ; so do the B-type roads. So, a binary search can be applied in designing the subroutines. Each searching step costs  $O(\log n)$  time due to Claim 2; so the total running time is  $O(\log^2 n)$ .

# **6.2** Which units does sector(V) intersect & which sector does V lie in?

Assume the endpoints of  $\operatorname{sector}(V) \cap \partial P$  are known for each vertex V, we proceed to compute the (consecutive) units that intersect  $\operatorname{sector}(V)$  and the (unique) sector that contains V.

# Compute the units that intersect sector(V).

Let  $u_L, u_R$  respectively denote the unit containing  $\mathcal{L}_V^* \cap \partial P$  and the unit containing  $\mathcal{R}_V^* \cap \partial P$ . They can be computed while we compute the two endpoints of  $\operatorname{sector}(V) \cap \partial P$ . Applying the Sector-Continuity, in most cases the units that intersect  $\operatorname{sector}(V)$  are the units from  $u_L$  to  $u_R$  in clockwise. Exceptional cases are discussed in the following note.

▶ Note 4. Sometimes an endpoint of  $\operatorname{sector}(V) \cap \partial P$  is not contained in the sector. This is because  $\operatorname{sector}(V)$  is not always a closed set (see Lemma 50 and 51). Under a degenerate case, this endpoint may happen to lie at a vertex  $V^*$  of P, and then, by definition, we could not include  $V^*$  into the set of units that intersect  $\operatorname{sector}(V)$ .

Judging whether the endpoints of  $\operatorname{sector}(V) \cap \partial P$  belong to  $\operatorname{sector}(V)$  requires some extra work. Nevertheless, there is a convenient alternative solution: We can craftily include  $V^*$  into "the units that intersect  $\operatorname{sector}(V)$ " even though  $V^*$  only lies on the boundary of  $\operatorname{sector}(V)$ . After that, the monotonicity property of  $\psi^+, \psi^-$  still holds and so the algorithm still works.

#### Compute the sector that contains V for each vertex V - a sweeping algorithm.

First, we introduce two groups of event-points. One group contains the points in  $\{\mathcal{L}_V^* \cap \partial P, \mathcal{R}_V^* \cap \partial P\}$ ; and the other contains the intersections between  $\sigma P$  and  $\partial P$ . (Recall  $\sigma P$  in Section 3.4 and the K-points in Subsection 4.5.) Notice that all the event-points lie in  $\partial P$ . Then, two tags are assigned to each event-point, which are called future-tag and current-tag respectively. The current-tag indicates the sector which contains the current event-point; the future-tag indicates the sector which contains the boundary-portion that starts at the current event-point and terminates at its (clockwise) next event-point. By sweeping around  $\partial P$ , we determine the sector containing each vertex by utilizing the tags of the event-points.

In the following, we define the event-points and their tags precisely.

We use two procedures – an adding procedure and a removing procedure. The removing procedure removes redundant event-points added in the first procedure.

**Adding procedure.** See Figure 42. The left picture exhibits the event-points in Group 1 defined below; the middle one exhibits the event-points in Group 2 defined below.

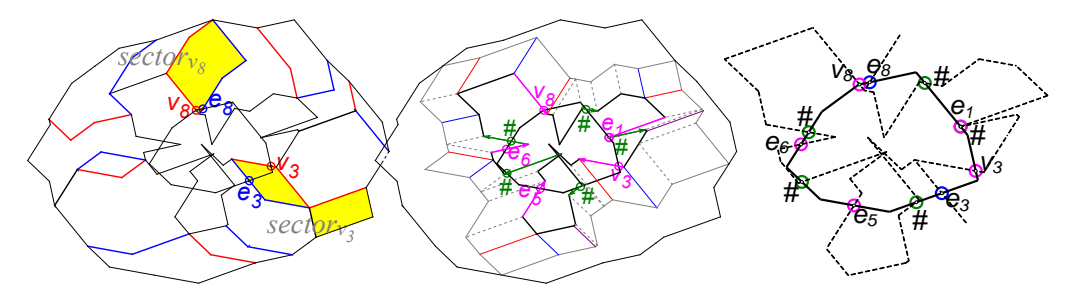


**Figure 42** Definition of the *event-points*. Their *future-tags* are labeled in the figure.

Group 1: Consider any vertex V for which  $\mathsf{sector}(V)$  intersects  $\partial P$ . We add two event-points  $\mathcal{L}_V^{\star} \cap \partial P$  and  $\mathcal{R}_V^{\star} \cap \partial P$ , and define their tags as follows.

$$\operatorname{Current}(\mathcal{L}_{V}^{\star} \cap \partial P) = V, \quad \operatorname{Future}(\mathcal{L}_{V}^{\star} \cap \partial P) = V,$$

$$\operatorname{Current}(\mathcal{R}_{V}^{\star} \cap \partial P) = V, \quad \operatorname{Future}(\mathcal{R}_{V}^{\star} \cap \partial P) = forw(V).$$
(30)

Group 2: For any intersection  $K_i$  between  $\sigma P$  and  $\partial P$ , we count it as an event-point and define its tags as follows. Notice that  $\sigma P$  is the concatenation of a few directional line segments. Assume that  $K_i$  comes from the directional line segment  $\overrightarrow{AB}$  of  $\sigma P$ . Notice that one of A, B lies in P while the other lies outside P since  $\overrightarrow{AB}$  intersects  $\partial P$ . Recall function g defined on  $\sigma P$  in Definition 33. Denote

$$Current(K_i) = `\#', \qquad Future(K_i) = \begin{cases} `\#', & \text{when } A \in P, B \notin P; \\ \mathbf{u}(g(K_i)), & \text{when } A \notin P, B \in P. \end{cases}$$
(31)

The special symbol '#' is introduced to indicate the outside of  $f(\mathcal{T})$ .

When Current(E) = '#', no sector contains event-point E.

When  $\operatorname{Future}(E) = '\#'$ , no sector contains the boundary-portion  $(E \circlearrowright E')$ , where E' denotes the clockwise next event-point of E.

▶ Note 5. Notice that  $Current(K_i) = '\#'$ . The reason for this is explained in Fact 42.

**Removing procedure.** If there are multiple event-points locating at the same position, we keep only one of them according to the following priority.

First, keep the event-point coming from  $\{\sigma P \cap \partial P\}$ .

Second, keep the event-point coming from  $\{\mathcal{R}_V^{\star} \cap \partial P\}$ .

As a consequence of the Sector-monotonicity and Interleavity-of-f, we get the following corollary which points out the sector containing each point on  $\partial P$ .

▶ Corollary 53. Take any point X in  $\partial P$ . If X lies at some event-point E, it belongs to  $\operatorname{sector}(\operatorname{Current}(E))$ . Otherwise, it belongs to  $\operatorname{sector}(\operatorname{Future}(E^*))$ , where  $E^*$  is the closest event-point preceding X in clockwise order.

Note: X belongs to no sector when we say it belongs to sector ('#').

To sum up, our algorithm works as follows.

- 1. ADD: Compute all of the event-points as well as their tags.
- 2. SORT: Sort the event-points in clockwise order.
- 3. REMOVE: Remove the redundant event-points.
- 4. SWEEP: Compute the closest event-point preceding each vertex and compute the sector containing each vertex by applying Corollary 53.

Next, we show the ADD step in detail. The other steps are trivial.

The event-points from Group 1 can be computed efficiently as shown in 6.1. We show how we compute the event-points from Group 2 as well as their tags in the following.

#### Compute the event-points in Group 2 (i.e. the K-points) and their tags

▶ Lemma 54. The polygonal curve  $\sigma P$  consists of O(n) sides and can be computed in O(n) time. The intersections in  $\sigma P \cap \partial P$  are of size O(n) and can be computed in  $O(n \log n)$  time. Moreover, the future-tag of each of such intersections can be computed in O(1) time. (The current tags for these event-points are the same and easy to compute; see Equation 31).

**Proof.** Recall frontier-pair-list, bottom borders, and frontier blocks in Section 3.4. Due to the following facts, the bottom borders have in total O(n) sides, i.e.  $\sigma P$  is of size O(n).

(i) the bottom borders of the blocks in the following set have in total O(n) sides.

```
\{\mathsf{block}(u,u') \mid (u,u') \in \mathsf{frontier}\text{-pair-list}, \text{ and } u,u' \text{ are both edges}\}.
```

(ii) the bottom borders of the blocks in the following set have O(n) sides.

```
\{\mathsf{block}(u,u') \mid (u,u') \in \mathsf{frontier}\text{-pair-list}, \text{ at least one of } u,u' \text{ is a vertex}\}.
```

Proof of (i): Clearly, the frontier-pair-list contains O(n) unit pairs, and the bottom border of  $\mathsf{block}(u, u')$  has at most two sides when u, u' are both edges. Therefore, we obtain (i).

Proof of (ii): Let  $(u_1, u_1'), \ldots, (u_m, u_m')$  denote the sublist of the frontier-pair-list that contains all of the edge pairs. Let  $Z_i = Z_{u_i}^{u_i'}$  for short. It can be simply observed that

- (ii.1) For any two neighboring edge pairs, e.g.  $(u_i, u_i')$  and  $(u_{i+1}, u_{i+1}')$ , there is another unit pair (denoted by u, u') in the frontier-pair-list between  $(u_i, u_i')$  and  $(u_{i+1}, u_{i+1}')$  (see Figure 25), and the bottom border of  $\mathsf{block}(u, u')$  is exactly the reflection of  $[Z_i \circlearrowright Z_{i+1}]$ .
- (ii.2)  $\{[Z_1 \circlearrowright Z_2], \ldots, [Z_m \circlearrowright Z_1]\}$  is a partition of  $\partial P$ . (This is because  $Z_1, \ldots, Z_m$  lie in clockwise order  $\partial P$ , which is due to the bi-monotonicity of the Z-points. See Figure 27.) Combining (ii.1) and (ii.2), we obtain (ii).

Next, we show that  $\sigma P$  can be computed in O(n) time.

We compute  $\sigma P$  in three steps; each costs O(n) time.

- Step 1. Compute the frontier-pair-list by Algorithm 1.
- Step 2. Compute  $Z_1, \ldots, Z_m$ . Note: This cost O(n+m) = O(n) time by Lemma 23.3 since they lie in clockwise order.
- Step 3. Generate each side in the bottom border of each frontier block. Note that each side costs O(1) time according to the definition of bottom borders.

To compute the intersections between  $\sigma P$  and  $\partial P$ , we can enumerate each side of  $\sigma P$  and compute its intersection with  $\partial P$ . According to the common computational geometric result, by O(n) time preprocessing, the intersection between a segment and the boundary of a fixed convex polygon P can be computed in  $O(\log n)$  time. Thus, this takes  $O(n \log n)$  time.

Finally, we show how we compute the future-tag of each intersection  $K_i$  in  $\sigma P \cap \partial P$ .

- By (31), it reduces to computing  $\mathbf{u}(g(K_i))$ . We state two observations: (1) Function  $\mathbf{u}(g(\cdot))$  has the property that it is identical within any side of  $\sigma P$ . This is due to the definition of g. (2) When computing  $\sigma P$ , we can at the same time compute the value of  $\mathbf{u}(g(\cdot))$  for each side of  $\sigma P$ . According to (1) and (2), by sweeping around  $\sigma P$ , we can compute  $\mathbf{u}(g(K_i))$  for all the intersections  $K_i$  in  $\sigma P \cap \partial P$  in linear time.
- ▶ Remark. In fact, the algorithm for computing  $\sigma P \cap \partial P$  can be optimized to linear time. Initially we select a pair of edges, one from  $\sigma P$  and one from  $\partial P$ . Every time we compute their intersection and change one edge to its clockwise next one. The selection of edge-to-change is according to specific rule. By selecting good initial edges and rule, we would not miss any intersection in  $\sigma P \cap \partial P$ . The analysis to this algorithm would be very complicated.

Running time of the sweeping algorithm. The ADD step requires  $O(n \log^2 n)$  time for Group 1 (as shown in Subsection 6.1), and  $O(n \log n)$  time for Group 2 (by Lemma 54). Also according to Lemma 54, there are in total O(n) event-points. So the SORT step runs in  $O(n \log n)$  time (or even in O(n) time). The REMOVE and SWEEP steps cost O(n) time.

#### 6.3 Two delimiting edges $e_{p_V}, e_{q_V}$ for block locating

Let block  $(u_1^*, u_2^*)$  denote the block containing V; we shall compute  $(u_1^*, u_2^*)$ . Recall Subsection tion 2.6 for a sketch. First, we want to find two **delimiting edges**  $e_{p_V}, e_{q_V}$  so that

$$e_p \prec e_q$$
. Moreover,  $(v_p \circlearrowright v_{q+1})$  contains  $V$ . (32)

Moreover, 
$$u_1^* \in [v_p \circlearrowright V)$$
, and  $u_2^* \in (V \circlearrowleft v_{q+1}]$ . (33)

Assume  $V = v_i$  henceforth in this subsection. First, we introduce a set of unit pairs  $\nabla_V$ .

$$\nabla_V := \{ (u, u') \mid \text{unit } u \text{ is chasing unit } u', u \in (\mathsf{D}_i \circlearrowright V), u' \in (V \circlearrowleft \mathsf{D}_{i-1}) \}. \tag{34}$$

▶ Fact 55.  $(u_1^*, u_2^*) \in \nabla_V$ .

**Proof.** By (34), it reduces to show that  $u_1^* \in (D_i \circlearrowright V)$  while  $u_2^* \in (V \circlearrowright D_{i-1})$ .

Let  $e_a = forw(u_1^*), e_{a'} = back(u_2^*)$ . Since  $u_1^*$  is chasing  $u_2^*$ , (i)  $e_a \leq e_{a'}$ . Notice that  $V \in \mathsf{block}(u_1^*, u_2^*) \subset \mathsf{quad}_{u_1^*}^{u_2^*} = \mathsf{quad}_a^{a'} \subseteq \mathsf{hp}_a^{a'}$ . (See Lemma 17) (Recall the half-planes  $\{hp\}$  introduced in Subsection 3.3.) Since  $V \in hp_a^{a'}$ , (ii)  $V = v_i \in (v_a \circlearrowright v_{a'+1})$ .

Combining (i) and (ii), we get  $e_a \prec e_i$  and  $e_{i-1} \prec e_{a'}$ .

Since  $e_a \prec e_i$ ,  $e_a \in (\mathsf{D}_i \circlearrowright V)$ , i.e.  $forw(u_1^*) \in (\mathsf{D}_i \circlearrowleft V)$ . So,  $u_1^* \in [\mathsf{D}_i \circlearrowleft V)$ .

Since  $e_{i-1} \prec e_{a'}$ ,  $e_{a'} \in (V \circlearrowleft \mathsf{D}_{i-1})$ , i.e.  $back(u_2^*) \in (V \circlearrowleft \mathsf{D}_{i-1})$ . So,  $u_2^* \in (V \circlearrowleft \mathsf{D}_{i-1}]$ .

In the following we further argue that  $u_1^* \neq D_i$  and  $u_2^* \neq D_{i-1}$ .

Because  $e_{a'} \in (V \circlearrowright \mathsf{D}_{i-1})$ , it also lies in  $(V \circlearrowleft \mathsf{D}_i)$ . So,  $e_{a'} \preceq back(\mathsf{D}_i)$ . Therefore,  $back(D_i) \not\prec e_{a'}$ , i.e.  $back(D_i) \not\prec back(u_2^*)$ . Therefore,  $D_i$  is not chasing  $u_2^*$ . This means that  $u_1^* \neq \mathsf{D}_i$  because  $u_1^*$  must be chasing  $u_2^*$ . Symmetrically,  $u_2^* \neq \mathsf{D}_{i-1}$ .

Following the definition of chasing (1), we see that all elements (u, u') in  $\nabla_V$ , when filled into a 2-dimensional matrix (as shown in Figure 43 (b)), where elements with the same u are in the same row and rows are sorted from top to bottom according to the clockwise order of u, whereas elements with the same u' are in the same column and columns are sorted from right to left according to the clockwise order of u', constitute into a "ladder" structure. See also Figure 43 (c) for an illustration of this structure. We define the "corners of this ladder" as the corner pairs. Formally, for any  $(e_x, e_{x'})$  in  $\nabla_V$ , it is a **corner pair**, if neither  $(e_{x-1}, e_{x'})$ nor  $(e_x, e_{x'+1})$  belongs to  $\nabla_V$ . (This concept is similar to extremal pair; see Definition 34.)

As demonstrated below, we are going to pick a corner pair of  $\nabla_V$  to be  $(e_p, e_q)$ .

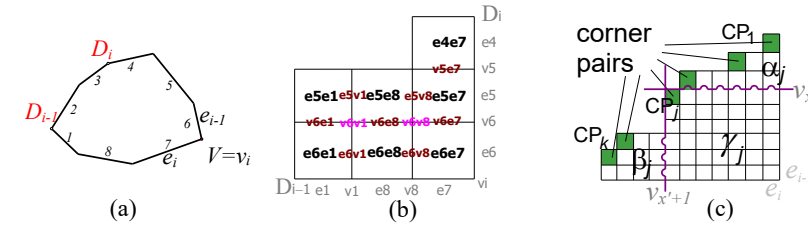


**Figure 43** An illustration of set  $\nabla_V$  and its corner pairs.

The definition of p,q relies on an interesting observation of  $\nabla_V$  stated in Fact 56 below. See Figure 43 (c). Denote by  $\mathsf{CP}_1,\ldots,\mathsf{CP}_k$  all the corner pairs and assume that they are sorted such that  $\mathsf{CP}_1$  is the topmost corner pair and  $\mathsf{CP}_k$  is the leftmost corner pair.

For each corner pair  $\mathsf{CP}_i = (e_x, e_{x'})$ , we define three subsets of  $\nabla_V$  as follows. If we cut  $\nabla_V$  along the horizontal line corresponding to  $v_x$  and the vertical line corresponding to  $v_{x'+1}$ ,

we get three chunks; the unit pairs in the top chunk are in  $\alpha_j$ ; those in the left chunk are in  $\beta_j$ ; and the rest have a rectangular shape and they contain the unit pairs in  $\gamma_j$ . Formally,

$$\begin{split} &\alpha_j = \{(u,u') \in \nabla_V \mid u \text{ lies in } (\mathsf{D}_i \circlearrowright v_x)\},\\ &\beta_j = \{(u,u') \in \nabla_V \mid u' \text{ lies in } (v_{x'+1} \circlearrowright \mathsf{D}_{i-1})\},\\ &\gamma_j = \{(u,u') \in \nabla_V \mid u \text{ lies in } [v_x \circlearrowright V), u' \text{ lies in } (V \circlearrowright v_{x'+1}]\}. \end{split}$$

For convenience, denote  $\alpha_{k+1} = \nabla_V$ . Recall the boundary-portions  $\{\langle \mathsf{quad} \rangle_u^{u'}\}$  introduced in Definition 14. For any subset S of  $\nabla_V$ , denote  $\langle \mathsf{quad} \rangle[S] = \bigcup_{(u,u') \in S} \langle \mathsf{quad} \rangle_u^{u'}$ .

▶ Fact 56. 
$$\langle \mathsf{quad} \rangle [\alpha_{j+1}] \cap \langle \mathsf{quad} \rangle [\beta_j] = \emptyset \ (1 \leq j \leq k).$$

This observation comes from the properties of the bounding-quadrants (Lemma 15, 16). Before proving it, we state explicit formulas for  $\langle \mathsf{quad} \rangle [\alpha_j]$  and  $\langle \mathsf{quad} \rangle [\beta_j]$ . For  $1 < j \leq k$ , let  $a_j, b_j$  respectively denote the edge pair at the upper right corner and lower left corner of  $\alpha_j$ ; for  $1 \leq j < k$ , let  $c_j, d_j$  respectively denote the edge pair at the upper right corner and lower left corner of  $\beta_j$ ; see Figure 44 (a). Recall that  $\rho$ .s and  $\rho$ .t denote the starting and terminal point of boundary-portion  $\rho$ . The following formulas immediately follow from the monotonicity of  $\langle \mathsf{quad} \rangle$  (Lemma 16).

$$\langle \mathsf{quad} \rangle [\alpha_j] = (\langle \mathsf{quad} \rangle [a_j].s \circlearrowleft \langle \mathsf{quad} \rangle [b_j].t), \text{ for any } 1 < j \le k.$$
 (35)

$$\langle \mathsf{quad} \rangle [\beta_i] = (\langle \mathsf{quad} \rangle [c_i].s \circlearrowleft \langle \mathsf{quad} \rangle [d_i].t), \text{ for any } 1 \le j < k.$$
 (36)

**Proof of Fact 56.** When j = k, set  $\beta_j$  is empty and the equation is trivial.

Next, we assume that j < k. We apply the following observations.

$$\langle \mathsf{quad} \rangle [a_{j+1}].s, \langle \mathsf{quad} \rangle [b_{j+1}].s, \langle \mathsf{quad} \rangle [c_j].s, \langle \mathsf{quad} \rangle [d_j].s$$
 lie in clockwise order. (37)

$$\langle \mathsf{quad} \rangle [a_{j+1}].t, \langle \mathsf{quad} \rangle [b_{j+1}].t, \langle \mathsf{quad} \rangle [c_j].t, \langle \mathsf{quad} \rangle [d_j].t$$
 lie in clockwise order. (38)

$$\langle \mathsf{quad} \rangle [a_{j+1}] \text{ has no overlap with } \langle \mathsf{quad} \rangle [d_j].$$
 (39)

$$\langle \mathsf{quad} \rangle [b_{j+1}] \text{ has no overlap with } \langle \mathsf{quad} \rangle [c_j].$$
 (40)

The first two facts follow from the monotonicity of  $\langle \mathsf{quad} \rangle$ ; the proof of (39) is given in the following; the proof of (40) is similar to that of (39) and omitted. Recall  $V = v_i$ . Notice that  $a_{j+1} = (forw(\mathsf{D}_i), e_i)$  and  $d_j = (e_{i-1}, back(\mathsf{D}_{i-1}))$ . Observing that edges  $forw(\mathsf{D}_i), e_i, e_{i-1}, back(\mathsf{D}_{i-1})$  do not lie in any inferior portion, applying the peculiar property of the bounding-quadrants (Lemma 15),  $\mathsf{quad}^i_{forw(\mathsf{D}_i)} \cap \mathsf{quad}^{back(\mathsf{D}_{i-1})}_{i-1}$  lie in the interior of P. So,  $\mathsf{quad}^i_{forw(\mathsf{D}_i)} \cap \partial P$  is disjoint with  $\mathsf{quad}^{back(\mathsf{D}_{i-1})}_{i-1} \cap \partial P$ . This further implies (39).

Now, see Figure 44 (b). Combining the four observations above, we see

$$\langle \mathsf{quad} \rangle [a_{i+1}].s, \langle \mathsf{quad} \rangle [b_{i+1}].s, \langle \mathsf{quad} \rangle [b_{i+1}].t, \langle \mathsf{quad} \rangle [c_i].s, \langle \mathsf{quad} \rangle [d_i].s, \langle \mathsf{quad} \rangle [d_i].t$$

lie in clockwise order around  $\partial P$ . In particular,

 $\langle \mathsf{quad} \rangle [a_{i+1}].s, \langle \mathsf{quad} \rangle [b_{i+1}].t, \langle \mathsf{quad} \rangle [c_i].s, \langle \mathsf{quad} \rangle [d_i].t$  lie in clockwise order around  $\partial P$ .

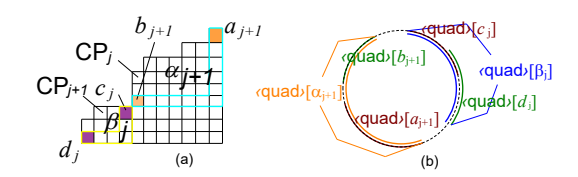


Figure 44 Illustration of Fact 56.

Therefore,  $(\langle \mathsf{quad} \rangle [a_{j+1}].s \circlearrowleft \langle \mathsf{quad} \rangle [b_{j+1}].t)$  is disjoint with  $(\langle \mathsf{quad} \rangle [c_j].s \circlearrowleft \langle \mathsf{quad} \rangle [d_j].t)$ . Further, by (35) and (36), this means  $\langle \mathsf{quad} \rangle [\alpha_{j+1}]$  is disjoint with  $\langle \mathsf{quad} \rangle [\beta_j]$ .

### Definition of $e_p, e_q$ and algorithm for computing $e_p, e_q$ .

(i) If  $(u_1^*, u_2^*)$  belongs to some set S, then  $V \in \langle \mathsf{quad} \rangle[S]$ .

$$\textbf{Proof.}\ \ V \in \mathsf{block}(u_1^*,u_2^*) \cap \partial P \subseteq \mathsf{quad}_{u_1^*}^{u_2^*} \cap \partial P \subseteq \langle \mathsf{quad} \rangle_{u_1^*}^{u_2^*} \subseteq \bigcup_{(u,u') \in S} \langle \mathsf{quad} \rangle_u^{u'} = \langle \mathsf{quad} \rangle[S].$$

By Fact 55, we have  $(u_1^*, u_2^*) \in \nabla_V$ . So  $V \in \langle \mathsf{quad} \rangle [\nabla_V]$  by (i). Further, since  $\emptyset = \alpha_1 \subset \ldots \subset \alpha_{k+1} = \nabla_V$ , there must be a unique index in  $1, \ldots, k$ , denoted by h, such that  $V \notin \langle \mathsf{quad} \rangle [\alpha_h]$  but  $V \in \langle \mathsf{quad} \rangle [\alpha_{h+1}]$ . We choose the corner pair  $\mathsf{CP}_h$  to be  $(e_{p_V}, e_{q_V})$ .

By defining  $p_V, q_V$  this way, we can verify that (32) and (33) both hold.

**Proof of (32).** Since 
$$(e_p, e_q) \in \nabla_V$$
, we get  $e_p \prec e_q$  and  $V \in (v_p \circlearrowright v_{q+1})$  by (34).

**Proof of (33).** By the definition of h, we know  $V \notin \langle \mathsf{quad} \rangle [\alpha_h]$  and  $V \in \langle \mathsf{quad} \rangle [\alpha_{h+1}]$ . Since  $V \notin \langle \mathsf{quad} \rangle [\alpha_h]$ , we know  $(u_1^*, u_2^*) \notin \alpha_h$  due to (i). Since  $V \in \langle \mathsf{quad} \rangle [\alpha_{h+1}]$ , we get  $V \notin \langle \mathsf{quad} \rangle [\beta_h]$  according to Fact 56, which further implies that  $(u_1^*, u_2^*) \notin \beta_h$  due to (ii). However, by Fact 55,  $(u_1^*, u_2^*) \in \nabla_V = \alpha_h \cup \beta_h \cup \gamma_h$ . So  $(u_1^*, u_2^*)$  must belong to  $\gamma_h$ , i.e.  $(u_1^*, u_2^*) \in \{(u, u') \in \nabla_V \mid u \text{ lies in } [v_p \circlearrowright V), u' \text{ lies in } (V \circlearrowright v_{q+1}]\}$ . This implies (33).

▶ **Lemma 57.** We can compute h (defined above) and thus compute  $(e_p, e_q)$  in  $O(\log n)$  time.

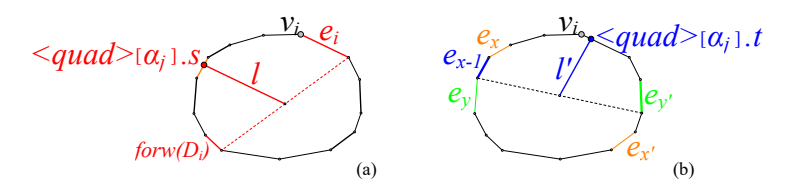


**Figure 45** Compute  $e_p, e_q$ .

**Proof.** To show that h can be computed in  $O(\log n)$  time, we use the following fact: Given  $1 \le j \le k$ , in O(1) time we can determine whether V lies in  $\langle \mathsf{quad} \rangle [\alpha_j]$ .

The case j=1 is trivial since  $\langle \mathsf{quad} \rangle [\alpha_j] = \emptyset$ . So, assume that j>1.

Assume  $\mathsf{CP}_j = (e_x, e_{x'}), \mathsf{CP}_{j-1} = (e_y, e_{y'}).$  (We can compute  $\mathsf{CP}_j$  and  $\mathsf{CP}_{j-1}$  in O(1) time. Except for the first and last element of  $\mathsf{CP}$ , the other corner pairs are extremal pairs. Moreover, we can obtain a list of extremal pairs beforehand and use it to compute  $\mathsf{CP}_j$ .)

- (i) By (35), we know  $\langle \mathsf{quad} \rangle [\alpha_j] = (\langle \mathsf{quad} \rangle [a_j].s \circlearrowleft \langle \mathsf{quad} \rangle [b_j].t)$ . Recall that  $a_j, b_j$  denotes the edge pair at the upper right corner and the lower left corner of  $\alpha_j$ , and we can see  $a_j = (forw(\mathsf{D}_i), e_i)$  and  $b_j = (e_{x-1}, e_{y'})$  by the definition of  $\alpha_j$ .
- (ii) By Definition 14,  $\langle \mathsf{quad} \rangle [a_j].s$  equals the unique intersection between l and  $[\mathsf{D}_i \circlearrowright v_{i+1}]$ , where l denotes the line at  $\mathsf{M}(\mathsf{D}_i, v_{i+1})$  that is parallel to  $e_i$  (see Figure 45 (a)).
- (iii) By Definition 14,  $\langle \mathsf{quad} \rangle [b_j].t$  equals the unique intersection between l' and  $[v_{x-1} \circlearrowright v_{y'+1}]$ , where l' denotes the line at  $\mathsf{M}(v_{x-1},v_{y'+1})$  that is parallel to  $e_{x-1}$  (see Figure 45 (b)).

Altogether,  $V \in \langle \mathsf{quad} \rangle [\alpha_j]$  if and only if V lies in the open half-plane bounded by l' and containing  $e_{x-1}$ . In O(1) time we can compute l' and then determine which side of l' the vertex V lies on. Therefore, we can determine whether  $V \in \langle \mathsf{quad} \rangle [\alpha_j]$  in O(1) time.

#### 6.4 Compute the block containing V

Given a vertex V. Assume  $V \in \mathsf{sector}(w)$  where w is known (computed by the algorithm in Subsection 6.2). Assume  $p_V, q_V$  are given which satisfy (32) and (33) (computed by the algorithm in Subsection 6.3). We now compute (the index of) the unique block containing V. Assume that  $\mathsf{block}(u_1^*, u_2^*)$  contains V; we shall compute  $(u_1^*, u_2^*)$ .

Recall the active pairs introduced in Subsection 2.6. For any unit pair (u, u') such that u is chasing u', it is **alive** if it satisfies (33); in other words, if  $u \in [v_p \circlearrowright V)$  and  $u' \in (V \circlearrowright v_{q+1}]$ . Moreover, for any alive pair (u, u'), we regard it as **active** if  $\zeta(u, u')$  intersects w.

For each active pair (u, u'), define

$$cell(u, u') := block(u, u') \cap sector(w), \tag{41}$$

and call it a cell.

▶ Fact 58.  $(u_1^*, u_2^*)$  is active, and  $\text{cell}(u_1^*, u_2^*)$  is the unique cell that contains V.

**Proof.** We know  $(u_1^*, u_2^*)$  is alive due to (33).

Assume  $f^{-1}(V) = (X_1, X_2, X_3)$ . Because  $V \in \mathsf{block}(u_1^*, u_2^*)$ , by Lemma 11.1,  $X_3 \in u_1^*$  and  $X_1 \in u_2^*$ . Because  $(X_1, X_2, X_3) \in \mathcal{T}$ , point  $X_2 \in \zeta(\mathbf{u}(X_3), \mathbf{u}(X_1))$ . Together,  $X_2 \in \zeta(u_1^*, u_2^*)$ . Because  $V \in \mathsf{sector}(w)$ , by Lemma 11.1,  $X_2 \in w$ . Therefore,  $\zeta(u_1^*, u_2^*)$  intersects w (at  $X_2$ ), which means that  $(u_1^*, u_2^*)$  is active.

Since  $\mathsf{block}(u_1^*, u_2^*)$  and  $\mathsf{sector}(w)$  both contain V, their intersection  $\mathsf{cell}(u_1^*, u_2^*)$  contains V. We argue that  $\mathsf{cell}(u_1^*, u_2^*)$  is the unique cell that contains V. If, to the opposite, V lies in two distinct cells, it lies in two distinct blocks, which contradicts  $\mathsf{BLock-Disjointness}$ .

By Fact 58, it reduces to find the unique cell that contains V. Next, we have to discuss two cases depending on whether w is an edge or a vertex. We first concentrate on the more typical case where w is an edge. The other case is discussed later. Here, assume that  $w = e_k$ .

**Outline.** We first state some observations of the cells (in particular, there is a monotonicity as stated in Fact 61 below), introduce another type of regions called "layers" (roughly, each layer consists of those cells cell(u, u') for which u or u' equals a given edge), and prove a monotonicity between the layers (Fact 63 below). Our algorithm is presented at last.

#### Observation 1 - consecutiveness of the active units.

A term *active edge* related to the active pairs is defined here.

An edge  $e_j$  in  $(v_p \circlearrowright V)$  is **active** if there is at least one unit u such that  $(e_j, u)$  is active; an edge  $e_j$  in  $(V \circlearrowright v_{q+1})$  is **active** if there is at least one unit u such that  $(u, e_j)$  is active.

- ▶ Fact 59. 1. For each active edge  $e_j$  in  $(v_p \circlearrowright V)$ , set  $\{u \mid (e_j, u) \text{ is active}\}$  consists of consecutive units, and its (clockwise) first and last unit can be computed in  $O(\log n)$  time. For each active edge  $e_j$  in  $(V \circlearrowleft v_{q+1})$ , set  $\{u \mid (u, e_j) \text{ is active}\}$  consists of consecutive units, and its (clockwise) first and last unit can be computed in  $O(\log n)$  time.
- **2.** The active edges in  $(v_p \circlearrowright V)$  (or  $(V \circlearrowleft v_{q+1})$ , respectively) are consecutive. Moreover, the (clockwise) first and last such edges can be computed in  $O(\log n)$  time.

**Proof.** For any edge 
$$e_j$$
 in  $(v_p \circlearrowright V)$ , denote  $b(j) = \begin{cases} q+1 & \text{if } e_j \prec e_{q+1}; \\ q & \text{otherwise.} \end{cases}$   
Denote  $b=b(j)$  when  $j$  is clear.

Assume  $V = v_i$ . Denote  $\Pi_j = (\zeta(e_j, e_i), \zeta(e_j, v_{i+1}), \dots, \zeta(e_j, v_b), \zeta(e_j, e_b))$ .

- (i)  $\Pi_j = \left(Z_j^i, [Z_j^i \circlearrowright Z_j^{i+1}], \dots, [Z_j^{b-1} \circlearrowright Z_j^b], Z_j^b\right)$ . (By definition of  $\zeta(e_j, u)$ ) (ii)  $Z_j^i, \dots, Z_j^b$  lie in clockwise order on  $\rho = [v_{b+1} \circlearrowright v_j]$ . (By bi-monotonicity of Z-points)

Proof of 1. Assume  $e_j \in (v_p \circlearrowright V)$ . The other case where  $e_j \in (V \circlearrowleft v_{q+1})$  is symmetric.

By (i) and (ii), the boundary-portions in  $\Pi_i$  that intersect  $e_k$  are consecutive. This simply implies that  $U = \{u \mid (e_j, u) \text{ is active}\}\$ consists of consecutive units.

Computing the first unit in U reduces to computing h such that  $Z_i^{h-1} \leq_{\rho} v_k <_{\rho} Z_i^h$ , which can be computed in  $O(\log n)$  time by a binary search by using Lemma 23.2.

The last unit in U can be computed similarly.

Proof of 2. Let  $\pi_j$  be the union of all portions in  $\Pi_j$ , which equals  $[Z_j^i \circlearrowright Z_j^{b(j)}]$  by (i) and (ii). By bi-monotonicity of the Z-points, the starting points of  $\pi_p, \ldots, \pi_{i-1}$  lie in clockwise order around  $\partial P$ , and so do their terminal points. So, the ones in  $\pi_p, \ldots, \pi_{i-1}$  that intersect  $e_k$  are consecutive. This means that the active edges in  $(v_p \circlearrowright V)$  are consecutive, since  $e_j$  is active if and only if  $\pi_i$  intersects  $e_k$ . Computing the first and last active edges in  $(v_p \circlearrowright V)$  reduces to computing the first and last portions in  $\pi_p, \ldots, \pi_{i-1}$  that intersect  $e_k$ . By Lemma 23.2, in O(1) time we can determine whether  $\pi_j$  is contained in  $[v_{b(j)+1} \circlearrowright v_k]$  or in  $[v_{k+1} \circlearrowright v_j]$ , or intersects  $e_k$ . So, by a binary search, in  $O(\log n)$  time we can compute these two edges.

#### Observation 2 - cell(u, u') is a parallelogram when at least one of u, u' is an edge.

▶ Fact 60. Given an active pair  $(e_j, u)$  (or  $(u, e_j)$ ), region  $\operatorname{cell}(e_j, u)$  (or  $\operatorname{cell}(u, e_j)$ ) is a parallelogram with two sides congruent to  $e_i$ , and it can be computed in O(1) time.

**Proof.** Assume  $(e_i, u)$  is active. By definition,  $\zeta(e_i, u)$  intersects with  $e_k$ , and

$$\operatorname{cell}(e_j, u) = f(\{(X_1, X_2, X_3) \mid X_1 = u, X_2 \in \zeta(e_j, u) \cap e_k, X_3 \in e_j\}). \tag{42}$$

Case 1: u is an edge, e.g.  $u = e_{j'}$ . In this case,  $\text{cell}(e_j, e_{j'})$  is the 2-scaling of  $e_j \oplus e_{j'}$  with respect to  $Z_j^{j'}$ , which is a parallelogram with two sides congruent to  $e_j$ . In addition, since  $\zeta(e_j,u)=Z_j^{j'}$  and it intersects  $e_k$ , point  $Z_j^{j'}$  lies in unit  $e_k$  and hence can be computed in O(1) time according to Lemma 23.1. Therefore,  $\operatorname{cell}(e_j,e_{j'})$  can be computed in O(1) time.

Case 2: u is a vertex, e.g.  $u = v_{j'}$ . First, we argue that  $\zeta(e_j, v_{j'})$  is not a single point. Suppose to the opposite that  $\zeta(e_j, v_{j'})$  is a single point. Then, its two endpoints  $Z_i^{j'-1}, Z_i^{j'}$ must be identical, and must lie in  $e_k$  since  $\zeta(e_j, v_{j'})$  intersects  $e_k$ . However, by Fact 21, when  $Z_j^{j'-1}, Z_j^{j'}$  lie in  $e_k$ , they lie at  $\mathsf{M}(\mathsf{I}_{j,k}, \mathsf{I}_{j'-1,k}), \mathsf{M}(\mathsf{I}_{j,k}, \mathsf{I}_{j',k})$ , respectively, which do not coincide because  $I_{j'-1,k} \neq I_{j',k}$ . Contradictory. Following this argument,  $\zeta(e_j,u) \cap e_k$  is a segment that is not a single point. Combining this fact with (42),  $\text{cell}(e_i, v_{i'})$  is a parallelogram with two sides congruent to  $e_i$ . (To see this more clearly, we refer to Figure 7 (c).)

Moreover, by Lemma 23.1 and Lemma 23.2, segment  $\zeta(e_i, v_{i'}) \cap e_k$  can be computed in O(1) time, and then  $\operatorname{cell}(e_i, v_{i'})$  can be computed in O(1) time.

The proof of the claim on  $cell(u, e_i)$  is symmetric and omitted.

#### Observation 3 - monotonicity of cells and definition of layers.

- ▶ Fact 61. 1. Let  $e_j$  be an active edge in  $(v_p \circlearrowright V)$ . Assume  $\{u \mid (e_j, u) \text{ is active}\} =$  $\{u_s,\ldots,u_t\}$  (in clockwise order). We claim that  $\mathsf{cell}(e_i,u_s),\ldots,\mathsf{cell}(e_i,u_t)$  are contiguous and lie monotonously in the opposite direction of  $e_k$ . See Figure 17 (a).
- 2. Let  $e_i$  be an active edge in  $(V \circlearrowright v_{q+1})$ . Assume  $\{u \mid (u, e_i) \text{ is active}\} = \{u_s, \ldots, u_t\}$ (in clockwise order). We claim that  $cell(u_s, e_i), \ldots, cell(u_t, e_i)$  are contiguous and lie monotonously in the opposite direction of  $e_k$ . See Figure 17 (b).

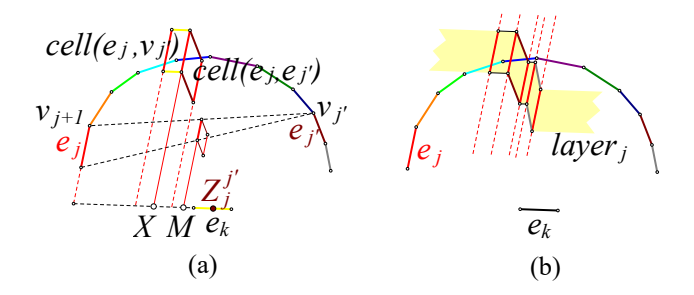


**Figure 46** Monotonicity of the cells and definition of the layers.

**Proof.** We prove 1; the proof of 2 is symmetric.

See Figure 46 (a). Let us consider the projections of these cells along direction  $e_j$  onto  $\ell_k$ , it reduces to prove that these projections are pairwise-disjoint and are arranged in order. Now, take two incident units in  $\{u_s, \ldots, u_t\}$ , e.g.  $v_{j'}$  and  $e_{j'}$ . (For incident units  $e_{j'}, v_{j'+1}$ , the proof is similar.) Let M be the projection of  $M(v_{j+1}, v_{j'})$ ; and X the reflection of  $Z_j^{j'}$  around M. We state that the projection of  $\text{cell}(e_j, e_{j'})$  terminates at X while the projection of  $\text{cell}(e_j, v_{j'})$  starts at X. This follows the definition of cells. More details are burdensome and omitted; see Figure 46 (a) for a clear illustration. Thus we obtain this lemma.

- ▶ **Definition 62** (Layers). See Figure 17 and Figure 46 (b). There are two types of layers.
- (A) Let  $e_j$  be an active edge in  $(v_p \circlearrowright V)$ . Assume  $\{u \mid (e_j, u) \text{ is active}\} = \{u_s, \ldots, u_t\}$  (in clockwise order). Let  $\mathsf{body}_j$  denote the region united by regions  $\mathsf{cell}(e_j, u_s), \ldots, \mathsf{cell}(e_j, u_t)$ . Clearly,  $\mathsf{body}_j$  is a region with two borders congruent to  $e_j$  since the cells have borders congruent to  $e_j$  (according to Fact 60). By removing these two borders, we can get an extension of  $\mathsf{body}_j$  which contains two strip regions parallel to  $e_k$ . This extension is defined as  $\mathsf{layer}_j$  and is called an  $\mathsf{A-type}$   $\mathsf{layer}$ .
- (B) Let  $e_j$  be an active edge in  $(V \circlearrowright v_{q+1})$ . Assume  $\{u \mid (u,e_j) \text{ is active}\} = \{u_s,\ldots,u_t\}$  (in clockwise order). Let  $\mathsf{body}_j$  denote the region united by regions  $\mathsf{cell}(u_s,e_j),\ldots,\mathsf{cell}(u_t,e_j)$ . Clearly,  $\mathsf{body}_j$  is a region with two borders congruent to  $e_j$  since the cells have borders congruent to  $e_j$  (according to Fact 60). By removing these two borders, we can get an extension of  $\mathsf{body}_j$  which contains two strip regions parallel to  $e_k$ . This extension is defined as  $\mathsf{layer}_j$  and is called a B-type  $\mathsf{layer}$ .

#### Observation 4 - monotonicity of layers.

- ▶ Fact 63. 1. All the layers lie in the closed half-plane bounded by  $\ell_k$  and containing P.
- 2. All the A-type layers are pairwise-disjoint and lie monotonously in the direction perpendicular to  $e_k$ . Symmetrically, all the B-type layers have the same monotonicity.

**Proof.** 1. Denote by H the half-plane bounded by  $\ell_k$  and containing P. Proving that all layers lie in H reduces to proving that all cells lie in H, which further reduces to proving that  $\operatorname{sector}(e_k) \subset H$ . Now, let X be an arbitrary point in  $\operatorname{sector}(e_k)$ , we shall prove  $X \in H$ .

Notice that there is  $(X_1, X_2, X_3) \in \mathcal{T}$  such that  $X_2 \in e_k$  and  $f(X_1, X_2, X_3) = X$ . Because  $X_1, X_3 \in \partial P$ , point  $M(X_1, X_3)$  lies in H. Since  $X_2 \in e_k$ , point  $X_2$  lies on the boundary of H. Together, the 2-scaling of  $M(X_1, X_3)$  with respect to  $X_2$ , which equals X, lies in H.

2. We know that each layer has two boundaries; we refer to them as the lower border and the upper border, so that the lower one is closer to  $\ell_k$  than the upper one. Assume that  $\mathsf{layer}_j$ 

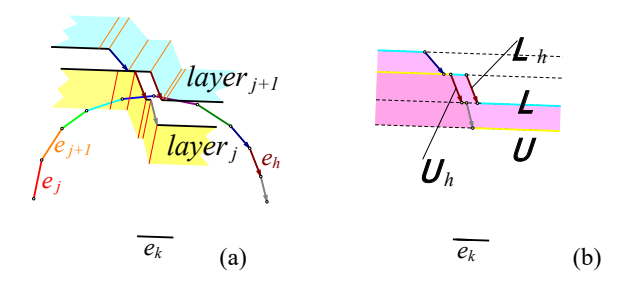


Figure 47 Monotonicity of the layers.

and  $\mathsf{layer}_{j+1}$  are A-type layers. See Figure 47 (a). We shall prove that the upper border of  $\mathsf{layer}_{i}$  (denoted by  $\mathcal{U}$ ) lies between  $\ell_k$  and the lower border of  $\mathsf{layer}_{i+1}$  (denoted by  $\mathcal{L}$ ).

Make an auxiliary line parallel to  $\ell_k$  at each vertex of the two borders; these auxiliary lines cut the plane into "slices", as shown in Figure 47 (b). It reduces to prove the following statement: (i) in each slice, the region under  $\mathcal{U}$  is contained in the region under  $\mathcal{L}$ .

Consider any slice that intersects both  $\mathcal{U}$  and  $\mathcal{L}$  (e.g. the middle one in the figure). (The proof for other slices are similar and easier.) Then, there is an edge  $e_h$ , such that the part of  $\mathcal{U}$  that lies in this slice (labeled by  $\mathcal{U}_h$  in the figure) and the part of  $\mathcal{L}$  that lies in this slice (labeled by  $\mathcal{L}_h$ ) are both translations of  $e_h$ . Applying the monotonicity of cells within layer<sub>h</sub> (Fact 61), we have a monotonicity between these two translations of  $e_h$  that implies (i).

#### Algorithm for computing $u_1^*, u_2^*$ .

- ▶ **Lemma 64.** Assume V, w, p, q are given as above.
- 1. Given an active edge  $e_i$ , we can do the following tasks in  $O(\log n)$  time:
  - $\textbf{a.}\ Determine\ whether\ V\ lies\ in\ \mathsf{layer}_{j};\ if\ not,\ determine\ which\ side\ of\ \mathsf{layer}_{j}\ it\ lies\ on.$
  - **b.** Determine whether V lies in body; if so, find the unique cell in body, containing V.
- **2.** We can compute  $u_1^*, u_2^*$  in  $O(\log^2 n)$  time.
- **Proof.** 1. Assume  $e_j \in (v_p \circlearrowright V)$ ; otherwise  $e_j \in (V \circlearrowleft v_{q+1})$  and it is symmetric. By Fact 60, the cells in  $\{\operatorname{cell}(e_j,u) \mid (e_j,u) \text{ is active}\}$  are parallelograms with two sides parallel to  $e_j$ . Those sides parallel to  $e_j$  can be extended so that they divide the plane into several regions as shown in Figure 46 (b). We refer to each of such region as a "chop" and denote the one containing  $\operatorname{cell}(e_j,u)$  by  $\operatorname{chop}_u$ . Notice that
- (1) We can compute  $\mathsf{chop}_u$  in O(1) time, since  $\mathsf{cell}(e_j, u)$  can be computed in O(1) time (Fact 60).
- (2) We can compute the first and last unit in  $\{u \mid (e_j, u) \text{ is active}\}\$  in  $O(\log n)$  time (Fact 59.1).
- (3) The chops have the same monotonicity as their corresponding cells.

Altogether, by a binary search, we can find the chop that contains V, which costs  $O(\log n)$  time. Knowing the chop containing V, we can easily solve tasks a and b in O(1) time.

2. To compute  $(u_1^*, u_2^*)$ , we design two *subroutines*. One assumes that V is contained in an A-layer (i.e. it assumes that  $u_1^*$  is an edge), the other assumes that V is contained in a B-layer (i.e. it assumes that  $u_2^*$  is an edge). We describe the first one in the following; the other is symmetrical. First, compute the first and last active edges  $e_g, e_{g'}$  in  $(v_p \circlearrowright V)$ , which costs  $O(\log n)$  time due to Fact 59.2. Then, using Claim 1.a and a binary search, find the only A-layer in  $\mathsf{layer}_g, \ldots, \mathsf{layer}_{g'}$  that contains V. If failed, terminate this subroutine. Otherwise, assume that  $\mathsf{layer}_j$  contains V, check whether  $\mathsf{body}_j$  contains V using Claim 1.b. If so, we find the cell containing V and thus obtain  $(u_1^*, u_2^*)$ . It costs  $O(\log^2 n)$  time.

CORRECTNESS: If  $u_1^*$  is an edge, the first subroutine obtains  $(u_1^*, u_2^*)$ ; if  $u_2^*$  is an edge, the second subroutine obtains  $(u_1^*, u_2^*)$ ; however, in a degenerate case,  $u_1^*, u_2^*$  can both be vertices, and the two subroutines both fail to find  $(u_1^*, u_2^*)$ . (This case is indeed degenerate because it implies a parallelogram inscribed in P with three anchored corners.) Nevertheless, our algorithms can handle the degenerate case after the following modification.

Notice that when  $(u_1^*, u_2^*)$  are both vertices, V lies on the boundary of some cell(u, u') such that at least one of u, u' is an edge. (This is stated precisely in (i) below.) We first find a cell that contains V or a cell whose boundary contains V. If we only find a cell whose boundary contains V, we use O(1) extra time to find the cell that contains V which is nearby.

(i) If  $(v_j, v_{j'})$  is active and point X lies in  $\text{cell}(v_j, v_{j'})$ , then it either lies in the boundary of  $\text{cell}(v_i, e_{i'-1})$ , or in the boundary of  $\text{cell}(e_i, v_{i'})$ .

Proof of (i): Denote  $M = \mathsf{M}(v_j, v_{j'})$  and denote by X' the reflection of X around M. Because  $\mathsf{cell}(v_j, v_{j'})$  is the reflection of  $\zeta(v_j, v_{j'}) \cap e_k$  around M, point X' lies in  $\zeta(v_j, v_{j'}) \cap e_k$ . Notice that  $\zeta(v_j, v_{j'})$  is the concatenation of  $\zeta(v_j, e_{j'-1})$  and  $\zeta(e_j, v_{j'})$ . Point X' either lies in  $\zeta(v_j, e_{j'-1}) \cap e_k$  or in  $\zeta(e_j, v_{j'}) \cap e_k$ . In the former case,  $(v_j, e_{j'-1})$  is active and the reflection of X' around M (which equals X) lies on the boundary of  $\mathsf{cell}(v_j, e_{j'-1})$ ; in the latter case,  $(e_j, v_{j'})$  is active and X lies on the boundary of  $\mathsf{cell}(e_j, v_{j'})$ .

▶ Remark. Comparing Lemma 52 to Lemma 64, we can see many similarities between our intersection-location algorithm for computing  $\mathcal{L}_V^{\star} \cap \partial P$  and point-location algorithm for computing the block containing V. On the objects being located, there are A-type and B-type roads in the former algorithm, and A-type and B-type layers in the latter. Moreover, roads and layers of the same type admit good monotonicities, and both algorithms incorporate two symmetric subroutines for applying these monotonicities.

#### Compute the block containing V when V lies in $sector(v_k)$ .

We now discuss the easier case where w is vertex. Assume that  $w = v_k$ .

Let  $(X_1, X_2, X_3)$  denote the preimage of V under function f. By Lemma 11.1,  $u_1^*, v_k, u_2^*$  are respectively the units containing  $X_3, X_2, X_1$ . Moreover, due to (33),  $[v_p \circlearrowright V)$  contains  $u_1^*$ ; and  $(V \circlearrowright v_{q+1}]$  contains  $u_2^*$ . Therefore,

$$X_1 \in (V \circlearrowright v_{q+1}], X_2 = v_k, X_3 \in [v_p \circlearrowright V).$$

In addition,  $VX_1X_2X_3$  is a parallelogram. By the following lemma, we can compute  $(X_1, X_2, X_3)$  in  $O(\log^2 n)$  time (given p, q). Then,  $(u_1^*, u_2^*) = (\mathbf{u}(X_3), \mathbf{u}(X_1))$  is obtained.

▶ **Lemma 65.** There is a unique parallelogram  $A_0A_1A_2A_3$  whose corners  $A_0, A_1, A_2, A_3$  respectively lie in  $V, (V \circlearrowright v_{q+1}], v_k, [v_p \circlearrowright V)$ , and we can compute it in  $O(\log^2 n)$  time.

**Proof.** Suppose to the contrary that there exist two such parallelograms, denoted by  $VAv_kA'$  and  $VBv_kB'$ . Because their centers both locate at  $\mathsf{M}(v_k,V)$ , quadrant ABA'B' is a non-degenerate parallelogram inscribed in  $[v_p \circlearrowright v_{q+1}]$ . However, by (32),  $[v_p \circlearrowright v_{q+1}]$  is an inferior portion. So there is a non-degenerate parallelogram with all corners lying on an inferior portion, which contradicts (i) stated in the proof of Fact 48.

To compute the parallelogram  $A_0A_1A_2A_3$ , we need to compute a pair of points  $A_3, A_1$  on  $[v_p \circlearrowright V), (V \circlearrowright v_{q+1}]$  so that their mid point lies at  $\mathsf{M}(v_k, V)$ . It is equivalent to compute the intersection between  $[v_p \circlearrowright V)$  and the reflection of  $(V \circlearrowright v_{q+1}]$  around  $\mathsf{M}(v_k, V)$ . We can compute it in  $O(\log^2 n)$  time by a trivial binary search. We omit further details.

In fact, by regarding  $v_k$  as a sufficiently small edge, the case  $V \in \mathsf{sector}(v_k)$  can be regarded as a special case of the edge case where  $V \in \mathsf{sector}(w)$  and w is an edge.

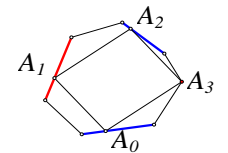
# 7 Algorithms for computing LMAPs

This section shows in detail how we compute all the LMAPs. Recall the sketch of our three routines in Subsection 2.3.

A classification of the corners of the inscribed parallelograms [15]. Assume that  $A_0A_1A_2A_3$  is a parallelogram inscribed in  $\partial P$ , and  $A_0, A_1, A_2, A_3$  lie in clockwise order. We classify every corner  $A_i$  as narrow, broad or even as follows. See Figure 48.

- $A_i$  is **narrow** if  $\mathbf{u}(A_{i-1})$  is chasing  $\mathbf{u}(A_{i+1})$ . (subscripts are taken modulo 4)
- $A_i$  is **broad** if its opposite corner is narrow; equivalently, if  $\mathbf{u}(A_{i+1})$  is chasing  $\mathbf{u}(A_{i-1})$ .
- **a**  $A_i$  is **even** if otherwise; i.e. if  $\mathbf{u}(A_{i+1})$  and  $\mathbf{u}(A_{i-1})$  are not chasing the other.

Note: If an inscribed parallelogram has two broad corners, they must be neighboring.



 $\mathbf{u}(A_2)$  is chasing  $\mathbf{u}(A_0)$ .

This means  $A_1$  is broad and  $A_3$  is narrow.

 $\mathbf{u}(A_1)$ , $\mathbf{u}(A_3)$  are not chasing each other. This means  $A_0$  and  $A_2$  are both even.

Figure 48 Illustration of broad, narrow and even corners.

By this definition, we can see

- Lemma 6 bounds the broad corner when its neighboring corners are fixed.
- Lemma 7 bounds the narrow corner when its neighboring corners are fixed.
- Lemma 9 bounds the narrow corner when its opposite corner is fixed.
- Lemma 10 states that if an LMAP has an narrow corner lying on X, then  $X \in f(\mathcal{T})$  and moreover, the other three corners lie at  $f_1^{-1}(X), f_2^{-1}(X), f_3^{-1}(X)$  respectively.
- Lemma 71 below bounds the even corner when its neighboring corners are fixed.
- Routine 1 aims to compute those LMAPs with an anchored narrow corner.
- Routine 2 aims to compute those LMAPs with two anchored broad corners.
- Routine 3 aims to compute those LMAPs with an anchored even corner.

A fact about the narrow corner; Lemma 10 of [15]. Assume that  $Q = A_0A_1A_2A_3$  is an LMAP, where  $A_0, A_1, A_2, A_3$  lie in clockwise order. Further assume that  $\mathbf{u}(A_3) = e_i$  and  $\mathbf{u}(A_1) = e_i$  and that  $e_i \prec e_j$ . Then, the (narrow) corner  $A_0$  must be anchored.

The following lemma shows that our three routines are sufficient for computing all LMAPs.

- ▶ **Lemma 66.** For any LMAP, at least one of the following holds.
- 1. It has an anchored narrow corner.
- 2. It has two anchored broad corners.
- 3. It has an anchored even corner.

**Proof.** Assume Q is an LMAP. If an opposite pair of corners of Q are both unanchored, one of the other two corners must be narrow (since edges are nonparallel to each other), and this narrow corner must be anchored due to the above fact. Thus Q has an anchored narrow corner. Now, assume that at least one corner is anchored among each pair of opposite corners. First, suppose Q has an even corner A. Then, either A or A's opposite corer is anchored, thus Q has an anchored even corner. Now, further assume that there is no even corner. Then, Q has at least two anchored corners that are narrow or broad. Thus, it either has an anchored narrow corner or has two anchored broad corners.

#### 7.1 Routine 1 - compute the LMAPs with an anchored narrow corner

Recall that Routine 1 applies Lemma 10 and works as follows (see Subsection 2.3).

```
1 foreach vertex\ V of P do

2 Determine whether V\in f(\mathcal{T});

3 If so, compute f^{-1}(V) and output parallelogram Vf_1^{-1}(V)f_2^{-1}(V)f_3^{-1}(V).

4 end
```

The difficulty lies in computing  $f^{-1}(V)$ , for which we need Lemma 11.

#### Restatement of Lemma 11

- **1.** Assume a point Y lies in  $f(\mathcal{T}) \cap \partial P$ . Then, (a)  $Y \in \mathsf{block}(u, u')$  is equivalent to  $[f_3^{-1}(Y) \in u, f_1^{-1}(Y) \in u']$ ; (b)  $Y \in \mathsf{sector}(w)$  is equivalent to  $f_2^{-1}(Y) \in w$ .
- **2.** Given a vertex V of P, we can determine whether  $V \in f(\mathcal{T})$  and compute  $f^{-1}(V)$  in O(1) time if we know "which block and sector V lies in."

**Proof of Lemma 11.** 1. Since  $Y = f(f_1^{-1}(Y), f_2^{-1}(Y), f_3^{-1}(Y))$ , due to (4) and (5), we get:  $Y \ lies \ in \ block(\mathbf{u}(f_3^{-1}(Y)), \mathbf{u}(f_1^{-1}(Y))) \ and \ sector(\mathbf{u}(f_2^{-1}(Y)))$ . The implies Claim 1.

2. If V does not lie in any block or sector, we determine that  $V \notin f(\mathcal{T})$ . (This applies the fact that  $f(\mathcal{T})$  is the union of all blocks and the union of all sectors.) Otherwise, we determine that  $V \in f(\mathcal{T})$  and compute  $f^{-1}(V)$  as follows.

Assume that V lies in  $\mathsf{block}(u, u')$  and  $\mathsf{sector}(w)$  (where u, u', w are known units). Assume  $f^{-1}(V) = (X_1, X_2, X_3)$ . We shall compute  $X_1, X_2, X_3$  so that the following statements hold.

- (i)  $X_1, X_2, X_3$  lie in units u', w, u, respectively. (According to Claim 1.)
- (ii)  $X_2 \in \zeta(u, u')$ . (Since  $(X_1, X_2, X_3) = f^{-1}(V) \in \mathcal{T}$  and by the definition (3) of  $\mathcal{T}$ )
- (iii)  $VX_1X_2X_3$  is a parallelogram. (Since  $f(X_1, X_2, X_3) = V$ )
- Case 1: u, u' are both edges, e.g.  $(u, u') = (e_i, e_j)$ . Because  $\zeta(u, u') = Z_i^j$ , we get  $X_2 = Z_i^j$  by (ii). Further since  $X_2 \in w$ , we know  $Z_i^j \in w$ . Since  $Z_i^j$  lies in unit w, by Lemma 23.1, it can be computed in O(1) time. Thus we compute  $X_2$ . Then  $X_1, X_3$  can be computed in O(1) time:  $X_1$  is the intersection between  $e_j$  and the reflection of  $e_i$  around  $M(V, X_2)$ ; and  $X_3$  is the intersection between  $e_i$  and the reflection of  $e_j$  around  $M(V, X_2)$ .
- Case 2: u is a vertex and u' is an edge, e.g.  $(u,u')=(v_i,e_j)$ . Let s denote the 2-scaling of  $v_i\oplus e_j$  with respect to V, which is a line segment. We first argue that s has at most one intersection with unit w. Applying Fact 21,  $\zeta(v_i,e_j)=[Z_{i-1}^j\circlearrowright Z_i^j]\subseteq [v_{j+1}\circlearrowright \mathsf{D}_j]$ , whereas  $X_2\in \zeta(v_i,e_j)$ ; together, the unit containing  $X_2$  (i.e. unit w) lies in  $[v_{j+1}\circlearrowleft \mathsf{D}_j]$ . Because s is parallel to  $e_j$ , each unit in  $[v_{j+1}\circlearrowleft \mathsf{D}_j]$ , including w, has at most one intersection with s.

Because  $X_3 \in u$  and  $X_1 \in u'$ , we know  $\mathsf{M}(X_1, X_3) = \mathsf{M}(V, X_2)$  lies in  $v_i \oplus e_j$ , so  $X_2$  lies in segment s. Further, since  $X_2 \in w$ , point  $X_2$  lies in both s and w. Therefore, in O(1) time we can compute  $X_2$  by computing the unique intersection of s, w. Moreover,  $X_3 = u = v_i$ . Finally, by (iii),  $X_1$  lies in the reflection of  $X_3$  around  $\mathsf{M}(V, X_2)$ .

Case 3: u is an edge and u' is a vertex. This case is symmetric to Case 2.

Case 4: u, u' are both vertices, e.g.  $(u, u') = (v_i, v_j)$ . Since  $X_3 \in u = v_i$  and  $X_1 \in u' = v_j$ , points  $X_1, X_3$  can be computed in O(1) time. Further, by (iii),  $X_2$  lies in the reflection of V around  $M(X_1, X_3)$  and thus can be computed in O(1) time.

◀

# 7.2 Routine 2 - compute the LMAPs with two anchored broad corners

#### Key symbols applied in this routine and their properties

Recall the arrays  $\mathbb{G}^-$ ,  $\mathbb{G}^+$ ,  $\psi^-$ ,  $\psi^+$  introduced above Lemma 12; two of which are restated below. The following lemma states some important properties of these arrays.

$$\mathbb{G}_V^- := \{ u \in \mathbb{G}_V \mid V \text{ is chasing } u \}. \qquad \psi_V^- := \bigcup_{u \in \mathbb{G}_V^-} \zeta(V, u).$$

- ▶ **Lemma 67.** 1. For each vertex V, sets  $\mathbb{G}_V^-$  and  $\mathbb{G}_V^+$  consist of consecutive units,  $\psi_V^-$  and  $\psi_V^+$  are boundary-portions of P. So, each of them can be stored implicitly in O(1) space.
- 2. Array  $\mathbb{G}$  has the following monotonicity. And  $\mathbb{G}^+, \mathbb{G}^-$  have the same monotonicity. Denote by  $g_V, g_V$  the (clockwise) first and last units in  $\mathbb{G}_V$ . Let  $V_1, \ldots, V_m$  be an enumeration (in clockwise) of all vertex V so that  $\mathbb{G}_V \neq \emptyset$ . Then,
  - The 2m units  $g_{V_1}, g_{V_1}, \dots, g_{V_m}, g_{V_m}$  lie in clockwise order. (Note that neighboring elements in this list could be identical.)
  - More importantly, the 2m edges  $back(g_{V_1}), forw(g_{V_1}), \ldots, back(g_{V_m}), forw(g_{V_m})$  lie in clockwise order. (Note that neighboring elements in this list could be identical.)
- 3. Array  $\psi^-$  has the monotonicity property that its elements  $\psi^-_{v_1}, \ldots, \psi^-_{v_n}$  are pairwise-disjoint (though neighboring elements may share a common endpoint) and lie in clockwise order on  $\partial P$ . Array  $\psi^+$  has the same monotonicity property as  $\psi^-$ .
- **4.** Given  $\mathbb{G}$ , we can compute  $\mathbb{G}^+, \mathbb{G}^-, \psi^+, \psi^-$  in linear time.

**Proof.** We only prove the properties of  $\mathbb{G}, \mathbb{G}^-, \psi^-$ . The others are symmetric.

 $\mathbb{G}_V$  consists of consecutive units due to the Sector-Continuity. Further since  $\{u \mid V \text{ is chasing } u\}$  is a unit interval, its intersection with  $\mathbb{G}$ , which equals  $\mathbb{G}_V^-$ , is a unit interval.

By Sector-monotonicity , we immediately get the monotonicity of  $\mathbb{G}$ . It further implies the monotonicity of  $\mathbb{G}^-$ , by noticing that each element  $\mathbb{G}_V^-$  is a subinterval of  $\mathbb{G}_V$ .

In the following, we give an equation which implies that  $\psi_V^-$  is always a boundary-portion. Let  $\dot{g}_V^-, \dot{g}_V^-$  denote the clockwise first and last units in  $\mathbb{G}_V^-$ .

$$\psi_{V}^{-} = \begin{cases} [Z_{back(V)}^{back(\hat{g}_{V}^{-})} \circlearrowright Z_{forw(V)}^{forw(\hat{g}_{V}^{-})}], & \text{when } \mathbb{G}_{V}^{-} \neq \emptyset; \\ \varnothing, & \text{when } \mathbb{G}_{V}^{-} = \varnothing. \end{cases}$$

$$(43)$$

Proof of (43): Assume  $\mathbb{G}_V^- \neq \emptyset$ , otherwise it is obvious. By definition of  $\zeta(V, u)$  in (2),

$$\zeta(V,u) = [Z^{back(u)}_{back(V)} \circlearrowright Z^{forw(u)}_{forw(V)}] \text{ for any unit } u \text{ in } \mathbb{G}^-_V.$$

Based on this formula and due to the bi-monotonicity of the Z-points (Fact 22), the union  $\bigcup_{u \in \mathbb{G}_V^-} \zeta(V, u)$  equals the boundary-portion that starts at the starting point of  $\zeta(V, g_V^-)$  and terminates at the terminal point of  $\zeta(V, g_V^-)$ , thus we obtain (43).

Next, we prove the monotonicity of  $\psi^-$ . Let  $V_1,\ldots,V_m$  be an enumeration (in clockwise) of all vertex V so that  $\mathbb{G}_V^- \neq \varnothing$ . By the monotonicity of  $\mathbb{G}^-$ , the 2m edges  $back(\acute{g}_{V_1}^-), forw(\grave{g}_{V_1}^-), \ldots, back(\acute{g}_{V_m}^-), forw(\grave{g}_{V_m}^-)$  lie in clockwise order around  $\partial P$ . Moreover, applying the bi-monotonicity of the Z-points (Fact 22), we have

$$Z_{back(V_1)}^{back(\hat{g}_{V_1}^-)}, Z_{forw(V_1)}^{forw(\hat{g}_{V_1}^-)}, \ldots, Z_{back(V_m)}^{back(\hat{g}_{V_m}^-)}, Z_{forw(V_m)}^{forw(\hat{g}_{V_m}^-)} \text{ lie in clockwise order around } \partial P. \tag{44}$$

Together with (43),  $\psi_{V_1}^-, \dots, \psi_{V_m}^-$  are pairwise-disjoint and lie in clockwise order.

 $\mathbb{G}^+, \mathbb{G}^-$  can easily be computed from  $\mathbb{G}$ ; we only show how we compute  $\psi^-$ . To compute this array is to compute those Z-points stated in (44). Given  $\mathbb{G}^-$ , we have  $g^-, g^-$  and so we can compute those points altogether in linear time by Lemma 23.3.

#### Restatement of Lemma 12 and its simple proof.

See Figure 49 below. Assume  $A_0A_1A_2A_3$  is an LMAP where  $A_0, A_1, A_2, A_3$  lie in clockwise order and where  $A_0, A_1$  are anchored broad corners, namely,

- 1.  $A_0$  is anchored and  $\mathbf{u}(A_1)$  is chasing  $\mathbf{u}(A_3)$ ; meanwhile,
- **2.**  $A_1$  is anchored and  $\mathbf{u}(A_2)$  is chasing  $\mathbf{u}(A_0)$ .

We claim that  $1.\mathbf{u}(A_2) \in \mathbb{G}_{A_0}^+, \mathbf{u}(A_3) \in \mathbb{G}_{A_1}^-;$  and  $2.A_1 \in \psi_{A_0}^+, A_0 \in \psi_{A_1}^-.$ 

**Proof of Lemma 12.** Because  $A_0$  is broad,  $A_2$  is narrow. By Lemma 9,  $A_2 \in \operatorname{sector}(A_0)$ . So  $\mathbf{u}(A_2)$  intersects  $\operatorname{sector}(A_0)$ . Since  $A_1$  is broad,  $\mathbf{u}(A_2)$  is chasing  $A_0$ . Together,  $\mathbf{u}(A_2) \in \mathbb{G}_{A_0}^+$ . This further implies  $\zeta(\mathbf{u}(A_2), A_0) \subseteq \bigcup_{\mathbf{u} \in \mathbb{G}_{A_0}^+} \zeta(u, A_0) = \psi_{A_0}^+$ . Moreover, using Lemma 6 on  $A_1$ , we get  $A_1 \in \zeta(\mathbf{u}(A_2), A_0)$ . So  $A_1 \in \psi_{A_0}^+$ . Symmetrically,  $\mathbf{u}(A_3) \in \mathbb{G}_{A_1}^-$  and  $A_0 \in \psi_{A_1}^-$ .

#### Algorithm for Routine 2 without the batch technique.

Let S denote the vertex pairs satisfying the relation between  $A_0, A_1$  given in Lemma 12.2. Formally,  $S = \{(V, V') \text{ is a vertex pair of } P \mid V' \in \psi_V^+ \text{ and } V \in \psi_{V'}^-\}$ . According to Lemma 12, Algorithm 2 correctly computes all those LMAPs with two anchored broad corners.

1 foreach  $(V,V') \in \mathcal{S}$  do
2 Compute and output all the non-slidable parallelograms  $A_0A_1A_2A_3$  such that  $A_0=V, A_1=V', \mathbf{u}(A_2) \in \mathbb{G}_V^+, \mathbf{u}(A_3) \in \mathbb{G}_{V'}^-, \text{ and } A_0, A_1, A_2, A_3 \text{ lie in clockwise.}$ 3 end

Algorithm 2: Routine 2 (without the batch technique)

The following lemma address in detail how we implement Sentence 2 in Algorithm 2.

- ▶ **Lemma 68.** 1. Given vertices V, V', apart from the following exceptional cases, there is a unique non-slidable inscribed parallelogram with two neighboring corners lying on V, V'.
  - Exception 1: P has an edge that is parallel to  $\overline{VV'}$  and is longer than segment  $\overline{VV'}$ . In this case, there are two such parallelograms.
  - Exception 2: All the segments in P that are parallel to  $\overline{VV'}$ , and other than  $\overline{VV'}$ , are shorter than  $\overline{VV'}$ . In this case, there is no such parallelogram.
- 2. Given two vertices V, V' and two unit interval U, U', in O(|U| + |U'|) time we can compute all the non-slidable parallelograms  $A_0A_1A_2A_3$  such that

$$A_0 = V, A_1 = V', \mathbf{u}(A_2) \in U, \mathbf{u}(A_3) \in U', \text{ and } A_0, A_1, A_2, A_3 \text{ lie in clockwise order.}$$

**Proof.** 1. Clearly, in this parallelogram, the opposite side of side VV' must be a chord of P that is a translation of VV' and is other than VV'. This implies 1.

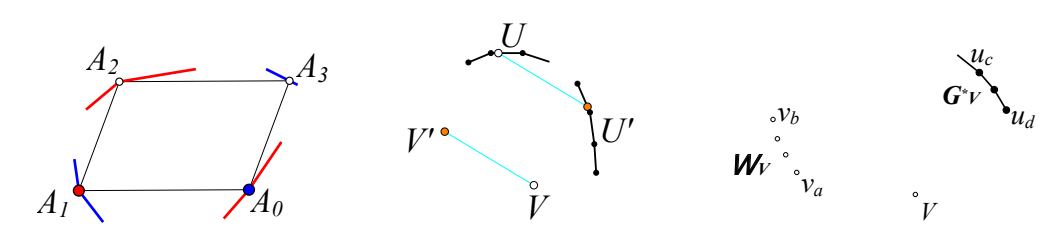


Figure 49 Ill. of Lemma 12 Figure 50 Ill. of Lemma 68 Figure 51 Ill. of Lemma 69

66

2. See Figure 50. For each unit u in U, we can determine weather the aforementioned chord  $(A_2A_3)$  has one endpoint  $(A_2)$  lying in u meanwhile the other  $(A_3)$  lying in some unit in U'. Because P is convex, if we enumerate u in order, we can maintain the unit containing  $A_3$  in order, and the running time of the entire process can be bounded by O(|U| + |U'|).

Running time analysis. Applying Lemma 68.2, the running time of Algorithm 2 is given by

$$\bigcup_{(V,V')\in\mathcal{S}} \left( \left| \mathbb{G}_V^+ \right| + \left| \mathbb{G}_{V'}^- \right| \right),$$

which is clearly  $O(n^2)$  because  $|\mathcal{S}| = O(n)$ . (The fact that  $|\mathcal{S}| = O(n)$  follows from the definition of  $\mathcal{S}$  and the monotonicities of  $\psi^+$  or  $\psi^-$ ; see Lemma 67.) Unfortunately, the running time is  $\Omega(n^2)$  in the worst case. For example, it is  $\Omega(n^2)$  when there exists a particular vertex V so that: (1) there are  $\Omega(n)$  vertices V' so that  $(V, V') \in \mathcal{S}$  (which is possible even though  $\psi^+, \psi^-$  has the monotonicities) and (2) there are  $\Omega(n)$  units in  $\mathbb{G}^+_V$ .

The basic idea of the batch technique. As introduced in Subsection 2.3, we can optimize Algorithm 2 by a common batch technique. Roughly, for any fixed vertex V, we can compute  $(A_2, A_3)$  for those pairs  $(A_0, A_1) \in \mathcal{S}$  in which  $A_0 = V$  in a batch. In this way, a monotonicity of  $A_2, A_3$  with respect to  $A_1$  can be utilized in the computation of  $A_2, A_3$ .

To describe this technique more clearly, we introduce the following notation. For each vertex V, define

$$\mathbb{W}_{V} := \{ V' \mid V' \text{ is a vertex in } \psi_{V}^{+} \text{ and } \psi_{V'}^{-}, \text{ is the single point } V \}. \tag{45}$$

Note that  $\mathbb{W}_V$  consists of consecutive vertices. (This follows the monotonicity of  $\psi^-$  stated in Lemma 67.) Next, we introduce a unit interval  $\mathbb{G}_V^*$  based on  $\mathbb{W}_V$ .

We define  $\mathbb{G}_V^*$  to be smallest unit interval containing  $\bigcup_{V' \in \mathbb{W}_V} \mathbb{G}_{V'}^-$ . (Note that  $\mathbb{G}_V^* = \emptyset$  if  $\mathbb{W}_V$  is empty.) More formally, we define  $\mathbb{G}_V^*$  as follows. See Figure 51. Let  $v_a, v_b$  denote the (clockwise) first and last vertex in  $\mathbb{W}_V$ . Because  $v_a \in \mathbb{W}_V$ , we have  $\psi_{v_a}^- = V$ , which implies that  $\mathbb{G}_{v_a}^-$  must be nonempty. Similarly,  $\mathbb{G}_{v_b}^-$  must be nonempty. Now, let  $u_c$  denote the (clockwise) first unit in  $\mathbb{G}_{v_a}^-$ , and  $u_d$  the (clockwise) last unit in  $\mathbb{G}_{v_b}^-$ , and we define  $\mathbb{G}_V^*$  to be the unit interval  $\{u_c, \ldots, u_d\}$  (in clockwise order).

We give some crucial observations of arrays  $\mathbb{W}, \mathbb{G}^*$  in the following lemma.

- ▶ Lemma 69. 1. Assume  $A_0A_1A_2A_3$  is an LMAP as depicted in Lemma 12. Further assume that  $A_1$  lies at some vertex in  $\mathbb{W}_{A_0}$ . Then,  $\mathbf{u}(A_3) \in \mathbb{G}_{A_0}^*$ .
- 2. For any vertex V, there exists an inferior portion such that it contains all units in  $\mathbb{W}_V$  and all units in  $\mathbb{G}_V^*$  and does **not** contain V.

**Proof.** 1. By Lemma 12,  $\mathbf{u}(A_3) \in \mathbb{G}_{A_1}^-$ . Further since  $A_1 \in \mathbb{W}_{A_0}$ , we get  $\mathbf{u}(A_3) \in \bigcup_{V' \in \mathbb{W}_{A_0}} \mathbb{G}_{V'}^-$ . Furthermore, by definition,  $G_{A_0}^*$  contains  $\bigcup_{V' \in \mathbb{W}_{A_0}} \mathbb{G}_{V'}^-$ , so  $\mathbf{u}(A_3) \in \mathbb{G}_{A_0}^*$ .

2. Assume  $\mathbb{W}_V$  is nonempty. Otherwise it is obvious. Recall  $e_s, e_t$  in Subsection 5.1. See Figure 51 for the following arguments.

Because  $u_c \in \mathbb{G}^-_{v_a}$ , by definition of  $\mathbb{G}^-_{v_a}$ ,  $v_a$  is chasing  $u_c$ . Also because  $u_c \in \mathbb{G}^-_{v_a}$ , we know  $\zeta(v_a, u_c) \subseteq \psi^-_{v_a} = V$ . So  $\zeta(v_a, u_c) = V$ . Together, by Fact 45,  $v_a, u_c$  lie in  $[v_s \circlearrowright v_{t+1}]$ . Because  $u_d \in \mathbb{G}^-_{v_b}$ , by definition of  $\mathbb{G}^-_{v_b}$ ,  $v_b$  is chasing  $u_d$ . Also because  $u_d \in \mathbb{G}^-_{v_b}$ , we know  $\zeta(v_b, u_d) \subseteq \psi^-_{v_b} = V$ . So  $\zeta(v_b, u_d) = V$ . Together, by Fact 45,  $v_b, u_d$  lie in  $[v_s \circlearrowleft v_{t+1}]$ .

Combining these arguments, we see that all units in  $\mathbb{W}_V$  and  $\mathbb{G}_V^*$  are contained in boundary-portion  $[v_s \circlearrowright v_{t+1}]$ . Further according to Fact 44, we obtain Claim 2.

#### Algorithm for Routine 2 with the batch technique.

Recall  $S = \{(V, V') \text{ is a vertex pair of } P \mid V' \in \psi_V^+ \text{ and } V \in \psi_{V'}^-\}$ . Further, denote

$$\begin{cases} \mathcal{S}_1 &= \{(V, V') \in \mathcal{S} \mid \psi_V^+ \neq V' \text{ and } \psi_{V'}^- \neq V\}, \\ \mathcal{S}_2 &= \{(V, V') \in \mathcal{S} \mid \psi_{V'}^- = V\}, \\ \mathcal{S}_3 &= \{(V, V') \in \mathcal{S} \mid \psi_V^+ = V'\}. \end{cases}$$

We design three subroutines for Routine 2. The first subroutine takes charge of the case  $(A_0, A_1) \in \mathcal{S}_1$ . The second and third take charge of the cases  $(A_0, A_1) \in \mathcal{S}_2$  and  $(A_0, A_1) \in \mathcal{S}_3$  respectively, which are symmetric to each other. Since  $\mathcal{S} = \mathcal{S}_1 \cup \mathcal{S}_2 \cup \mathcal{S}_3$ , and recall that  $(A_0, A_1) \in \mathcal{S}$  due to Lemma 12.2, these subroutines together are sufficient for Routine 2.

The first subroutine adopts the same strategy as presented in Algorithm 2, except for changing S in Sentence 1 to  $S_1$ . The second subroutine incorporates the aforementioned batch technique and is presented in Algorithm 3. The third is omitted due to symmetry.

```
1 Compute array \mathbb{W} and \mathbb{G}^*.
2 foreach vertex V such that \mathbb{W}_V \neq \emptyset do
3 | Let v_i be the first vertex in \mathbb{W}_V. So \mathbb{W}_V = \{v_i, v_{i+1}, \dots, v_{i+|\mathbb{W}_V|-1}\}.
4 | Let v_j denote the terminal vertex of the portion consisting by the units in \mathbb{G}_V^*.
5 | (Note: By Lemma 69.2, [v_i \circlearrowright v_j] is an inferior portion that does not contain V)
6 | Let U denote the subset of \mathbb{G}_V^+ that lies in [v_i \circlearrowright v_j].
7 | Let U' denote the subset of \mathbb{G}_V^* that lies in [v_i \circlearrowright v_j].
8 | Compute and output all the non-slidable parallelograms such that A_0 = V, A_1 \in \mathbb{W}_V, \mathbf{u}(A_2) \in U, \mathbf{u}(A_3) \in U', and A_0, A_1, A_2, A_3 lie in clockwise.
9 end
```

Algorithm 3: Second part of Routine 2 for computing the LMAPs

Suppose  $A_0A_1A_2A_3$  is an LMAP as assumed in Lemma 12 satisfying the additional assumption that  $A_0 = V$  and  $(A_0, A_1) \in \mathcal{S}_2$ . Since  $(A_0, A_1) \in \mathcal{S}_2$ , we get  $\psi_{A_1}^- = A_0$  and  $A_1 \in \psi_{A_0}^+$ , which means  $A_1 \in \mathbb{W}_{A_0}$  (i.e.  $A_1 \in \mathbb{W}_V$ ) by Definition (45). This further implies that  $\mathbf{u}(A_3) \in \mathbb{G}_V^+$  by Lemma 69.1. Also, recall that  $\mathbf{u}(A_2) \in \mathbb{G}_{A_0}^+ = \mathbb{G}_V^+$  by Lemma 12.2.

By the definitions of  $v_i, v_j$ , we know  $[v_i \circlearrowright v_j]$  contains all units in  $\mathbb{W}_V$  and  $\mathbb{G}_V^*$ . Further since  $\mathbb{W}_V$  contains  $\mathbf{u}(A_1)$  while  $\mathbb{G}_V^*$  contains  $\mathbf{u}(A_3)$  meanwhile  $A_1, A_2, A_3$  lie in clockwise order,  $A_1, A_2, A_3$  all lie in  $[v_i \circlearrowleft v_j]$ . Therefore, we get  $\mathbf{u}(A_2) \in U$  and  $\mathbf{u}(A_3) \in U'$ .

Altogether, Algorithm 3 correctly outputs all those LMAPs for which  $(A_0, A_1) \in \mathcal{S}_2$ .

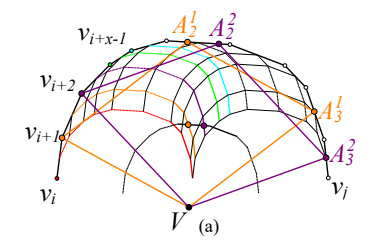
The core of Algorithm 3 lies in Sentence 8, whose implementation is clarified by the following lemma. (Hint: A key assumption in this lemma is that  $[v_i \circlearrowright v_j]$  must be an inferior portion; this assumption implies the monotonicities of  $A_2$ ,  $A_3$  with respect to  $A_1$ .)

- **Lemma 70** (Lemma 68.2 with batch technique). Given  $V, v_i, v_i, x, U, U'$  such that
- $V, v_i, v_j$  are vertices of P, and x is some positive integer.
- $[v_i \circlearrowright v_j]$  is an inferior portion that does not contain V.
- U, U' are unit intervals contained in  $[v_i \circlearrowright v_j]$ .

In O(x+|U|+|U'|) time we can compute all the non-slidable parallelograms  $A_0A_1A_2A_3$  such that

$$A_0 = V, A_1 \in \{v_i, v_{i+1}, \dots, v_{i+x-1}\}, \mathbf{u}(A_2) \in U, \mathbf{u}(A_3) \in U',$$

and that  $A_0, A_1, A_2, A_3$  lie in clockwise order.



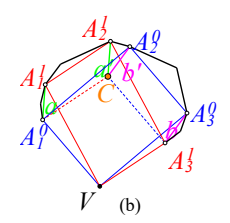


Figure 52 Illustration of Lemma 70

**Proof.** For simplicity, ignore the exceptional cases discussed in Lemma 68.1. See Figure 52 (a). For  $0 \le k < x$ , denote by  $A_0^k A_1^k A_2^k A_3^k$  the (unique) parallelogram such that  $A_0^k = V$ ,  $A_1^k = v_{i+k}$ . We aim to compute those  $(A_2^k, A_3^k)$  for which  $\mathbf{u}(A_2^k) \in U$  and  $\mathbf{u}(A_3^k) \in U'$ . We state:

- (i)  $A_2^0, \dots, A_2^{x-1}$  lie in clockwise order, and
- (ii)  $A_3^0, \dots, A_3^{x-1}$  also lie in clockwise order.

Proof of (i). Let  $\rho = [v_i \circlearrowright v_j]$ . Suppose to the opposite that  $A_2^1 <_{\rho} A_2^0$  as shown in Figure 52 (b). Make a line at  $A_1^0$  parallel to  $VA_3^1$ ; and a line at  $A_3^1$  parallel to  $VA_1^0$ ; and assume they intersect at C. Because  $VA_1^0A_2^0A_3^0$  and  $VA_1^1A_2^1A_3^1$  are parallelograms, we can see  $CA_1^0A_1^1A_2^1$  and  $CA_2^0A_3^0A_3^1$  are also parallelograms. It follows that  $forw(A_1^0)$  is not chasing  $back(A_3^1)$ , so  $\rho$  is not an inferior portion. Contradictory.

*Proof of (ii).* This one immediately follows from (i). We omit the details.

In general, we adopt the algorithm given in Lemma 68.2 to compute  $A_2^k$  and  $A_3^k$  for each k. However, due to the monotonicities (i) and (ii), the unit containing  $A_2^k$  and the unit  $A_3^k$  can be computed in amortized O(1) time, and thus the total time is O(x + |U| + |U'|).

Running time analysis of optimized Routine 2. We state some key observations first.

- (i)  $\bigcup_{(V,V')\in\mathcal{S}_1} \left( |\mathbb{G}_{V'}^-| + |\mathbb{G}_V^+| \right) = O(n).$
- (ii)  $\sum_{V} (|\mathbb{W}_{V}| + |\mathbb{G}_{V}^{+}| + |\mathbb{G}_{V}^{*}|) = O(n).$
- (iii) Given  $\mathbb{G}^-, \mathbb{G}^+, \psi^-, \psi^+$  (which can be computed from  $\mathbb{G}$  in linear time according to Lemma 67.4), we can compute arrays  $\mathcal{S}, \mathbb{W}, \mathbb{G}^*$  in linear time.

According to Lemma 68.2, the first subroutine runs in  $\bigcup_{(V,V')\in\mathcal{S}_1}\left(|\mathbb{G}_{V'}^-|+|\mathbb{G}_{V}^+|\right)$  time. This is O(n) time according to (i). According to Lemma 70, the second subroutine runs in  $\sum_{V}\left(|\mathbb{W}_{V}|+|\mathbb{G}_{V}^+|+|\mathbb{G}_{V}^*|\right)$  time after the computation of  $\mathbb{W}$  and  $\mathbb{G}^*$ . This is O(n) time (after the preprocessing of  $\mathbb{G}$ ) according to (ii) and (iii). The third subroutine runs in the time as the second. Altogether, Routine 2 runs in linear time after preprocessing  $\mathbb{G}$ .

Proof of (i). The monotonicity of  $\psi^-$  stated in Lemma 67 implies that there exist at most two different V such that  $\psi^-_V$  contains V' but does not equal V. Therefore,  $\Sigma_{(V,V')\in\mathcal{S}_1}|\mathbb{G}^-_{V'}|\leq 2\Sigma_{V'}|\mathbb{G}^-_{V'}|$ . Moreover, by the monotonicity of  $\mathbb{G}^-$  (Lemma 67),  $\Sigma_{V'}|\mathbb{G}^-_{V'}|=O(n)$ . Together,  $\Sigma_{(V,V')\in\mathcal{S}_1}|\mathbb{G}^+_{V'}|=O(n)$ . Similarly,  $\Sigma_{(V,V')\in\mathcal{S}_1}|\mathbb{G}^+_V|=O(n)$ . Together, we get (i).

Proof of (ii). Following the monotonicity of  $\psi^+$ , vertex sets  $\mathbb{W}_{v_1}, \dots, \mathbb{W}_{v_n}$  are pairwise-disjoint and lie in clockwise order. So  $\sum_V |\mathbb{W}_V| = O(n)$ . This monotonicity of  $\mathbb{W}$  and the monotonicity of  $\mathbb{G}^-$  imply a similar monotonicity of  $\mathbb{G}^*$  which guarantees that  $\sum_V |\mathbb{G}_V^*| = O(n)$ . Moreover,  $\sum_V |\mathbb{G}_V^+| = O(n)$  by the monotonicity of  $\mathbb{G}^+$ . Altogether, we get (ii).

*Proof of (iii)*. This claim simply follows from the definition of  $\mathcal{S}$ ,  $\mathbb{W}$ , and  $\mathbb{G}^*$ .

▶ Remark. Routine 2 is for sure some magic. It applies every piece of our knowledge to the LMAPs perfectly and has an amazing accumulated time complexity.

#### 7.3 Routine 3 - compute the LMAPs with an anchored even corner

Routine 3 computes those LMAPs who have an anchored even corner. (Recall that  $A_i$  is an even corner if  $\mathbf{u}(A_{i-1}), \mathbf{u}(A_{i+1})$  are not chasing the other.) Unlike the first two routines, this one runs in  $O(n \log n)$  time and does not require any preprocessed information.

The strategy of this routine is similar to that of Routine 2. An important difference is that it applies bounds for even corners (below) rather than the bounds for broad corners.

### A generalization of $\zeta(u,u')$ and bounds for even corners.

Previously,  $\zeta(u, u')$  is defined for any unit pair u, u' such that u is chasing u'. In the following, we extend the scope of definition of  $\zeta(u, u')$  to every pair of distinct units u, u'.

Recall that  $D_i$  is the unique vertex of P with largest distance to the extended line of  $e_i$ . For each pair of units u, u' that are distinct, we define

$$\zeta(u, u') = [Z_a^{a'} \circlearrowright Z_b^{b'}], \text{ where } \begin{cases}
e_a &= back(u) \\
e_{a'} &= \begin{cases} back(u'), & \text{if } back(u) \prec back(u'); \\
back(\mathsf{D}_a), & \text{otherwise.} \end{cases} \\
e_{b'} &= forw(u') \\
e_b &= \begin{cases} forw(u), & \text{if } forw(u) \prec forw(u'); \\
forw(\mathsf{D}_{b'}), & \text{otherwise.} \end{cases}
\end{cases} (46)$$

Be aware that it is always true that  $e_a \prec e_{a'}$  and  $e_b \prec e_{b'}$ , so  $\zeta(u, u')$  is well-defined. See Figure 53 for illustrations. Also be aware that (46) degenerates to (2) when u is chasing u'.

▶ **Lemma 71** (Bounds on even corners; Lemma 12 of [15]). Given the same assumption as Lemma 6. We claim that  $A_i$  lies in  $\zeta(u, u')$  if u, u' are not chasing each other.

Note that Lemma 71 is a cousin of Lemma 6. Its proof is slightly more complicated.

Applying Lemma 71, we can deduce other bounds as presented in the next lemma. They bound a corner when one of its neighboring corner is anchored on a known vertex, which have the same favor as Lemma 12.2. See Figure 54. For each vertex V of P, denote

$$\mathbb{H}_{V} = \text{the set of units that lie in } (\mathsf{D}_{back(V)} \circlearrowright \mathsf{D}_{forw(V)}).$$
 (47)

$$\kappa_V^+ = \bigcup_{u \in \mathbb{H}_V} \zeta(V, u). \tag{48}$$

$$\kappa_{V}^{-} = \bigcup_{u \in \mathbb{H}_{V}} \zeta(u, V). \tag{49}$$

- ▶ Lemma 72. If  $A_0A_1A_2A_3$  is an LMAP where  $A_0, A_1, A_2, A_3$  lie in clockwise order and  $A_i$  is an even corner, (at least) one of the following holds.
- (a) Corner  $A_{i+1}$  lies at some vertex V and  $A_i$  lies in  $\kappa_V^+$ .
- (b) Corner  $A_{i-1}$  lies at some vertex V and  $A_i$  lies in  $\kappa_V^-$ .

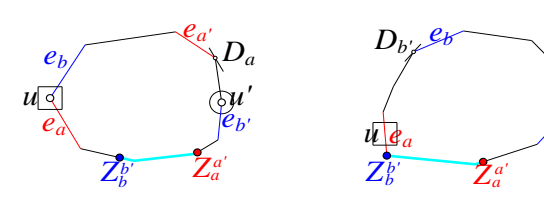


**Figure 53** Definition of  $\zeta(u, u')$  when u, u' are not chasing each other.

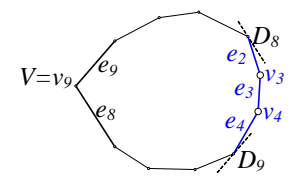


**Figure 54** Definition of  $\mathbb{H}_V$ . Here,  $\mathbb{H}_{v_9}$  contains the units in  $(\mathsf{D}_8 \circlearrowright \mathsf{D}_9)$ .

**Proof.** Since  $A_i$  is even, units  $\mathbf{u}(A_{i+1}), \mathbf{u}(A_{i-1})$  are distinct, non-incident, and not chasing each other. If two units u, u' are distinct, non-incident, and not chasing each other, one of the following occurs: u is a vertex and  $u' \in \mathbb{H}_u$ ; or, u' is a vertex and  $u \in \mathbb{H}_{u'}$  (a proof can be found in Section 6.4 of [15]). Therefore, one of the following holds.

- (a')  $\mathbf{u}(A_{i+1})$  is a vertex and  $\mathbf{u}(A_{i-1}) \in \mathbb{H}_{\mathbf{u}(A_{i+1})}$ .
- (b')  $\mathbf{u}(A_{i-1})$  is a vertex and  $\mathbf{u}(A_{i+1}) \in \mathbb{H}_{\mathbf{u}(A_{i-1})}$ .

Clearly, (a') implies (a). Suppose (a') is true. Let  $V = \mathbf{u}(A_{i+1}), u = \mathbf{u}(A_{i-1})$ . Because (a'),  $u \in \mathbb{H}_V$ . Moreover, by Lemma 71,  $A_i \in \zeta(\mathbf{u}(A_{i+1}), \mathbf{u}(A_{i-1})) = \zeta(V, u)$ . Together,  $A_i \in \bigcup_{u \in \mathbb{H}_V} \zeta(V, u) = \kappa_V^+$ . Symmetrically, (b') implies (b).

# The algorithm for Routine 3 and its analysis.

```
1 foreach vertex pair V, V' such that V' \in \kappa_V^+ or V' \in \kappa_V^- do
```

- Compute and output all the parallelograms that are inscribed, non-slidable, and have two neighboring corners lying on V, V'.
- з end

**Algorithm 4:** Routine 3 for computing the LMAPs

- ▶ **Lemma 73.** 1. For each vertex V, notation  $\kappa_V^+, \kappa_V^-$  are boundary-portions of  $\partial P$ . In addition, we can compute arrays  $\kappa^+, \kappa^-$  in linear time.
- 2. Array  $\kappa^+, \kappa^-$  have the same monotonicity property as  $\psi^+, \psi^-$  stated in Lemma 67.
- 3. Given two vertices V, V' of P, in  $O(\log n)$  time we can compute all the non-slidable inscribed parallelograms which have two neighboring corners lying on V, V'.
- **4.** Algorithm 4 computes the LMAPs with an anchored even corner in  $O(n \log n)$  time.

**Proof.** 1. and 2. By the definition of  $\zeta$  in (46), we get

$$\left\{ \begin{array}{ll} \zeta(v_i,e_j) &= [Z_{i-1}^{back(\mathsf{D}_{i-1})} \circlearrowleft Z_i^j], \text{ for } e_j \in \mathbb{H}_{v_i}; \\ \zeta(v_i,v_j) &= [Z_{i-1}^{back(\mathsf{D}_{i-1})} \circlearrowleft Z_i^j], \text{ for } v_j \in \mathbb{H}_{v_i}. \end{array} \right.$$

Further, applying the bi-monotonicity of Z-points, we get

$$\kappa_{v_i}^+ = \begin{cases} [Z_{i-1}^{back(\mathsf{D}_{i-1})} \circlearrowright Z_i^{back(\mathsf{D}_i)}], & \text{When } \mathsf{D}_{i-1} \neq \mathsf{D}_i; \\ \varnothing, & \text{When } \mathsf{D}_{i-1} = \mathsf{D}_i. \end{cases}$$
(50)

This implies that  $\kappa_V^+$  is a boundary-portion. Moreover, due to the bi-monotonicity of the Z-points,  $Z_1^{back(\mathsf{D}_1)}, \dots, Z_n^{back(\mathsf{D}_n)}$  lie in clockwise order around  $\partial P$ , which implies the monotonicity of  $\kappa^+$ . Computing  $\kappa^+$  reduces to computing these Z-points. We can first compute D and then apply Lemma 23.3 to compute the Z-points, which costs O(n) time.

The properties of  $\kappa^-$  can be proved symmetrically.

- 3. It reduces to find a chord of P other than  $\overline{VV'}$  but is a translation of  $\overline{VV'}$ , which can be found in  $O(\log n)$  time by the Tentative Prune-and-Search technique. See Theorem 3.3 in [20]. (Alternatively, an  $O(\log^2 n)$  method exists which uses a simple binary search.)
- 4. By Claim 2, there are O(n) pairs of vertices (V, V') such that  $V' \in \kappa_V^+$  or  $V' \in \kappa_V^-$ . Further by Claim 3, Algorithm 4 runs in  $O(n \log n)$  time.

The correctness of Algorithm 4 follows from Lemma 72.

**Acknowledgements.** The author thanks our god for his amazing creation. I have a feeling that everything is rotating and is perfect after understanding the novel structure.

The author thanks Haitao Wang for fruitful discussions and for his considerate advices and helps on writing this paper, and thanks Andrew C. Yao, Jian Li, and Danny Chen for instructions, and Matias Korman, Wolfgang Mulzer, Donald Sheehy, Kevin Matulef, and anonymous reviewers from past conferences for many precious suggestions. Last but not least, the author appreciates the developers of Geometer's Sketchpad<sup>®</sup>.

#### References -

- 1 A. Aggarwal, M. M. Klawe, S. Moran, P. Shor, and R. Wilber. Geometric applications of a matrix-searching algorithm. *Algorithmica*, 2(1-4):195–208, 1987.
- 2 A. Aggarwal, B. Schieber, and T. Tokuyama. Finding a minimum-weight k-link path in graphs with the concave monge property and applications. *Discrete & Computational Geometry*, 12(1):263–280, 1994.
- 3 N. Anghel. A maximal parallelogram characterization of ovals having circles as orthoptic curves. In *Forum Geometricorum*, volume 10, pages 21–25, 2010.
- 4 C. Bertram-Kretzberg, Hofmeister T., and Lefmann H. An algorithm for heilbronn's problem. SIAM Journal on Computing (SICOMP), 30(2):383–390, 2000.
- **5** B. Bhattacharya and A. Mukhopadhyay. On the Minimum Perimeter Triangle Enclosing a Convex Polygon, pages 84–96. Springer Berlin Heidelberg, 2003.
- **6** A. Bielecki and K. Radziszewski. Sur les parallélépipèdes inscrits dans les corps convexes. Ann. Univ. Mariae Curie-Sklodowska, Sect. A, 8:97–100, 1954.
- J. E. Boyce, D. P. Dobkin, R. L. Drysdale, III, and L. J. Guibas. Finding extremal polygons. In 14th Symposium on Theory of Computing, STOC '82, pages 282–289. ACM, 1982.
- 8 S. Cabello, O. Cheong, and L. Schlipf. Finding largest rectangles in convex polygons. European Workshop on Computational Geometry, 2014.
- 9 S. Chandran and D. M. Mount. A paraellel algorithm for enclosed and enclosing triangles. *International Journal of Computational Geometry & Applications*, 02(02):191–214, 1992.
- 10 A. Connes and D. Zagier. A property of parallelograms inscribed in ellipses. American Mathematical Monthly, 114:909, 2007.
- 11 D.P. Dobkin and L. Snyder. On a general method for maximizing and minimizing among certain geometric problems. In 20th Annual Symposium on Foundations of Computer Science, pages 9–17. IEEE Computer Society, 1979.
- 12 C. M. Fulton and S. K. Stein. Parallelograms inscribed in convex curves. American Mathematical Monthly, 67:257–258, 1960.
- 13 Y. Gordon, A. E. Litvak, M. Meyer, and A. Pajor. John's decomposition in the general case and applications. *Journal of Differential Geometry*, 68(1):99–119, 2004.
- O. Hall-Holt, M. J. Katz, P. Kumar, J. S. B. Mitchell, and A. Sityon. Finding large sticks and potatoes in polygons. In *Symposium on Discrete Algorithms*, pages 474–483, 2006.
- **15** K. Jin. Finding all maximal area parallelograms in a convex polygon. *CoRR*, abs/1711.00181, 2017.
- 16 K. Jin. Maximal area triangles in a convex polygon. CoRR, abs/1707.04071, 2017.
- 17 K. Jin and K. Matulef. Finding the maximum area parallelogram in a convex polygon. In 23rd Proceeding of Canadian Conference on Computational Geometry, 2011.
- **18** F. John. Extremum problems with inequalities as subsidiary conditions. *Courant Anniversary Volume*, pages 187–204, 1948.
- 19 V. Keikha, M. Löffler, J. Urhausen, and I. v. d. Hoog. Maximum-area triangle in a convex polygon, revisited. *CoRR*, abs/1705.11035, 2017.

- D. Kirkpatrick and J. Snoeyink. Tentative prune-and-search for computing fixed-points 20 with applications to geometric computation. Fundamenta Informaticae, 22(4):353–370, December 1995.
- M. Lassak. Approximation of convex bodies by centrally symmetric bodies. Geometriae Dedicata, 72(1):63-68, 1998.
- 22 M. Lassak. Parallelotopes of maximum volume in a simplex. Discrete & Computational Geometry, 21(3):449-462, Apr 1999.
- 23 H. Lefmann and N. Schmitt. A deterministic polynomial-time algorithm for heilbronn's problem in three dimensions. SIAM Journal on Computing, 31(6):1926–1947, 2002.
- 24 G. Leng, Y. Zhang, and B. Ma. Largest parallelotopes contained in simplices. Discrete Mathematics, 211(1-3):111-123, January 2000.
- 25 A. Miernowski. Parallelograms inscribed in a curve having a circle as  $\pi/2$ -isoptic. Annales UMCS, Mathematica, 62:105–111, 2008.
- J. O'Rourke, A. Aggarwal, S. Maddila, and M. Baldwin. An optimal algorithm for finding 26 minimal enclosing triangles. Journal of Algorithms, 7(2):258 –269, 1986.
- 27 N.A.D. Pano, Y. Ke, and J. O'Rourke. Finding largest inscribed equilateral triangles and squares. In Proceeding of Annual Allerton Conference on Communication, Control, and Computing, pages 869–878, 1987.
- K. Radziszewski. Sur une probléme extrémal relatif aux figures inscrites et circonscrites aux fiures convexes. Ann. Univ. Mariae Curie-Skłodowska, Sect. A, 6, 1954.
- 29 J. M. Richard. Safe domain and elementary geometry. European Journal of Physics, 25:835, 2004.
- 30 W. M. Schmidt. On a problem of heilbronn. Journal of the London Mathematical Society, 4:545-550, 1971.
- 31 C. Schwarz, J. Teich, A. Vainshtein, E. Welzl, and B.L. Evans. Minimal enclosing parallelogram with application. In Proceedings of the Eleventh Annual Symposium on Computational Geometry, SCG '95, pages 434–435, New York, NY, USA, 1995. ACM.
- M. Sharir and S. Toledo. Extremal polygon containment problems. Computational Geometry: Theory and Applications, 4(2):99-118, jun 1994.
- 33 G. Toussaint. Solving geometric problems with the rotating calipers. In IEEE MELE-CON'83, pages 1-4, 1983.